



DWLBC REPORT


Hydrogeophysical mapping of fracture orientation and groundwater flow in the Western Mount Lofty Ranges, South Australia

2008/32



Government of South Australia

Department of Water, Land and
Biodiversity Conservation



Hydrogeophysical mapping of fracture orientation and groundwater flow in the Western Mount Lofty Ranges, South Australia

Adrian Costar, Graham Heinson and Tania Wilson

**Knowledge and Information Division
Department of Water, Land and Biodiversity Conservation**

December 2008

Report DWLBC 2008/32



Science, Monitoring and Information Division

Department of Water, Land and Biodiversity Conservation

25 Grenfell Street, Adelaide

GPO Box 2834, Adelaide SA 5001

Telephone National (08) 8463 6946

International +61 8 8463 6946

Fax National (08) 8463 6999

International +61 8 8463 6999

Website www.dwlbc.sa.gov.au

Disclaimer

The Department of Water, Land and Biodiversity Conservation and its employees do not warrant or make any representation regarding the use, or results of the use, of the information contained herein as regards to its correctness, accuracy, reliability, currency or otherwise. The Department of Water, Land and Biodiversity Conservation and its employees expressly disclaims all liability or responsibility to any person using the information or advice. Information contained in this document is correct at the time of writing.

© Government of South Australia, through the Department of Water, Land and Biodiversity Conservation 2010

This work is Copyright. Apart from any use permitted under the Copyright Act 1968 (Cwlth), no part may be reproduced by any process without prior written permission obtained from the Department of Water, Land and Biodiversity Conservation. Requests and enquiries concerning reproduction and rights should be directed to the Chief Executive, Department of Water, Land and Biodiversity Conservation, GPO Box 2834, Adelaide SA 5001.

ISBN 978-1-921528-77-4

Preferred way to cite this publication

Costar A, Heinson G, and Wilson T, 2008, *Hydrogeophysical mapping of fracture orientation and groundwater flow in the Western Mount Lofty Ranges, South Australia*, DWLBC Report 2008/32, Government of South Australia, through Department of Water, Land and Biodiversity Conservation, Adelaide.

FOREWORD

South Australia's unique and precious natural resources are fundamental to the economic and social wellbeing of the State. It is critical that these resources are managed in a sustainable manner to safeguard them both for current users and for future generations.

The Department of Water, Land and Biodiversity Conservation (DWLBC) strives to ensure that our natural resources are managed so that they are available for all users, including the environment.

In order for us to best manage these natural resources it is imperative that we have a sound knowledge of their condition and how they are likely to respond to management changes. DWLBC scientific and technical staff continues to improve this knowledge through undertaking investigations, technical reviews and resource modelling.

Scott Ashby
CHIEF EXECUTIVE
DEPARTMENT OF WATER, LAND AND BIODIVERSITY CONSERVATION

ACKNOWLEDGEMENTS

The Department of Water Land and Biodiversity Conservation (DWLBC) would firstly like to acknowledge the National Water Commission for funding the project.

Acknowledgement should also be given to the South Australian Murray–Darling Basin Natural Resources Management Board and Adelaide University (particularly Associate Professor Graham Heinson) for their numerous discussions regarding methodology and any technical issues that arose during the course of this project.

A special thank you to the land owners of various properties in the Western Mount Lofty Ranges (WMLR) who facilitated in allowing access to various sites and groundwater wells.

Finally thank you to all the people who helped in fieldwork operations including, Associate Professor Graham Heinson, Simone Stewart, Dan Wohling, Tania Wilson, Dragana Zulfic, Heather Mazengarb, Ceridwen Synnot, Volmer Berens and the French contingent which consisted of Alexis Rochat, Mathieu Derunes and Florent Sztikar.

CONTENTS

FOREWORD	iii
ACKNOWLEDGEMENTS	v
SUMMARY	1
1. INTRODUCTION	3
1.1 PURPOSE	3
1.2 THE STUDY AREA	3
1.3 BACKGROUND	7
2. HYDROGEOLOGY	9
2.1 GEOLOGY	9
2.1.1 Hydrogeology	9
2.1.2 Climate	9
2.1.3 Fractured Rock Aquifers	12
3. METHODOLOGY	13
3.1 BACKGROUND THEORY	13
3.2 GEOPHYSICAL TECHNIQUES	15
3.2.1 Borehole-to-surface DC resistivity Method	15
3.2.2 Self-potential Method	16
4. RESULTS	19
4.1 ELECTRICAL RESISTIVITY	19
4.2 SELF-POTENTIAL (SP) METHODS	29
5. DISCUSSION	35
5.1 CALIBRATION STUDIES	35
5.1.1 Watervale Oval, Clare Valley	35
5.1.2 Balhanah, Western Mount Lofty Ranges	36
5.2 GENERATING HYDRAULIC ANISOTROPY	40
6. CONCLUSION	43
7. RECOMMENDATIONS	45
APPENDICES	47
A. SURFACE MAPS OF ELECTRICAL POTENTIAL FOR ALL 18 SITES IN THE WESTERN MOUNT LOFTY RANGES	47
B. WELLS SELECTED FOR SURVEY IN THE WESTERN MOUNT LOFTY RANGES WITH GEOLOGICAL DESCRIPTION	66
UNITS OF MEASUREMENT	69
GLOSSARY	71
REFERENCES	73
BIBLIOGRAPHY	77

LIST OF FIGURES

Figure 1a.	Study area within the Western Mount Lofty Ranges.....	5
Figure 1b.	Site selection across the Western Mount Lofty Ranges	6
Figure 2.	Typical groundwater contours for an aquifer test in fractured rock (Cook 2003) ...	7
Figure 3.	Geology of the Western Mount Lofty Ranges.....	10
Figure 4.	Well yield in the Mount Lofty Ranges, South Australia	11
Figure 5.	Groundwater wells in a fractured rock environment	12
Figure 6.	Illustration of a well and its area of influence	13
Figure 7.	Schematic of DC resistivity survey and output surface potential map	16
Figure 8.	Within the fluid that resides in the fracture there are ions. The movement of these ions sets up what is called advective current.....	17
Figure 9.	Map of 21 sites located in the Western Mount Lofty Ranges.....	20
Figure 10.	Borehole-to-surface DC resistivity surface setup arrangement.....	22
Figure 11.	Apparent resistivity of electrodes at 25 m away from the well as a function of bearing. (a) If the graph is symmetrical then it is inferred that there is one major orientation for the conductive fractures. If conductive structures are approximately vertical there is symmetry observed around the borehole. (b) If the graph is asymmetrical, there may be a second differently orientated fracture set. The dip of structures gives rise to anisotropy of the response and will be biased to the upside fracture sets.	23
Figure 12.	Average apparent resistivity (Ωm) for sites with available data vs salinity (TDS) 25	
Figure 13.	Normalised potential contour map from Site 5, dashed line denotes strike orientation, solid line with arrow denotes a direction of dip	26
Figure 14.	Map of fracture strike and dip for each of the 18 available sites in the Western Mount Lofty Ranges.....	28
Figure 15.	Self-potential surface setup arrangement	31
Figure 16.	SP results for Site 9. The white dashed line represents the point at which the pump was switched on. Length of record shown here is only the first 5-7 minutes of the pumping duration	31
Figure 17.	SP results for Site 10. The white dashed line represents the point at which the pump was switched on. Length of record shown here is only the first 5-7 minutes of the pumping duration	32
Figure 18.	SP results for Site 7. The white dashed line represents the point at which the pump was switched on. Length of record shown here is only the first 5-7 minutes of the pumping duration	33
Figure 19.	SP results for Site 6. The white dashed line represents the point at which the pump was switched on. Length of record shown here is only the first 5-7 minutes of the pumping duration	34
Figure 20.	Aquifer test conducted in October 2003. Drawdown contours shown here are after 230 minutes of pumping from well 6628-21203. Well unit numbers are in blue, water levels (mAHD) for each well are in red. Note that water level contours (also mAHD) are approximate and coloured black	37
Figure 21.	Normalised potential distribution contour map for Balhannah site.....	38
Figure 22.	Apparent resistivity of electrodes at 15 m away from the well as a function of bearing.....	39

CONTENTS

Figure 24. Hypothetical example of anisotropic direction and ratio as applied to circular buffering system. Assuming circular buffer radius of 200 m with a anisotropic strike direction of NW/SE and a hydraulic anisotropic ratio of 3.	41
Figure 23. Sequence of events which facilitate fracture development in a fractured rock environment	44

LIST OF TABLES

Table 1. Wells selected for survey in the Western Mount Lofty Ranges	19
Table 2. Summary of electrical data interpretations for 18 selected sites in the Western Mount Lofty Ranges.....	27
Table 3. Summary of anisotropic ratios for the calibration sites	40
Table 4. Summary of electrical data interpretations for 18 selected sites in the Western Mount Lofty Ranges.....	40

SUMMARY

Fractured rock aquifers are becoming increasingly important water supplies as traditional sedimentary aquifers become more fully utilised. Characterisation of groundwater flow in fractured rocks is difficult as hydraulically conductive fractures are inherently complex and often unpredictable. As fractures act as conduits for flow of both groundwater and electrical charge, methods that can efficiently detect the distribution of electrical pathways may be used to infer characteristics of significant hydrological parameters.

Electrical data from direct current borehole-to-surface resistivity and self-potential measurements were used for the interpretation of major hydrological structures at 18 sites in the Western Mount Lofty Ranges, South Australia. Application of borehole-to-surface methods generated an interpretation of sub-vertical fracture strike and dip. The natural-voltage self-potential signals generated during pumping tests are of a complex nature, but, the magnitude of changes in the electrokinetic measurement can be attributed to fluid flow rates and yield the dominant direction of groundwater flow.

Borehole-to-surface measurements at the majority of sites showed a dominant trend of conductive zones with a fracture strike of north – north-west to north – north-east which are consistent with major regional structural trends.

Electrokinetic measurements are highly variable in the region with large (up to 60 mV) variations with time. Although self-potential is a relatively new technique, a combination of the two electrical methods provides valuable information about in-situ hydraulic pathways and leads to a greater understanding of the subsurface flow in fractured rock aquifers.

1. INTRODUCTION

1.1 PURPOSE

This work is part of a larger Australian Government Water Fund project intended to further the understanding of groundwater flow mechanisms in fractured rock aquifers (FRAs) to improve water resource management decisions.

It is anticipated that the project will be comprised of four key components, each representing areas with significant knowledge gaps and requiring further investigation. These are as follows:

- Surface water-groundwater interaction and the implications for conjunctive use of the resource
- Extent of the zones of influence from pumped wells
- Groundwater movement across regional scale faults and
- Predicting catchment scale processes in a fractured rock environment.

While the project spans these four key areas of study the focus of this report is on the extent of the zones of influence from pumped wells in the Western Mount Lofty Ranges (WMLR) (Program 2).

Methods and technologies proposed in this project are considered innovative or non-traditional, as they have not previously been applied to investigations of processes occurring in fractured rock systems. As such, the approach adopted in this project intends to address many of these issues and knowledge gaps which have not previously been approached with such scientific rigor.

1.2 THE STUDY AREA

The Mount Lofty Ranges are the range of mountains to the east of the city of Adelaide in South Australia. They stretch from the southern most point of the Fleurieu Peninsula at Cape Jervis and extend northwards for over 300 kilometres before petering out north of the southern Flinders Ranges. In the vicinity of Adelaide, they separate the Adelaide Plains from the extensive plains that surround the Murray River and stretch eastwards to Victoria.

The WMLR Prescribed Water Resource Area (PWRA) occupies an area on the western side of the Mount Lofty Ranges (Fig. 1a). This region extends from Gawler south to Cape Jervis and covers parts of the Adelaide Hills and the Fleurieu Peninsula.

While the WMLR PWRA covers a much larger area, the study area was focused on the middle section of the WMLR, where the Barossa PWRA forms the most northern boundary and the McLaren Vale Prescribed Wells Area (PWA) forms the southern boundary. This region comprises the Torrens River, Onkaparinga River and Little Para River catchments.

The Torrens River Catchment (TRC) covers an area of approximately 501 km² (Fig. 1a). The catchment runs in a westerly direction, which follows the Torrens River as it traverses the Adelaide Plains and discharges to the sea at West Beach. The catchment contains two

INTRODUCTION

major reservoirs at Kangaroo Creek and Millbrook. The major land uses in the catchment are dairying, irrigated pasture for livestock grazing, fruit trees, and viticulture. The western part of the catchment, on the lower side of the Eden Burnside Fault, is extensively urbanised.

The Onkaparinga River Catchment (ORC) covers an area of 555 km² and adjoins the southern boundary of the TRC (Fig. 1a). The major watercourse is the Onkaparinga River which discharges into the Onkaparinga Estuary. The course of the river is interrupted by the Mount Bold reservoir in the southwest of the catchment. The major land uses in the catchment are dairying, irrigated pasture for livestock grazing, and some viticulture.

The Little Para River Catchment (LPRC) covers an area of 94 km² and adjoins the northwestern boundary of the TRC (Fig. 1a). The major watercourse within the catchment is the Little Para River which discharges into Barker Inlet. The course of the river is interrupted by the Little Para reservoir in the northwest of the catchment.

Initially 21 sites across the WMLR study area were selected (Fig. 1b), however 3 sites were abandoned due to unsuitable wells. Therefore data from 18 sites are presented in this report. Site selection was based on lithological variations, position within the regional structure, and accessibility of wells (Table 1). The sites span over 40 kilometres of the WMLR, from Gumeracha in the north to Mylor in the south.

Surveys were also undertaken at sites near Balhannah in the WMLR and the Clare Valley. The information was used to calibrate the hydrogeophysical methods against known hydrogeological parameters.

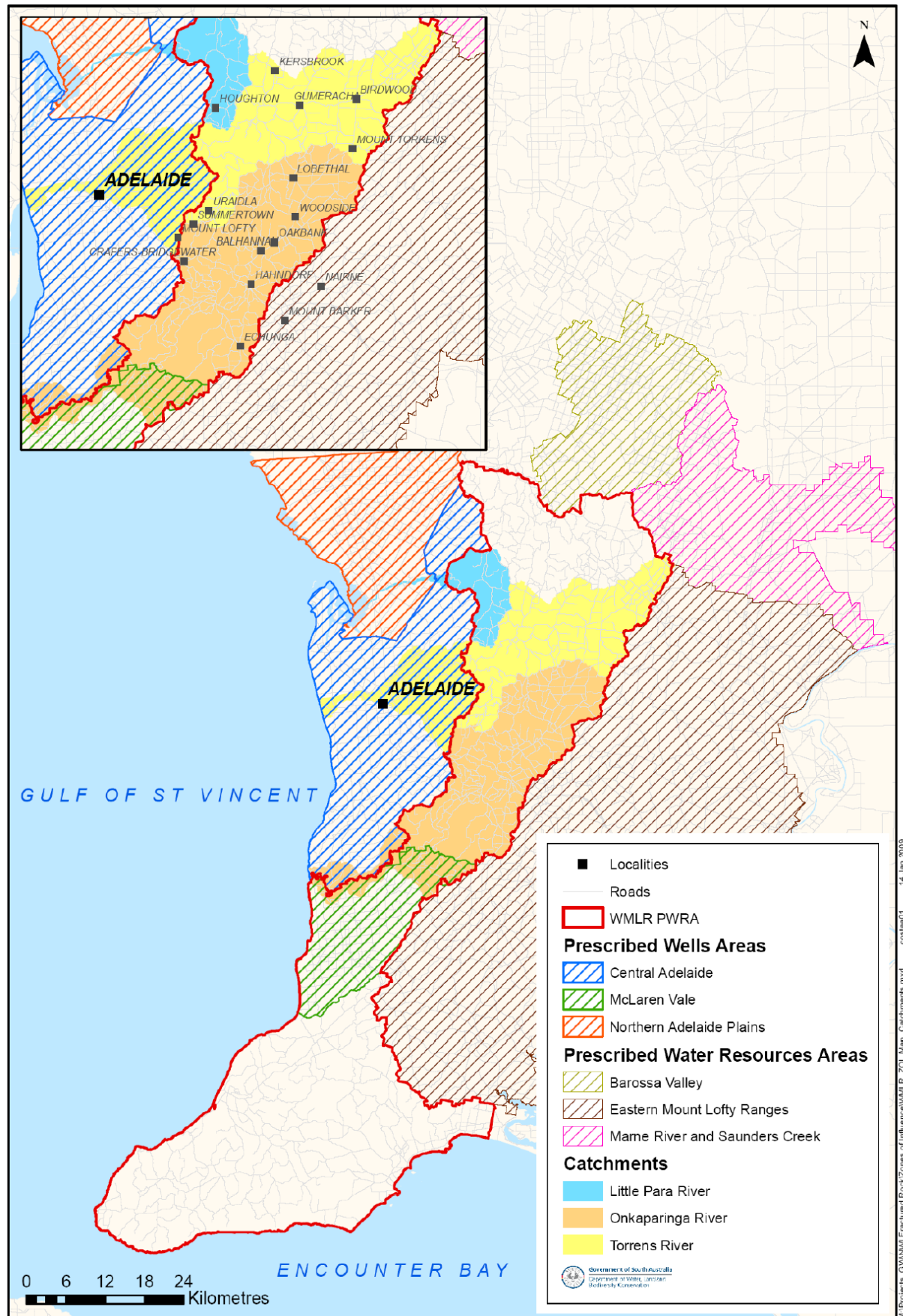


Figure 1a. Study area within the Western Mount Lofty Ranges

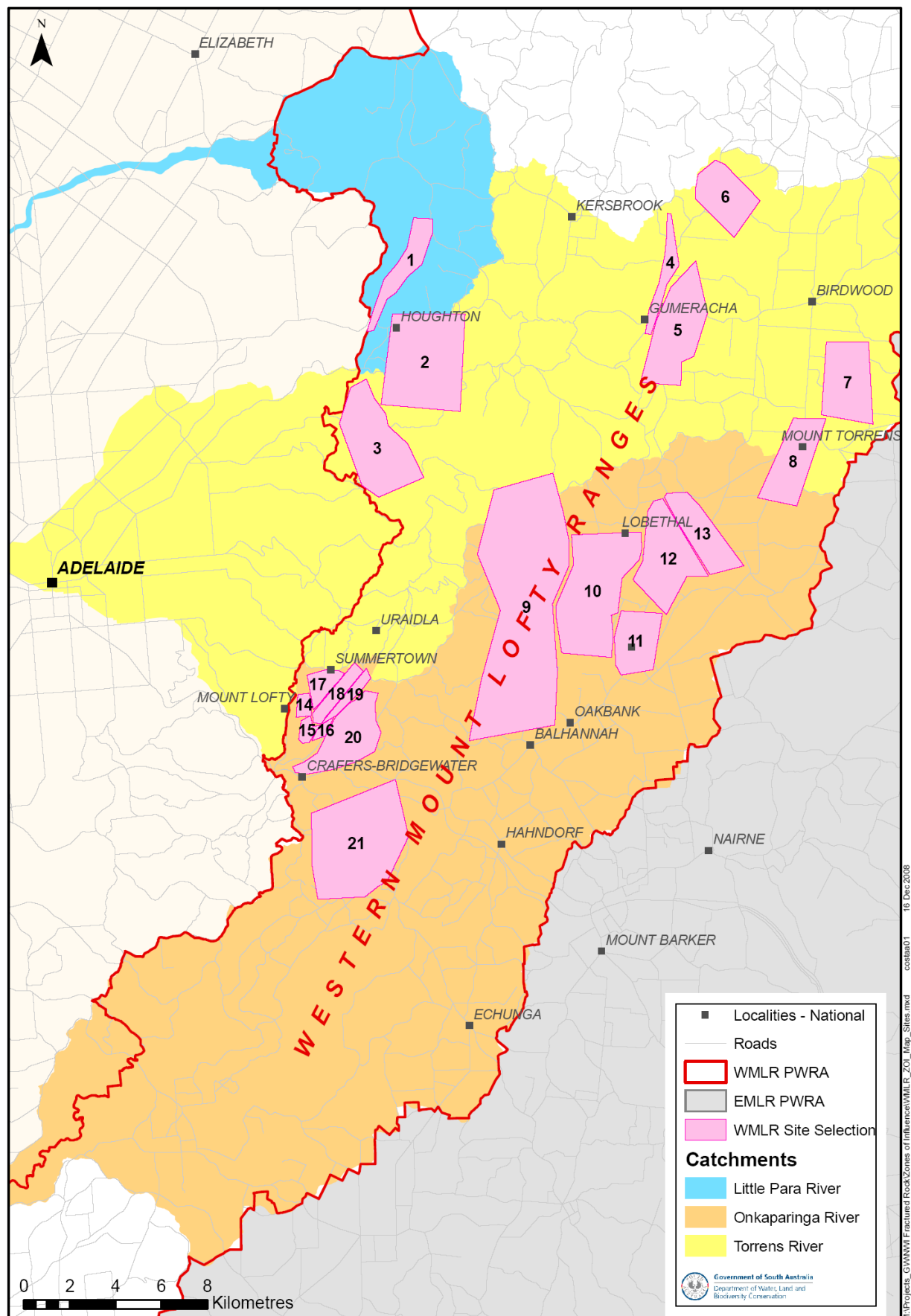


Figure 1b. Site selection across the Western Mount Lofty Ranges

1.3 BACKGROUND

FRAs underlie approximately 40% of the Australian continent and are becoming increasingly important water supplies as traditional sedimentary aquifers (porous media) are becoming fully utilised (Cook et al. 2001). Despite their importance, it is extremely difficult to quantify the bulk properties controlling fluid transport through fractured rock.

FRAs occur where groundwater is stored and moves primarily through joints and fractures in the basement rocks. Groundwater moves from the higher points in the landscape towards the lowest areas where discharge normally occurs through the sedimentary aquifers in the valleys to the streams.

Currently management of well interference in FRAs utilises buffer zones that assume a circular zone of influence around a pumped well. Due to the heterogeneous nature of FRAs the true zones of influence are more likely to be elliptical and controlled by regional fracture systems (Fig. 2).

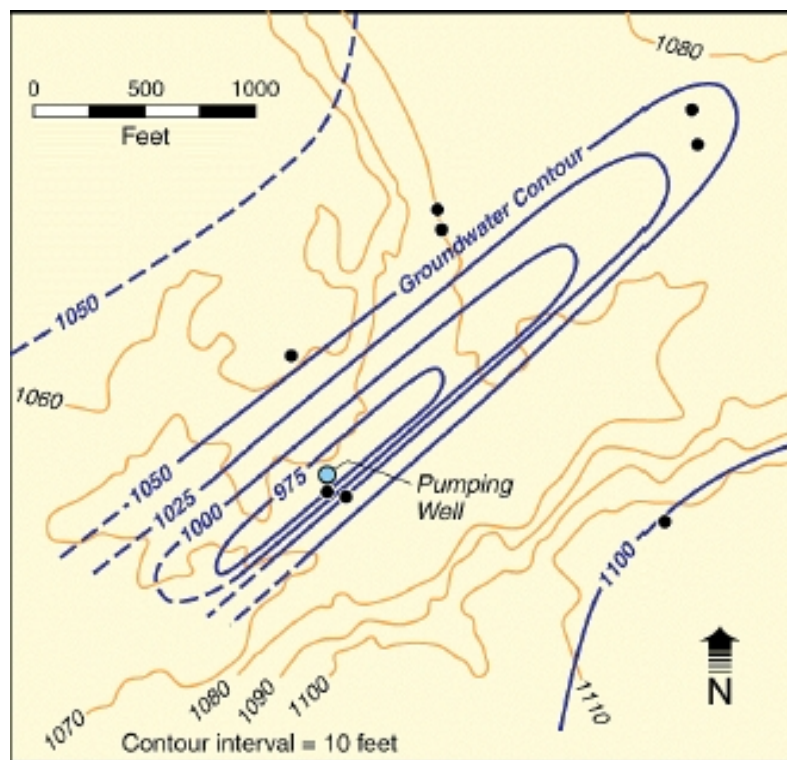


Figure 2. Typical groundwater contours for an aquifer test in fractured rock (Cook 2003)

Geophysical techniques (resistivity and self-potential) have been used previously to delineate groundwater flow paths under pumped conditions. These techniques can also be used to estimate the extent of elliptical zones of influence.

Variations in the zones will be dependent on:

- Location within regional structure (i.e. hinge vs. limb)
- Lithology – control on fracture spacing and aperture
- Extraction rate.

INTRODUCTION

Analysis of data provided from detailed mapping and geophysical surveys would indicate any correlations between these parameters.

The Department of Water, Land and Biodiversity Conservation (DWLBC) has completed several investigations throughout the WMLR in order to provide technical advice for the impending Water Allocation Plans.

This program (Program 2) will be incorporated into a wider project that will result in an increased understanding of groundwater flow mechanisms and surface water – groundwater interactions at local and regional scales. As a result, improved management strategies for fractured rock environments will be implemented. The techniques used and outcomes obtained from this project will also contribute significantly to water resource management strategies at national levels.

2. HYDROGEOLOGY

2.1 GEOLOGY

The geology of the study area across the TRC, ORC and LPRC varies from the Proterozoic Barossa Complex and Adelaidean sequences to the Cambrian Kanmantoo Group (Fig. 3).

The Proterozoic Barossa Complex dominates the northern corner of the TRC, with minor outcrops in the ORC, and forms the basement to the Adelaidean and Cambrian sequences of the Adelaide Geosyncline. Outcrops occur as inliers, thought to represent anticlinal cores, typically with faulted contacts with the overlying Adelaidean sequences. These originally high-grade metamorphic rocks underwent retrograde metamorphism to greenschist facies during the Cambro-Ordovician Delamarian Orogeny (Preiss, 1987).

The remaining geology encompasses a significant proportion of the stratigraphic sequence associated with the Adelaide Geosyncline. Outcropping stratigraphic sequences of the Neoproterozoic Burra Group (Emeroo Subgroup, Mundallio Subgroup, Stonyfell Quartzite, Saddleworth Formation and Belair Subgroup), Umberatana Group and Wilpena Group occur in both catchments, as well as the Cambrian Kanmantoo Group. Deformation associated with the Delamarian Orogeny has resulted in north-south trending, south plunging folds and complex faulting.

2.1.1 HYDROGEOLOGY

Groundwater in the TRC, ORC and LPRC exists primarily in fractured rock aquifers within the sedimentary and metasedimentary rocks of the Neoproterozoic Adelaidean sequence. In the northern part of the TRC, around Kersbrook, and in a small area of the ORC, significant FRAs exist in the metamorphic rocks of the Proterozoic Barossa Complex. In the eastern extremes of both catchments, groundwater resides in the sedimentary and metamorphic rocks of the Cambrian Kanmantoo Group. To the west of the Eden-Burnside Fault, the FRA systems of the upper catchment discharge into the sedimentary aquifers of the Adelaide Plains.

Recharge to both these aquifers occurs from rainfall, which percolates down to the watertable through the soil profile.

2.1.2 CLIMATE

The study area across the TRC, ORC and LPRC experience cool wet winters and typically hot dry summers. Annual average rainfall in the TRC ranges from 500 mm^y⁻¹ to 1000 mm^y⁻¹, with the higher rainfall in the southern part of the catchment, in areas of higher elevation close to Mt Lofty. Rainfall is significantly less in the topographically lower, western reaches of the TRC where the annual average is less than 600 mm^y⁻¹. The long-term average annual rainfall in the upper part of the TRC, measured at the townships of Gumeracha, Kersbrook and Birdwood is 799, 739 and 723 mm^y⁻¹ respectively. Rainfall is winter dominant, falling between the months of April and October.

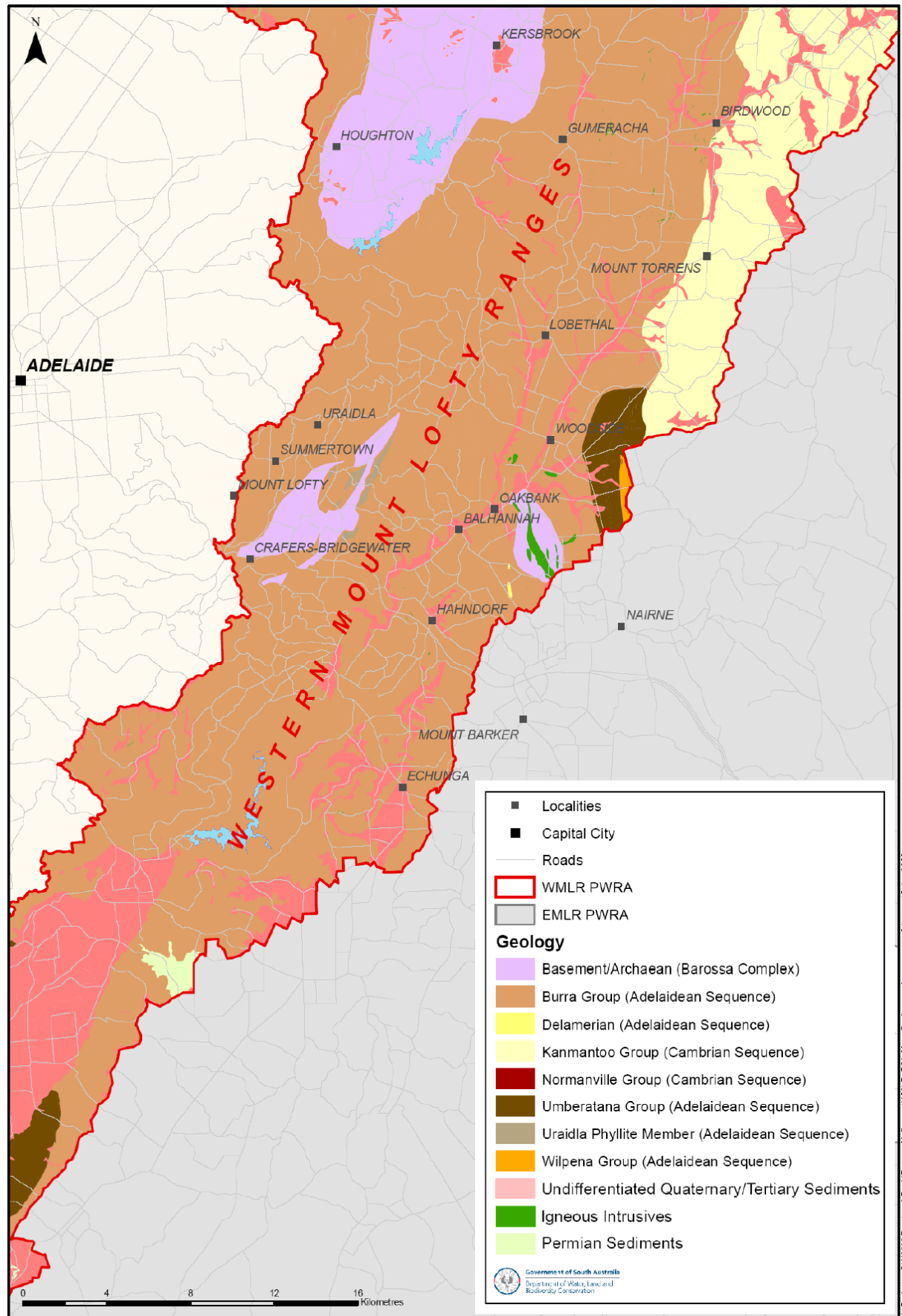


Figure 3. Geology of the Western Mount Lofty Ranges

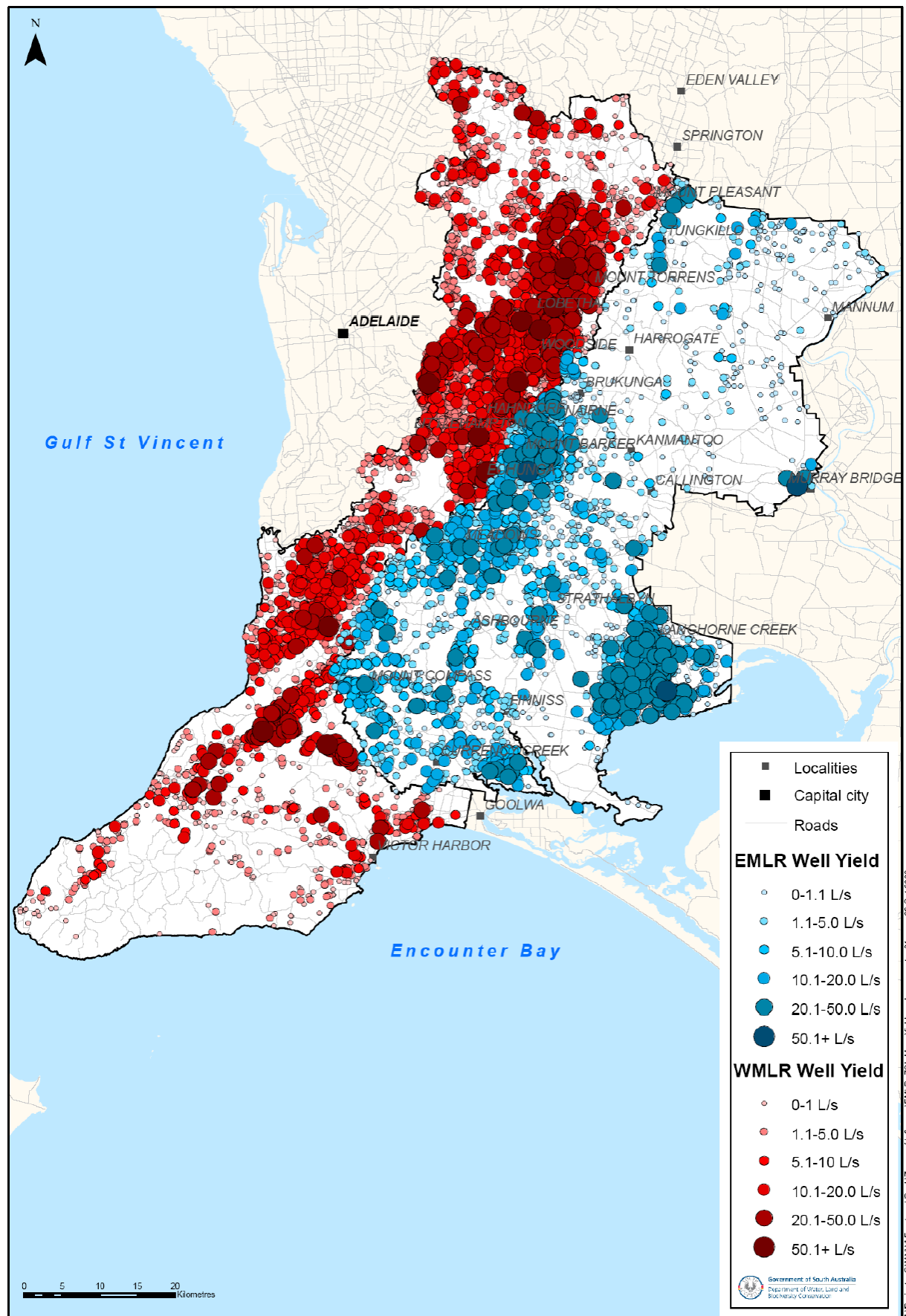


Figure 4. Well yield in the Mount Lofty Ranges, South Australia

The majority of the ORC has an average annual rainfall of 800 mm y^{-1} to 900 mm y^{-1} , except for a section to the northwest of the catchment, toward Mt Lofty, in which the annual average is up to 1200 mm y^{-1} . Rainfall is winter dominant, falling between the months of April and October. The long-term average annual rainfall in the upper part of the ORC, measured at the townships of Lobethal, Bridgewater and Echunga is 886, 1042 and 807 mm y^{-1} respectively.

2.1.3 FRACTURED ROCK AQUIFERS

In fractured rock systems, groundwater fills voids formed by fractures, fissures, faults and joint planes, which are invariably unevenly distributed within the rock formation. Due to their nature they present unique problems in their investigation, evaluation and management, largely because of their heterogeneous nature, and the dependence of aquifer properties on fracture distribution, connectivity and extent.

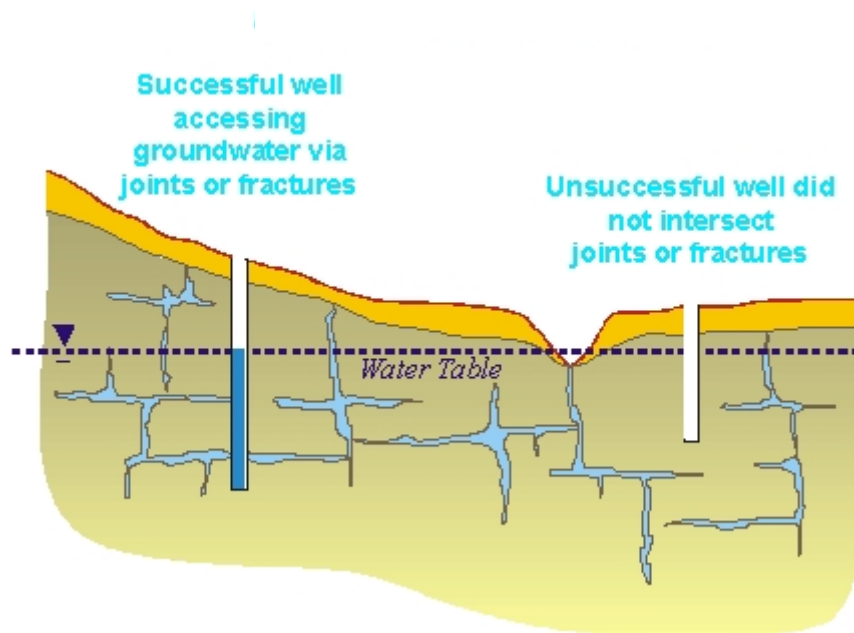


Figure 5. Groundwater wells in a fractured rock environment

FRAs are characterised by high spatial variability in hydraulic conductivity, making traditional hydraulic methods for estimating groundwater flow difficult to apply. Despite the importance of fractured rock aquifers, there is a lack of available knowledge of groundwater processes within these systems, and hence, there is a great need to develop techniques to better characterize hydraulic properties.

3. METHODOLOGY

3.1 BACKGROUND THEORY

Due to the current lack of understanding, management practices for groundwater in fractured rock environments adopt a precautionary approach. The approach currently used is similar to that of traditional sedimentary aquifers.

Water extraction from any well will form an associated cone of depression around the well (Fig. 6). This cone of depression will map out a circle (or zone of influence) on the surface and any neighbouring well that is constructed within this zone will have its water level affected by the extraction. This is called well interference.

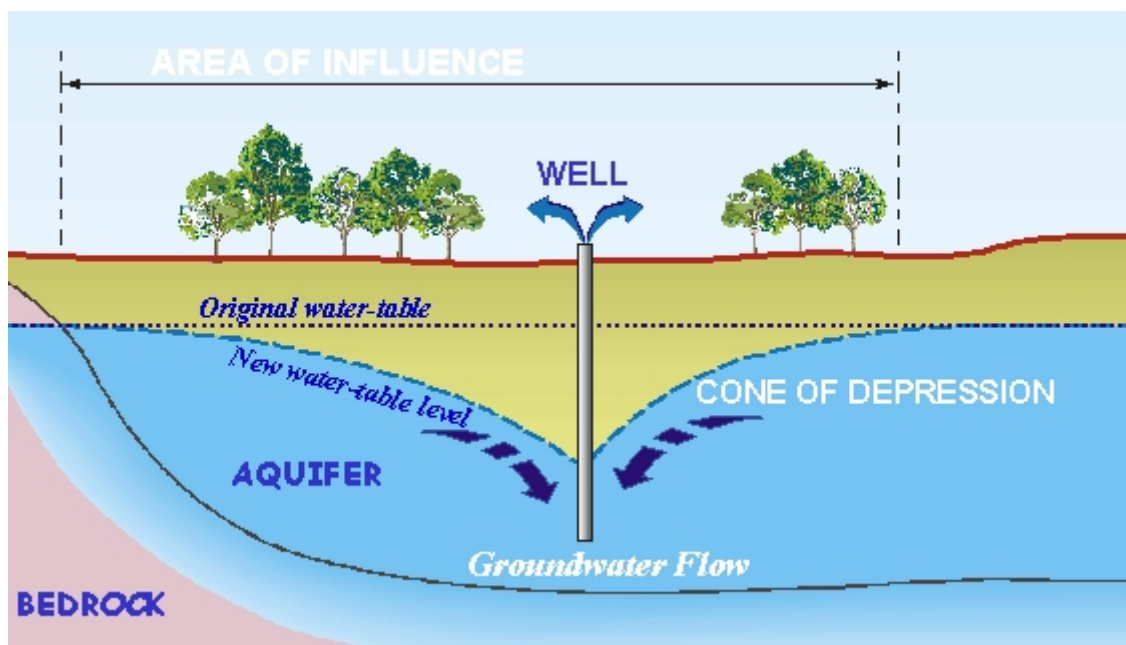


Figure 6. Illustration of a well and its area of influence

At present, management of well interference in fractured rock environments has commonly utilised these circular zones of influence typically associated with sedimentary aquifers. However due to the heterogeneous nature of fractured rock aquifers, the zones of influence are more likely to be elliptical and controlled by regional fracture systems. Improving correlations between geology and the spatial extent and distribution of zones of influence would potentially provide a more accurate and predictive management tool than is currently available and could in theory be applied anywhere in a fractured rock environment.

As discussed in the previous section (illustrated by Fig. 2), groundwater flow in a fractured rock environment is influenced by the fracture network. The geometry of the fractures results in a hydraulic anisotropy such that groundwater extraction produces a drawdown cone that is not radially uniform.

The preferential strike orientation of fracture sets cause the rock to be both electrically and hydraulically anisotropic, and the variation in the size and opening of fractures causes additional heterogeneity. Groundwater will tend to flow along these preferential flow paths at

rates that may be several orders of magnitude greater than in directions perpendicular to it. Therefore the zone of influence is no longer circular but rather elliptical in shape.

To quantify fractured aquifer properties, a relationship must be found between fluid transport and some other measurable property, such as electrical resistivity (Freeze and Cherry 1979; Brown 1989; Sahimi 1995). The electrical resistivity of rocks depends on several factors including the presence of conductive minerals such as base metal sulphides or oxides and graphite in the rock. Most rocks without these minerals are usually poor conductors and their resistivity is governed primarily by their porosity, degree of fracturing, salinity of pore water and the degree of saturation of the pore spaces (Cook et al. 2001).

As fractures act as conduits for flow of both groundwater and electrical charge, methods that can efficiently detect the distribution of electrical pathways may be used to infer characteristics of significant hydrological parameters (Brown 1989). Geophysical methods used to detect the electrical conductivity are typically fast, repeatable, relatively low-cost and non-intrusive, thus making them a practical alternative to traditional approaches (Skinner and Heinson 2004).

Electrical methods have been used to successfully monitor groundwater occurrence within fractured rock and have provided information on fluid electrical conductivity, fracture orientation and the overall bulk porosity (Dailey et al. 1992; Slater et al. 1996; Skinner and Heinson 2004; Adepelumi et al. 2006; Batayneh 2006; Weiss et al. 2006). Fracture characterisation and understanding fluid flow in fractured environments is not only crucial to monitoring groundwater resources in FRAs but has also been used for:

- Geothermal applications (Robinson and Tester 1984; Fehler 1989; Block et al. 1994)
- Hazardous waste disposal (Davies et al. 1991; Robinson et al. 1993)
- Predicting the movement of contaminants (Nicholas and Healy 1988; Shapiro and Hsieh 1991; Benson et al. 1997)
- Mapping of conductive plumes (Nimmer et al. 2007).

An alternative geophysical approach that is often more closely coupled to the groundwater flow field is to measure the electrical potential occurring naturally on the ground surface, known as the self-potential (SP). The main sources of SP are diffusive charge separation due to difference in mobility between ions in solution, electrical energy produced from redox reactions around ore bodies and buried metallic objects and charge separation as a result of fluid flow (Sato and Mooney 1960; Sill 1983; Revil et al. 1999; Wishart et al. 2006). This latter electrokinetic process involves the movement of water through porous or fractured rock media which generates an electric potential gradient, sometimes known as streaming potential (Revil et al. 1999; Fagerlund and Heinson 2003; Sheffer and Oldenburg 2007). SP has the advantage that it is minimally intrusive and that the hydrological system is not perturbed by the presence of the boreholes, as is the case for borehole-to-surface electrical methods. The method is also very cheap as it requires only simple apparatus that is quick to deploy.

Streaming potentials have been used in many applications including earthquake prediction (Jouniaux and Pozzi 1995), geothermal exploration (Corwin and Hoover 1979; Sill 1983; Ishido and Pritchett 1999) and hydrogeological investigations (Fagerlund and Heinson 2003; Rizzo et al. 2004; Wishart et al. 2006). In addition, Wishart et al. (2006) demonstrated the potential benefits of combining the self potential method with resistivity surveys to improve characterization of hydraulically-conductive fractures in tight rocks.

This program reports on the capabilities of direct current (DC) borehole-to-surface and SP techniques for the interpretation of hydrogeological processes and, in particular, to delineate groundwater flow paths under pumped conditions in fractured rock aquifers.

3.2 GEOPHYSICAL TECHNIQUES

3.2.1 BOREHOLE-TO-SURFACE DC RESISTIVITY METHOD

For most surface characterisation techniques, overburden introduces difficulties because of its attenuation properties and the high contrast in its properties compared to the underlying rock. Methods that place a source and/or receiver in a borehole and in direct contact with groundwater can reduce these limitations. These can however be more costly than comparable surface surveys due to higher drilling and measurement costs (Karasaki et al. 2000).

Geophysical borehole methods are used in several approaches including electrical (Dailey et al. 1992; Slater et al. 1996; Johnson et al. 2002), radar (Stevens et al. 1995) and seismic (Majer et al. 1997).

The borehole-to-surface DC (direct current) resistivity technique involves placing a current source electrode down a borehole below the watertable and completing the circuit with a current sink electrode at a distance far enough away to be considered infinity (Skinner and Heinson 2004). In practise this current sink should be a minimum of 200 m away.

Current from the down-hole point source electrode will flow radially away from the electrode within a homogenous, isotropic medium. Equipotential surfaces (surfaces of equal voltage) are spherically symmetrical around the current electrode and decrease with distance away from the current source. When the medium is heterogeneous and anisotropic, electrically conductive fractures in the vicinity of the current source will distort the potential field.

Deviations from the spherical equipotential surfaces can be measured between a reference electrode and potential electrodes on the surface. The distortion of the field around electrically conductive features produces a phenomenon known as the *paradox of resistivity anisotropy*. Measured maximum observed apparent resistivity (ρ_a) is parallel to the principal direction of fracture strike and the maximum true resistivity (ρ) is perpendicular to the principal direction of fracture strike (Taylor and Flemming 1988). This counterintuitive occurrence is a result of using current magnitude in the calculation of apparent resistivity, while the actual potential differences are determined by the current density (Keller and Frischknecht 1966).

Thus the measured electrical anisotropy can indicate the preferential direction of hydraulically conductive fractures and the degree of connectivity between the source and receiver electrode (Fig. 7).

This can then be used to determine porosity as a function of angle away from the hole through an empirical relationship that relates bulk resistivity to pore fluid resistivity and porosity at low frequencies established by Archie (1942):

$$\frac{\rho_r}{\rho_w} = F = \alpha \phi^{-n} \quad \text{Equation (1)}$$

where ρ_r is the bulk resistivity of the rock, ρ_w is the pore fluid resistivity, F is the formation factor, ϕ is the porosity, n is the cementation factor and α is a dimensionless parameter.

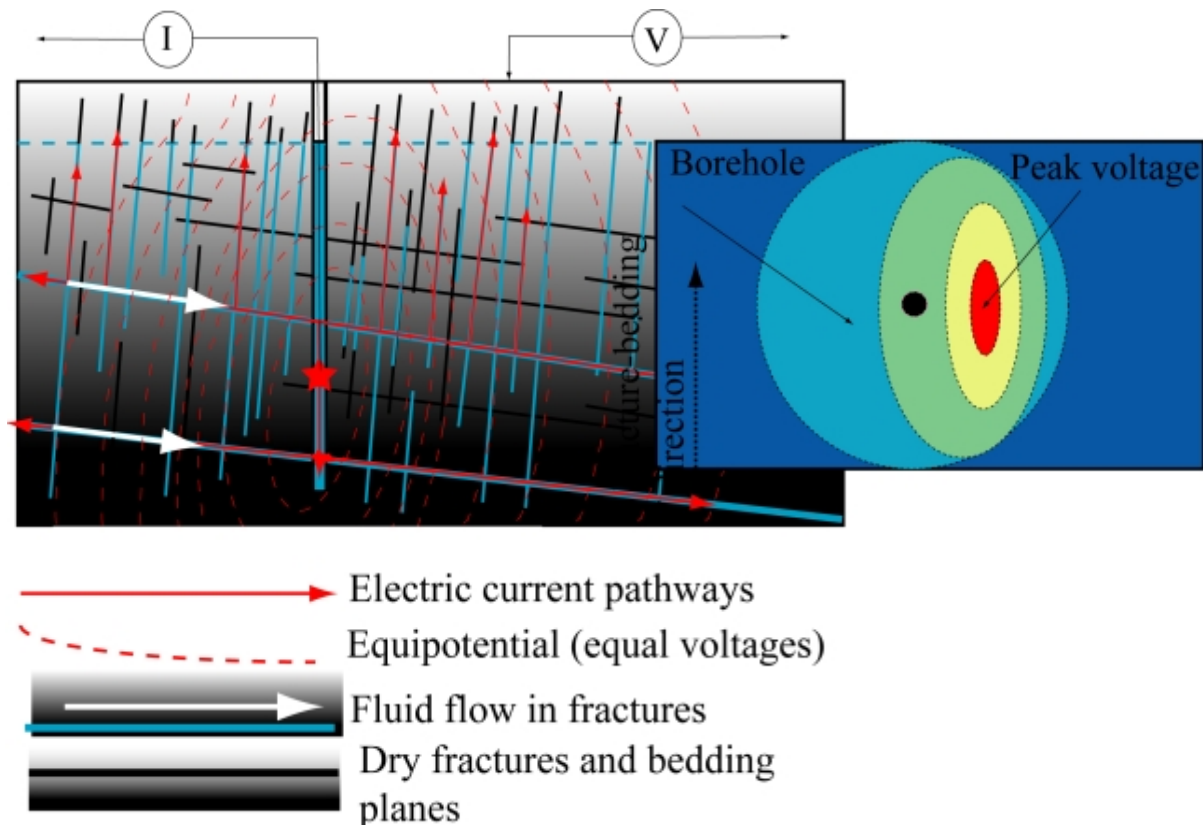


Figure 7. Schematic of DC resistivity survey and output surface potential map

This technique is more sensitive to vertical structures and cannot detect the presence of horizontal fractures (Watson and Barker 1999). Therefore, lower-angle fractures are likely to produce more isotropic responses, as electrical connection with the surface is not as pronounced. Although there must be horizontal fractures to feed the borehole, there is vertical control of the near-surface recharge.

3.2.2 SELF-POTENTIAL METHOD

The self-potential (SP) method is a simple electrical technique that requires no source and involves measuring the natural electrokinetic potentials, or streaming potentials, in the earth. Streaming potentials arise due to a naturally-occurring diffusion electrical potential, often known as the zeta potential (ζ -potential), across boundaries between a fluid electrolyte and mineral grains in fractured rock and porous media (Sato and Mooney 1960).

Consider a system consisting of two separate phases such as liquid and a solid medium, in which the phases must be electrically neutral. Thus, the net charge within the liquid medium and the charge on the surface of the solid medium have to be equal in magnitude and of opposite signs (Fagerlund and Heinson 2003). At the interface of the two phases there is an aggregation of excess charge on each side, which establishes an electrical double layer (Fig. 8). When the fluid moves relative to the solid medium, the mobile part of the electrical double layer is dragged along with the flow creating the transport of electric charge with the flow. The amount of charge transported is directly related to the potential on the slipping plane, the ζ -potential, with the magnitude equalling the potential change in the mobile phase. The more negative the ζ -potential the more positive ions are transported with the flow and thus the greater the net transport of negative charge ions (Fagerlund and Heinson 2003).

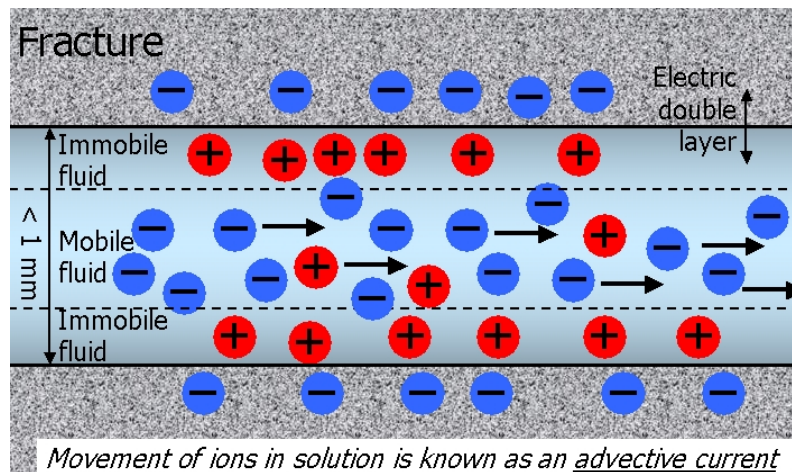


Figure 8. Within the fluid that resides in the fracture there are ions. The movement of these ions sets up what is called advective current

The ζ -potential is shown to increase with increasing temperature and pH and to decrease with increasing salinity (Gustafsson et al. 2000; Saka 2006). Consider particles in suspension with a negative ζ -potential. If more alkali is added to the suspension then particles tend to acquire more negative charge. However, if more acid is added to this suspension then a point will be reached where the charge will be neutralised and eventually build up to a positive charge. Thus, in general, ζ -potentials will be positive at a low pH and slightly positive or negative at a high pH (Gustafsson et al. 2000; Saka 2006).

RESULTS

4.1 ELECTRICAL RESISTIVITY

Borehole-to-surface DC resistivity surveys were conducted at 18 available sites in the WMLR (Fig. 9). Within these sites, which were determined by lithology, a well was selected based upon its location, construction, depth and ideally was unequipped for access to the open well (Table 1). Note that the geological unit noted in Table 1 features the contributing unit only. Refer to Appendix B for a more detail on the unit and structural description.

At each site the source current electrode was located either down hole, placed at the surface or connected to the metal borehole casing. The location of the source electrode was variable but, ideally, was set at depths below weathered surface material in an open hole and below the watertable. However, this was not possible at some sites due to the well being equipped and sealed off completely at the surface. In the case that access to the well was not possible, the current electrode was then attached to the metal casing to ensure the borehole was energised to the depth of the casing and below the watertable.

Table 1. Wells selected for survey in the Western Mount Lofty Ranges

Site	Unit Number	Easting	Northing	Depth (m)	Date of DTW	DTW (m)	Date of Yield	Yield (L/s)	Date of TDS	TDS (mg/L)	Geological Unit
1	-	-	-	-	-	-	-	-	-	-	-
2	6628-5502	296757	6142124	76.2	Apr-74	6	Apr-76	2.5	Aug-08	1804	Lb
3	6628-6109	294289	6140602	152	Apr-08	10.0	May-78	2.25	Apr-08	567	Nmc
4	-	-	-	-	-	-	-	-	-	-	-
5	6628-11979	308093	6145325	104	Aug-08	15.9	Mar-82	4.5	Feb-02	517	Ndw
6	6628-4602	309335	6149412	71	Aug-08	16.2	Apr-03	2	Aug-08	1086	Ndw
7	6628-11780	314557	6142934	118	Apr-08	12.4	May-81	2.75	Apr-08	4465	Eeb
8	6628-10781	313518	6137833	41	Apr-08	8.8	Jan-74	7.6	Apr-08	4816	Eec
9	6628-12605	300105	6133223	123.4	Jun-08	12.5	Oct-83	6.25	Oct-83	871	Ndw
10	6628-22603	304342	6132176	91	Apr-08	50 +	Jun-06	2.5	Apr-08	887	Ndt
11	6628-9333	305658	6129771	40	-	-	Oct-78	6.37	Oct-78	462	Nds
12	6628-14068	308696	6133979	110	Dec-87	3	Dec-87	30	Dec-87	2432	Nds
13	6628-10214	309402	6135199	56.8	Jun-08	10.6	Nov-78	6.37	Nov-78	728	Nds
14	6628-6576	291850	6127138	82.32	Jun-08	5.6	Apr-78	2.29	Jun-08	169	Ndw
15	-	-	-	-	-	-	-	-	-	-	-
16	6628-6835	292900	6126978	59.13	Jun-08	10.0	Apr-78	9.55	Apr-94	184	No
17	6628-6739	292202	6128388	83.76	-	-	Mar-78	5.28	Mar-78	309	No
18	6628-10954	293922	6129276	66.5	Jun-08	17.1	Aug-79	1.25	Aug-79	132	No
19	6628-21741	293816	6128280	140	Jun-08	28.1	Apr-04	5	Jun-08	550	No
20	6628-6854	293356	6126442	129	Jun-08	4.2	Oct-82	11.4	Mar-01	510	Lb
21	6627-2721	292311	6121051	50	Apr-77	12.5	Apr-77	1.63	Aug-08	180	No

Eeb – Backstairs Passage Formation

Eec – Carrickalinga Head Formation

Lb – Barossa Complex

Nds – Saddleworth Formation

Ndt – Stonyfell Quartzite

Ndw – Woolshed Flat Formation

Nmc – Castambul Formation

No – Emeroo Subgroup

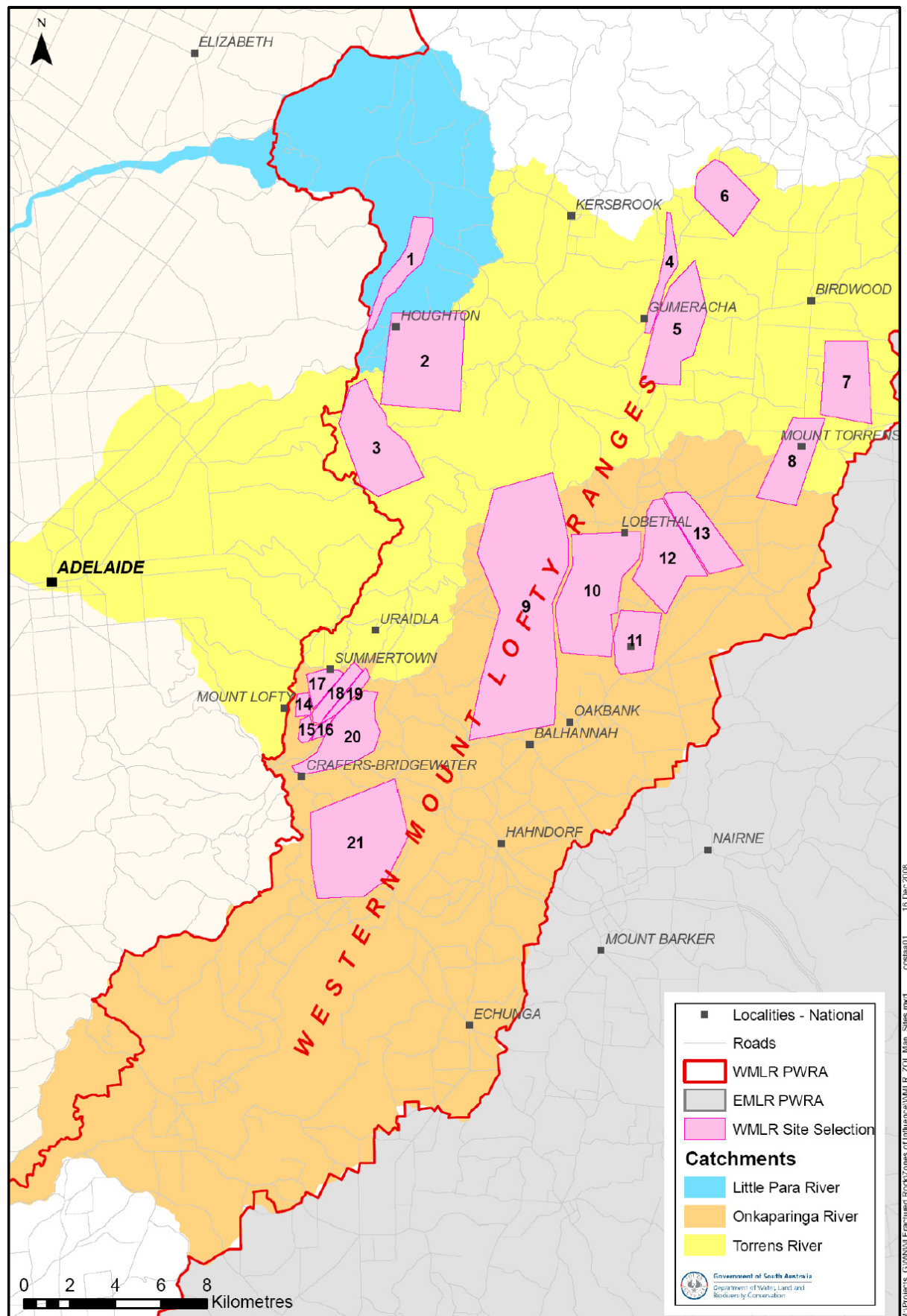


Figure 9. Map of 21 sites located in the Western Mount Lofty Ranges

RESULTS

The electric circuit was completed with a return current electrode located at a distance far enough to be considered at infinity (typically >200 m). Surface electrical potential measurements were made in reference to an electrode at a distance at which the potential is defined to be zero from the borehole (typically >100 m, but in the opposite direction to the return current electrode).

An array of 72 surface electrodes were located radially from the borehole at 5 m intervals, with six electrodes on each line between 5 and 30 m, along 12 lines at 30° angular increments (Fig. 10). However, in some survey areas, obstacles either prevented the placement of certain surface electrodes or caused shifts in the angular increments of the lines. Contoured surface maps were then produced showing the electrical potential measured, normalised by the input current (sometimes called the transverse resistance; Skinner and Heinson 2004). It is possible to convert the transverse resistance to apparent resistivity from equation 2, assuming a point current source.

$$\rho_a = 2\pi r \left(\frac{V}{I} \right) \quad \text{Equation (2)}$$

Where ρ_a is the apparent resistivity measured in the field, r is the distance from the borehole and (V/I) is the transverse resistance. This is useful in determining the background resistivity (that is, the overall resistivity of the regolith–bedrock–fluid system), however, interpreting apparent resistivity in terms of fluid pathways is more complex due to the paradox of anisotropy.

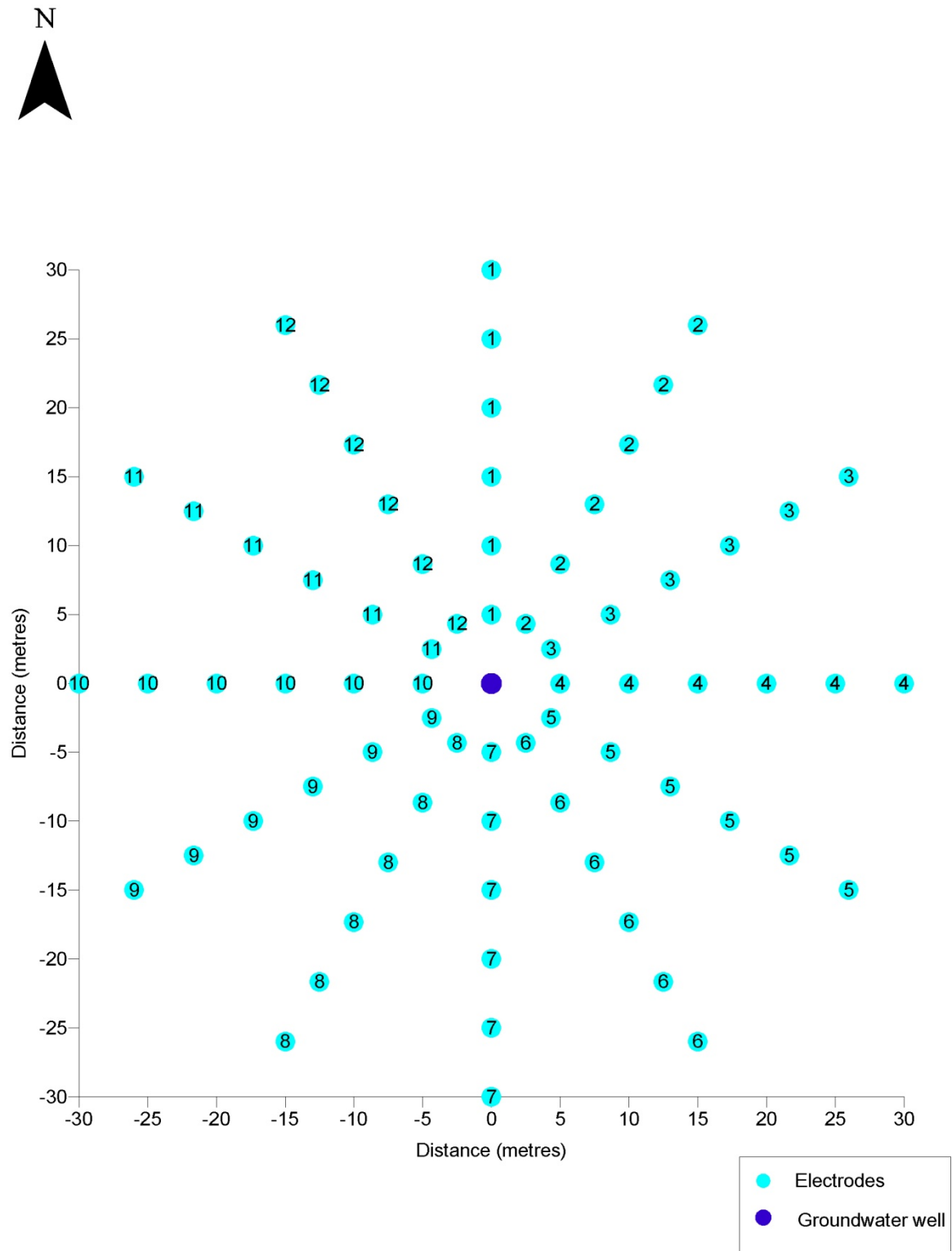


Figure 10. Borehole-to-surface DC resistivity surface setup arrangement

Average apparent resistivity over the 12 lines was calculated for a distance of 25 m away from the borehole. It was then related to bulk porosity using Archie's Law, assuming $n = 2$ and $\alpha = 1$, for surveys where the electrical conductivity of the water was known (equation 3).

RESULTS

$$\phi = \sqrt{\frac{\rho_w}{\rho_a}} \quad \text{Equation (3)}$$

Where ϕ is the bulk porosity, ρ_w is the pore fluid resistivity and ρ_a is the bulk apparent resistivity.

A 25 m radius was chosen because (a) errors in location of the current and voltage electrodes are less important than for those closer to the borehole, and (b) the approximation of a line source is better.

Simple graphs comparing the apparent resistivity of electrodes at a certain distance away from the borehole as a function of the bearing were then produced to aid in interpretation of strike on conductive fractures. Firstly, by highlighting the bearings where the peaks of apparent resistivity occur, strike can be inferred in much the same way as from surface maps (Skinner and Heinson 2004). Secondly, the nature of the asymmetry may provide more information about conductive fractures. If the graph is symmetrical then it is inferred that there is one major orientation for the conductive fractures (Fig. 11a). However if the graph is asymmetrical, it may indicate a second conductive zone (Fig. 11b). The ratio of maximum to minimum apparent resistivity for a 25 m radius was made to show the relative conductivity of different zones.

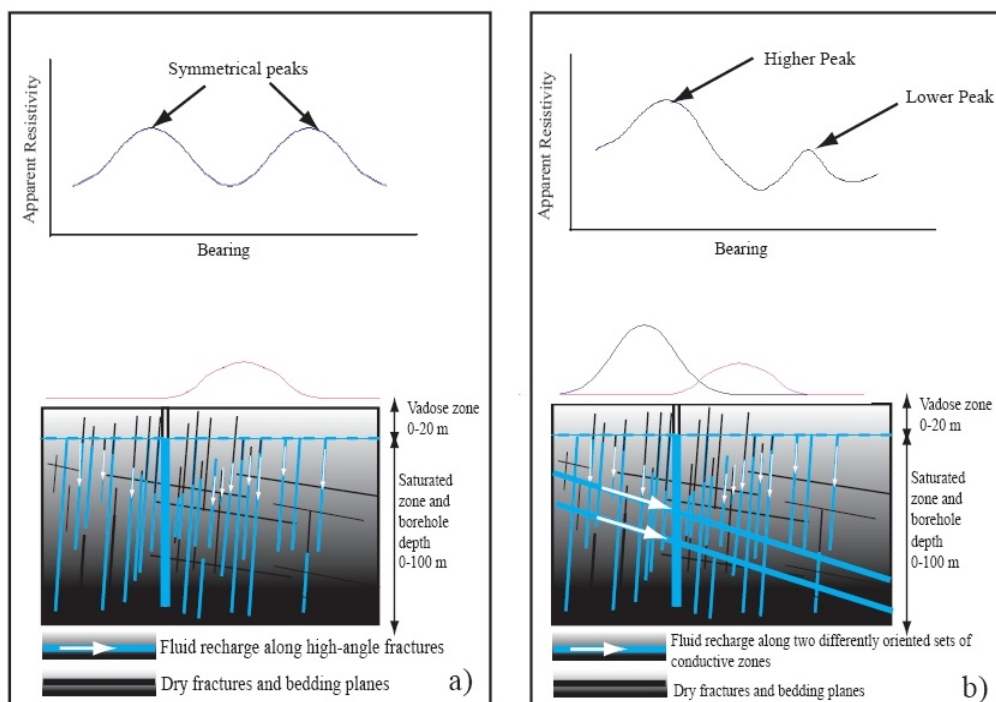


Figure 11. Apparent resistivity of electrodes at 25 m away from the well as a function of bearing. (a) If the graph is symmetrical then it is inferred that there is one major orientation for the conductive fractures. If conductive structures are approximately vertical there is symmetry observed around the borehole. (b) If the graph is asymmetrical, there may be a second differently orientated fracture set. The dip of structures gives rise to anisotropy of the response and will be biased to the upside fracture sets.

The strike of the most conductive feature at each site was primarily inferred from the orientation of the maximum axis of the equipotential ellipse of the surface maps (Skinner and Heinson 2004). Surface maps of normalised potential – measured potential (V) divided by

RESULTS

the current (I) – were more complex to interpret and, in conjunction with the graphs of apparent resistivity, were used as supporting information. In particular, apparent resistivity was often unexpectedly lower around boreholes; perhaps an artefact produced by assuming a point source of current when in reality the source is more complex by virtue of the connection to the casing. Zones of high electric potential (normalised by the input current) were interpreted as having good electrical connection with the borehole, indicating the location of fractures and/or bedding planes in the orientation of the zone.

Figure 13 shows the borehole-to-surface DC resistivity results for Site 5. The results are plotted as a normalised potential (V/I) distribution contour map. The dip and strike of the most conductive elements at this site were inferred from the data. Dip values were calculated by measuring the distance of lateral offset of the maximum transfer resistance value from its expected location (directly above the current electrode). The strike was determined from the orientation of the maximum axis of the equipotential ellipse. In this case, the centre of the highest potentials were offset indicating a dipping structure to the south west while the strike was determined to be in a north-west direction.

Sites were classified in terms of the degree of heterogeneity, electrical resistivity and dominant fracture orientation (Table 2). Due to the large variations in absolute potential, the same colour contour interval was not applied to each surface map otherwise many features would be masked. However, comparisons between sites could be made by classifying each site in terms of high (>1 V/I), medium (0.1 – 1 V/I) and low (<0.1 V/I) normalised potential (Table 2).

Results for each of the parameters were highly variable, ranging from 3–210 Ωm for the bulk apparent resistivity, 35–60% for bulk porosity and 1 to 2.5 for the ratio of maximum to minimum apparent resistivity.

The calculated range for bulk porosity is consistent with what one would expect for a bulk porosity in a fractured rock environment. It should be noted that porosity values for four sites were outside this range (sites 14, 16, 17, 18) and are considered not representative. Archie's Law (Equation 1) is quite sensitive to the salinity. It is possible that the values used for salinity are not representative of these sites, particularly since salinity values for sites 16, 17 and 18 could not be measured in the field and were historic readings taken from the State database (SAGEodata).

As expected there is clearly an inverse correlation between apparent resistivity and water salinity, as sites with lower apparent resistivity tend to have higher salinity (Fig. 12).

Variations in magnitude of electrical potential measurement are indicative of different porosities and saturations. In general, larger potential at all electrodes indicate that the ground has lower electrical resistivity and hence more groundwater.

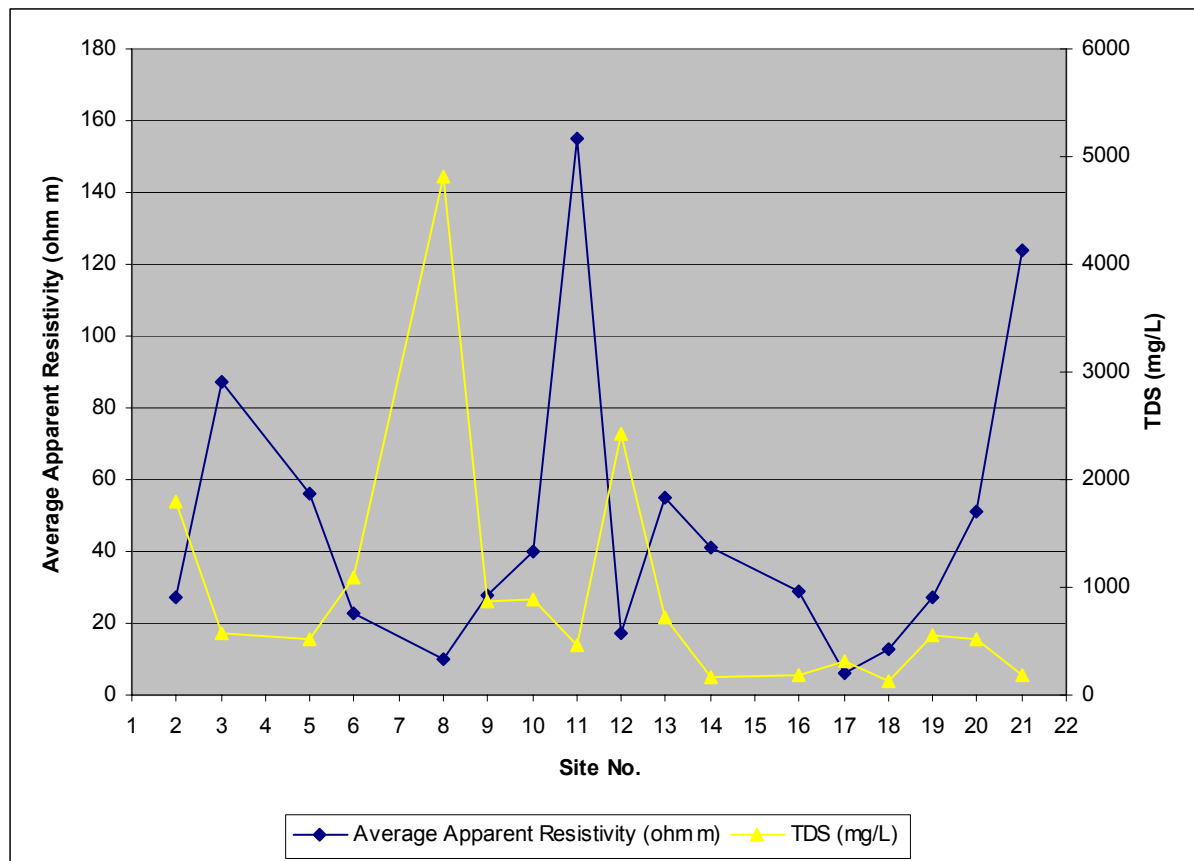


Figure 12. Average apparent resistivity (Ωm) for sites with available data vs salinity (TDS)

It is implied that there is an overall dipping conductive structure if the maximum normalised potential was offset from above the borehole (Skinner and Heinson 2004). The direction of dip of the conducting structures could be inferred at some sites as being at right angles to the strike and towards the more resistive structures. As mentioned above, dip values were calculated by measuring the distance of lateral offset of the maximum transverse resistance value from its expected location (directly above the current electrode).

Borehole-to-surface potential maps were completed for all 18 sites and are presented in Appendix A. Surface maps for some surveys showed very little anisotropy, with the normalised potential essentially showing a concentric pattern around the borehole. Slight anisotropy around the borehole may be due to errors in positioning of the electrodes. Any errors in positioning will affect the electrodes closer to the borehole much more than those further out.

Figure 13 shows the borehole-to-surface potential contour map for Site 5 and the associated derivation of strike and dip direction (Table 2). In this case Site 5 exhibits a north-western strike direction with a dip direction to the south-west.

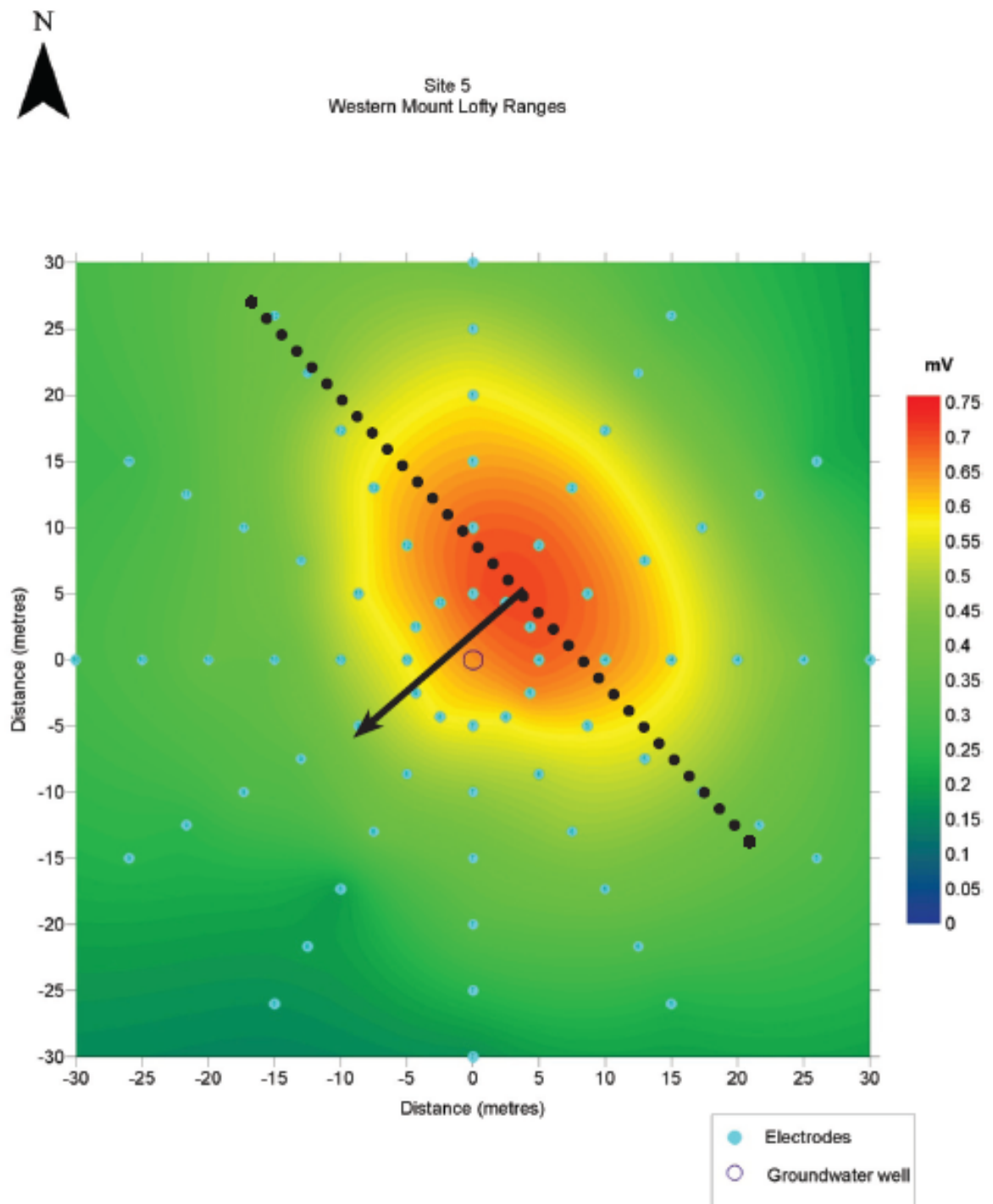


Figure 13. Normalised potential contour map from Site 5, dashed line denotes strike orientation, solid line with arrow denotes a direction of dip

The majority of sites surveyed exhibited some anisotropy and showed dominant conductive zones with north-east and north-west strikes. These are consistent with the overall north-east to south-west structural trend in the area.

RESULTS

Table 2. Summary of electrical data interpretations for 18 selected sites in the Western Mount Lofty Ranges

Site	Unit Number	Anisotropy (Yes/No)	Strike	Dip	Magnitude (V/I)	Symmetry (Yes/No)	Porosity (%)	Geophysical Anisotropic Ratio
1	-	-	-	-	-	-	-	-
2	6628-5502	Y	NW	SW	Med	N	35	1.5
3	6628-6109	Y (low)	NNW	-	High	Y	35	1.3
4	-	-	-	-	-	-	-	-
5	6628-11979	Y	NW	SW	Med	N	45	1.5
6	6628-4602	Y	ukn (NE*)	SE	Med	N	45	2.5
7	6628-11780	-	-	-	-	-	-	-
8	6628-10781	Y	N	E	Med	N	35	1.5
9	6628-12605	ukn	ukn (NE/SW*)	SE	Med	N	50	ukn
10	6628-22603	ukn	ukn (N/S*)	E	Med	N	35	ukn
11	6628-9333	Y	NW	-	High	Y	30	1.5
12	6628-14068	Y	NE	SE	Med	N	35	2.0
13	6628-10214	Y	NE	SE	Med	N	35	1.5
14	6628-6576	Y	NNE	-	High	Y	90	1.5
15	-	-	-	-	-	-	-	-
16	6628-6835	Y (low)	NNE	ESE	Med	N	100 +	1.2
17	6628-6739	Y	WNW	-	Med	Y	100 +	2.0
18	6628-10954	Y	NE	-	Med	Y	100 +	1.5
19	6628-21741	Y	NNW	ENE	Med	N	60	2.0
20	6628-6854	Y	NW	-	Med	Y	45	1.5
21	6627-2721	Y	NE	-	High	N	50	1.5

N (strike/dip) – north

E (strike/dip) – east

S (strike/dip) – south

W (strike/dip) – west

Med – medium

ukn – unknown (not enough data)

* Dip direction implies orthogonal strike direction

Note: Porosity values for sites 14, 16-19 are unrealistic, resulting from inaccurate groundwater salinity used in calculation

A collective map with the fracture strike and dip for each of the eighteen sites demonstrates a high degree of correlation between fracture orientation and regional structural trends (Fig. 14).

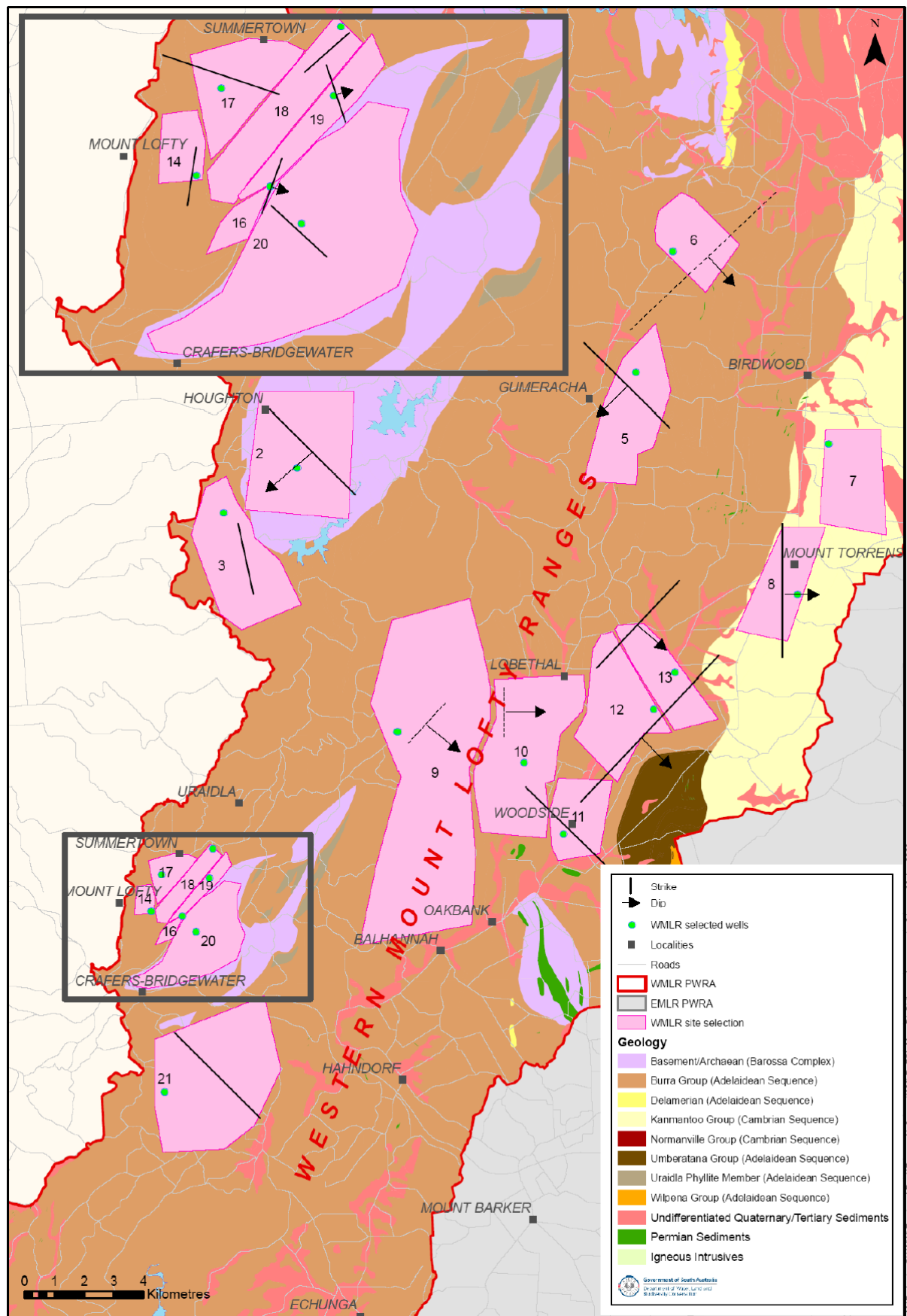


Figure 14. Map of fracture strike and dip for each of the 18 available sites in the Western Mount Lofty Ranges

4.2 SELF-POTENTIAL (SP) METHODS

SP surveys were carried out at a number of sites in the WMLR. However as discussed in an earlier DWLBC report 'Hydrogeophysical mapping of fracture orientation and groundwater flow in the Eastern Mount Lofty Ranges, South Australia' (Costar et al. 2008), the SP data requires further research and discussion into the technique. For this reason and that many of the sites selected in the WMLR were unsuitable for SP surveys, focus was shifted to the borehole-to-surface DC resistivity results. While the discussion of the SP survey is discussed here for the WMLR and was conducted in the same manner as that conducted in the Eastern Mount Lofty Ranges (EMLR), the following results are those from the EMLR study.

SP surveys were carried out using an array of 36 surface electrodes at each site. Each array consisted of 6 radial lines (60° separations), with 6 electrodes at 5 m intervals along each line between 5 and 30 m from array centre (Fig. 15). The electrodes were ordered and numbered from outermost through to innermost, such that Line 1 has electrodes 1–6, Line 2 has electrodes 7–12, etc. Potentials were measured every 5 seconds at each electrode relative to a distant reference electrode, located far enough away to be considered unaffected by pumping (typically >200 m).

SP measurements were recorded continuously from 5–10 minutes before the start of pumping, through the pumping cycle and also 5–10 minutes after pumping to measure recovery. It has been assumed that the measured SP values are stable before the start of pumping.

The electrodes measure a transient change in surface electrical potential surrounding the pumped well of up to 60 mV. Such changes occur over time-scales varying from a few seconds after turning the pump on, to a few tens of minutes when equilibrium flow is established.

In many cases wells were equipped with pumps, however, for those that were unequipped a pump was brought onto site.

Electrokinetic potential measurements are presented as a function of time away from borehole for all 36 electrodes, with the inset map showing the orientation of the electrodes relative to the borehole (Fig. 16). Four examples showing a range of outcomes are illustrated in Figures 16, 17, 18 and 19 with the red colours indicating high electrokinetic potentials, and the blues indicating low potentials. Most of the changes are seen over the first few minutes of pumping when, presumably, near-surface fractures are quickly drained and the electrokinetic sources are closest to the surface.

At Site 9 (Fig. 16) for each line the largest change in potential is observed for those electrodes closest to the borehole as expected, with the amount of change decreasing the further out the electrodes are from the borehole (e.g. electrode 6 shows large change in potential, electrode 1 shows little change in potential). There is almost no change observed for those electrodes 30 m away from the borehole, suggesting that little change would be seen for distances greater than this. Change in potential also decreases with magnitude after time, with no change after almost 5 minutes, indicating that only the shallow zones are being drained. The largest and longest duration potentials are seen in Line 3, approximately on a bearing of 120°, suggesting that groundwater flow is greatest in this direction and indicating fluid flow being dominant from the south-east. To the north, the fluid flow is presumably deeper, and produces smaller electrokinetic signals. The potential changes are of order of 4 mV over a time span of about 5 minutes. Several electrodes were off-scale,

RESULTS

such as electrodes 8 and 9 from the line 2, which were made noisy by the pump outflow passing by the metal electrodes.

A similar pattern is exhibited by the electrokinetic measurements at Site 10 (Fig. 17). There is a pronounced change in potential at this site, of opposite polarity, and of magnitude 4 mV. The largest and longest potential change is along Line 3 (bearing of 120°), similarly showing that the dominant flow direction appears to be from the south-east. The negative polarity could be attributed to more alkaline conditions compared to Site 9 (Gustafsson et al. 2000).

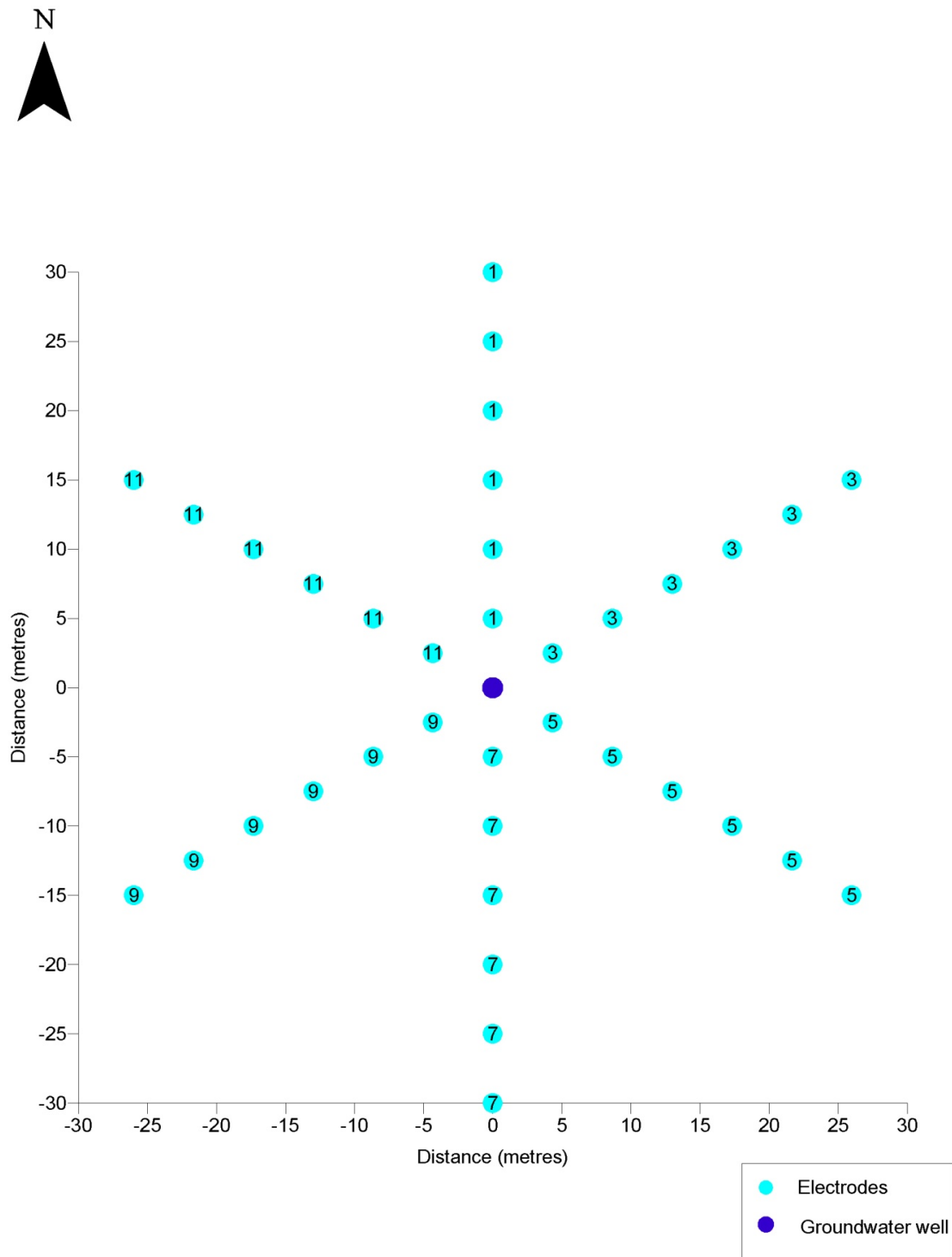


Figure 15. Self-potential surface setup arrangement

RESULTS

Electrokinetic potentials as a function of time for Site 7 are shown in Figure 18, with the inset map showing the orientation of the electrode lines 1–6 from north spaced 60°, 120°, 180°, 240° and 300°. The electrokinetic voltage change is much smaller than observed at Site 9, of order 0.3 mV, which is close to the ambient noise levels of the data logger. There is a small positive change at the start of the pump tests for less than 1 minute and Line 3 shows the largest voltage change, but the effect is marginal. These observed smaller voltages are interpreted as being due to much lower fluid flow rates at this site and the main hydraulic fractures are deeper and hence produce a smaller signal.

At Site 6 it is evident that lines south to north-west have largest polarity change, on the order of magnitude 60 mV (Fig. 19). This is substantially larger than many of the sites and is interpreted to be a much higher flow rate at this site, or that the main hydraulic fractures are quite shallow. In particular the largest and longest potential changes are seen for Lines 5 and 6 indicating direction of dominant flow appears to be from the north-west. Again, the opposite polarity may be due to pH variations between sites (Gustafsson et al. 2000).

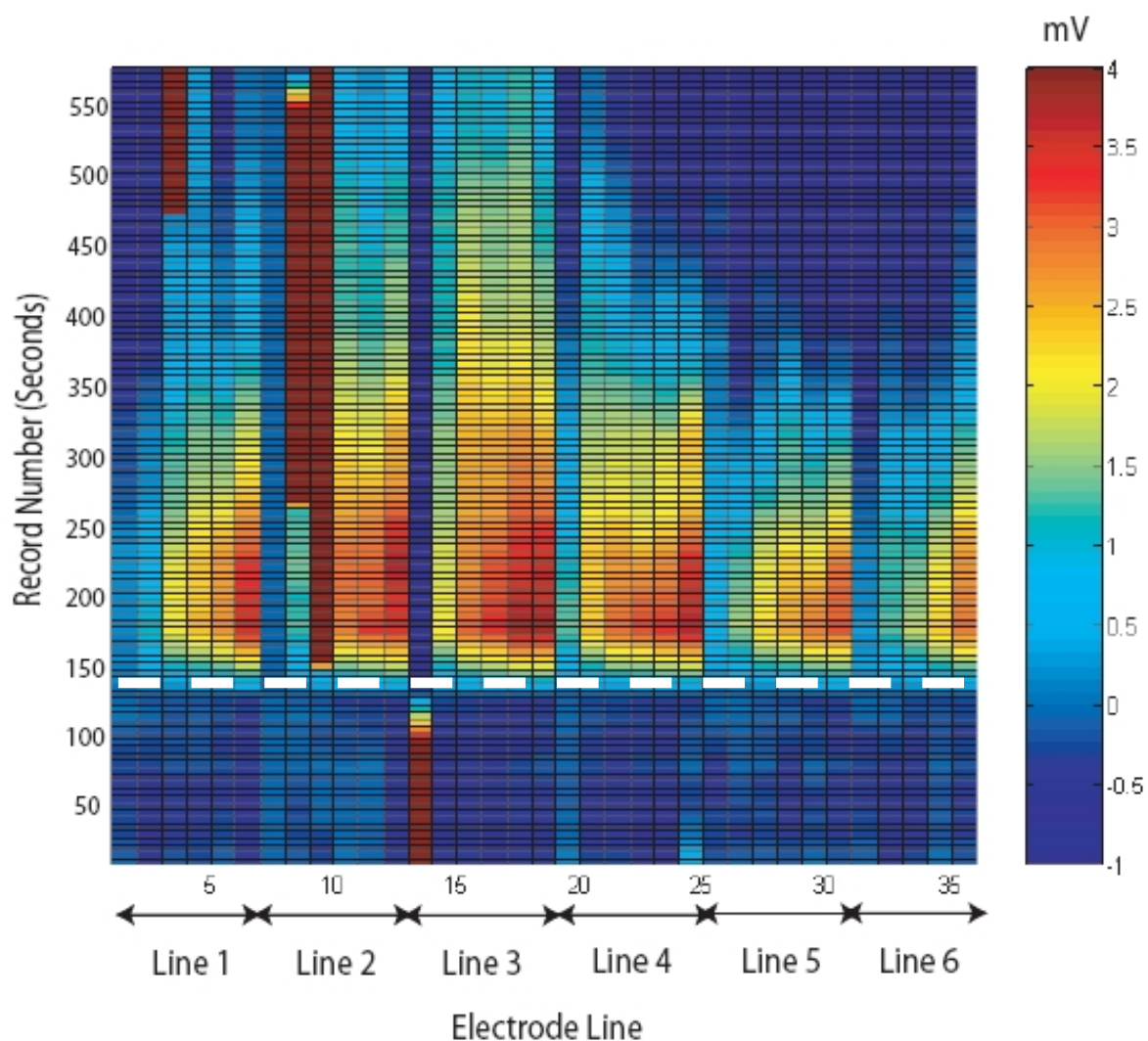


Figure 16. SP results for Site 9. The white dashed line represents the point at which the pump was switched on. Length of record shown here is only the first 5-7 minutes of the pumping duration

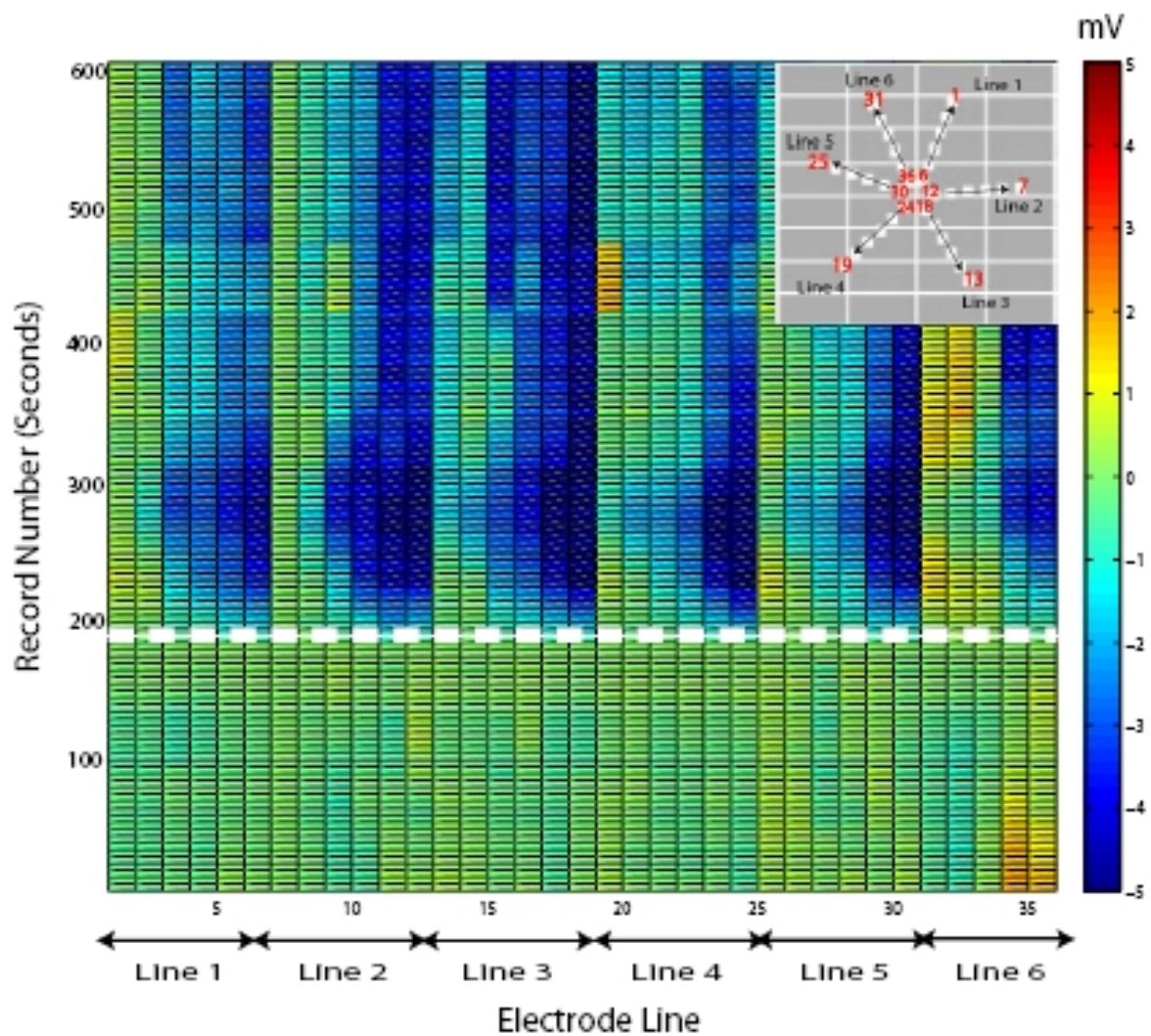


Figure 17. SP results for Site 10. The white dashed line represents the point at which the pump was switched on. Length of record shown here is only the first 5-7 minutes of the pumping duration

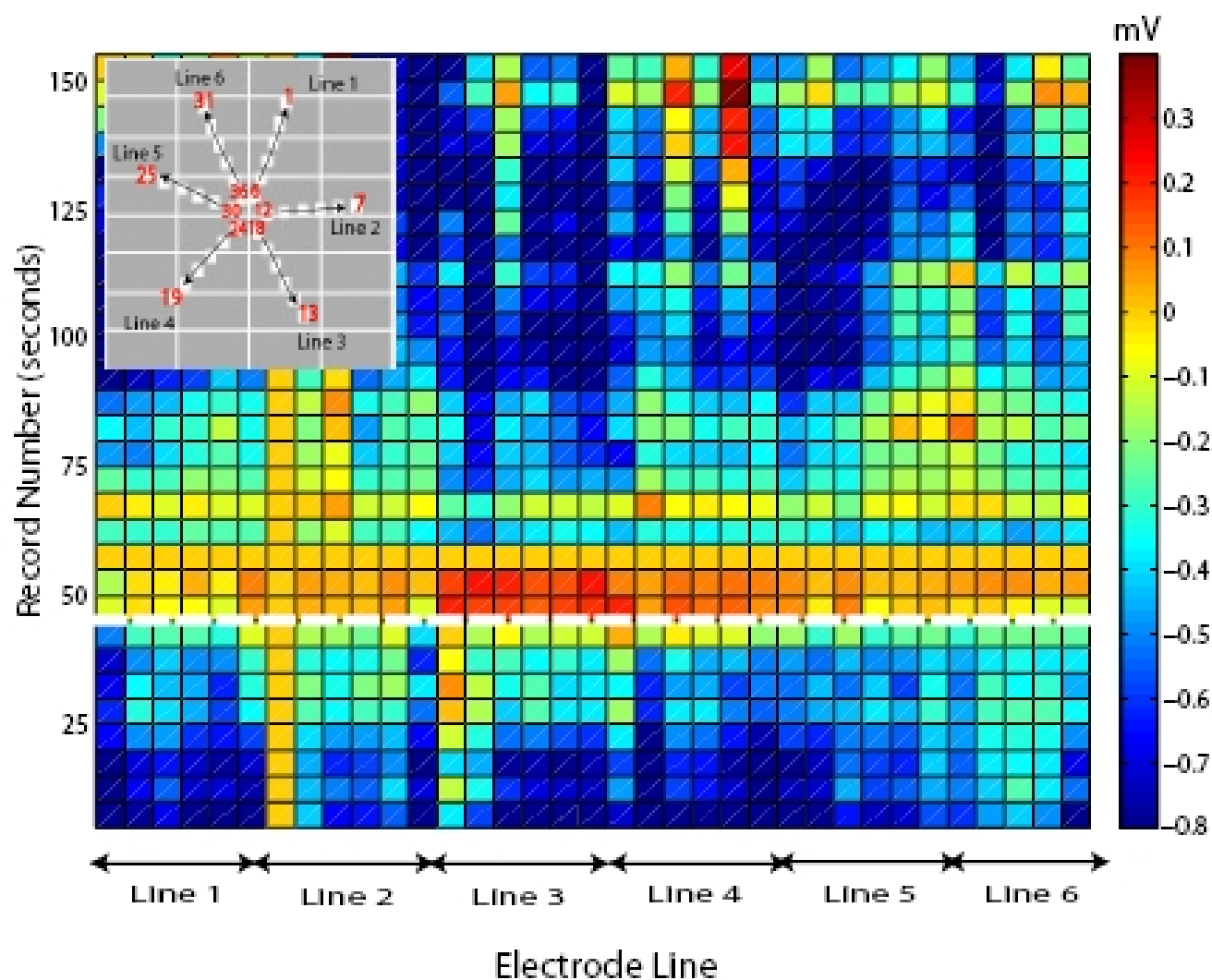


Figure 18. SP results for Site 7. The white dashed line represents the point at which the pump was switched on. Length of record shown here is only the first 5-7 minutes of the pumping duration

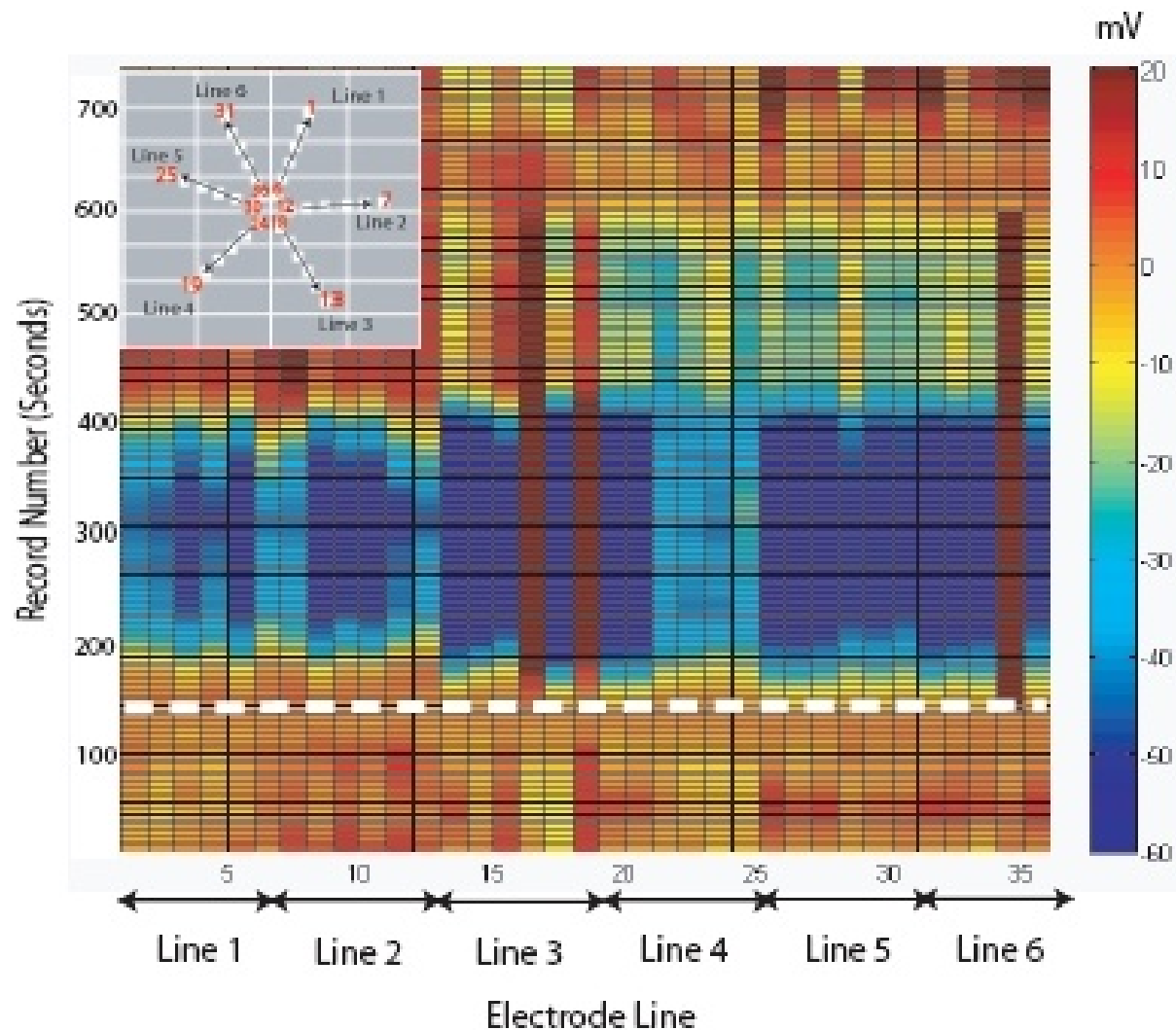


Figure 19. SP results for Site 6. The white dashed line represents the point at which the pump was switched on. Length of record shown here is only the first 5-7 minutes of the pumping duration

Many of the wells in the EMLR (and WMLR) are equipped with pumps and are totally sealed at the surface, proving a challenge to gather data. In addition, many of the pumps were suited to stock and domestic use and therefore yielded small flow rates. Studies have been shown that drawdown (drop in water level) of more than 10 m was advantageous to facilitate adequate movement of water within fractured systems. With such a low yield, and without being able to accurately measure the water level throughout the pumping cycle, it is likely that sufficient drawdowns were not being reached.

5. DISCUSSION

5.1 CALIBRATION STUDIES

As expressed in the previous section, the SP methodology is still being developed. Calibration of this method in regard to comparing the geophysical data measured to pumping test data has been documented and the reader is referred to published work by Fagerlund and Heinson (2003).

In an attempt to calibrate geophysical survey data (namely the borehole-to-surface DC resistivity) to pumping test and hydrogeological data, results from two different sites were used in the calibration process.

The two sites used were:

1. Balhannah site, located in the WMLR approximately 50 kilometres east of Adelaide; and
2. Watervale Oval site, located in the Clare Valley approximately 100 kilometres north of Adelaide.

Both of these sites are located in a fractured rock environment, exhibit a network of closely spaced wells (hence these sites have been used extensively for many other hydrogeological and geophysical investigations) and they have pumping test data readily available.

5.1.1 WATERVALE OVAL, CLARE VALLEY

The Watervale Oval site is located south of the township of Clare. This site was chosen initially by Primary Industries and Resources South Australia (PIRSA) as a possible location for an aquifer storage and recovery (ASR) site primarily due to the accessible nature of the site.

Fagerlund and Heinson (2003) used this site for detecting subsurface groundwater flow in fractured rock using SP methods. In order to undertake such work a pumping test was conducted at the Watervale Oval site in April 2001.

The pumping well used was well 6630-3063, referred to as 'Borehole 4' in the text. Well 6630-3063 was continuously pumped at a rate of 2 L/s for the first 100 minutes followed by 1.5 L/s for the remainder of the test which had an entire duration of approximately 500 minutes (Fagerlund and Heinson 2003). Water levels in four neighbouring observation wells were constantly monitored for the entire test.

While these neighbouring observation wells were not strategically placed, in that they limited the water level data to the western side of the pumping well, an area of influence and a direction of greatest drawdown could be ascertained. It is evident from the water levels in neighbouring wells that well 6630-2796 ('Borehole 3') showed the greatest drawdown (almost 7 m).

Analysing all the observation well data available and the findings of the SP data in Fagerlund and Heinson (2003) it could be inferred that the direction of preferential fracturing is to the north – north-west.

Warren (2001) used this data to establish a calculation of observed hydraulic anisotropic ratio. This was achieved by normalising maximum drawdown values recorded in each of the observation wells. A value of approximately 5 was calculated for the observed hydraulic anisotropic ratio.

Borehole-to-surface DC resistivity results conducted by Skinner and Heinson (2004) reveal normalised potential distribution contour maps for the same well 6630-3063. At $r = 25$ m the maximum potential = ~ 0.72 ; the minimum for the same distance = ~ 0.45 . Therefore an anisotropic ratio using geophysical methods is approximately 2.

The dip and strike of the most conductive elements at this site were inferred from the data. Dip values were calculated by measuring the distance of lateral offset of the maximum transfer resistance value from its expected location (directly above the current electrode). The strike was determined from the orientation of the maximum axis of the equipotential ellipse.

For well 6630-3063 ('Borehole 4') the calculated dip of the conductive structures was $\sim 80^\circ$ east and the strike was determined to be $\sim 340^\circ$ which is north – north-west (Skinner and Heinson 2004).

This finding of strike direction is consistent with and supports the investigations and pumping test data conducted by Fagerlund and Heinson (2003).

5.1.2 BALHANAH, WESTERN MOUNT LOFTY RANGES

The Balhannah site is located approximately 2 kilometres west of the township of Balhannah in the Mount Lofty Ranges. The site has been used extensively for various studies and investigations due to the number of wells constructed in close proximity to one another.

In October 2003 a pumping test was conducted by DWLBC (formerly the Department of Water Resources) as part of a separate investigation, however, the information gathered can be used in this work to further calibrate the geophysical data and relate it to the hydrogeology.

The pumping well used was well 6628-21203 which was continuously pumped for approximately 230 minutes at 2 L/s. Ten neighbouring wells were monitored for water level during the pumping test.

The greatest amount of drawdown was measured in well 6628-21211 which was located to the north-east of the pumping well. Over 3 m of drawdown was observed after 230 minutes of continuous pumping.

The observation well data imply that the direction of preferential fracturing is to the north-east.

Figure 20 shows drawdown contours surrounding the pumping well. The elliptical shape is elongated in a north-east to south-west direction which would indicate the direction of preferential flow. By simple calculation, a hydraulic anisotropic ratio of approximately 2 can be determined from these contours.

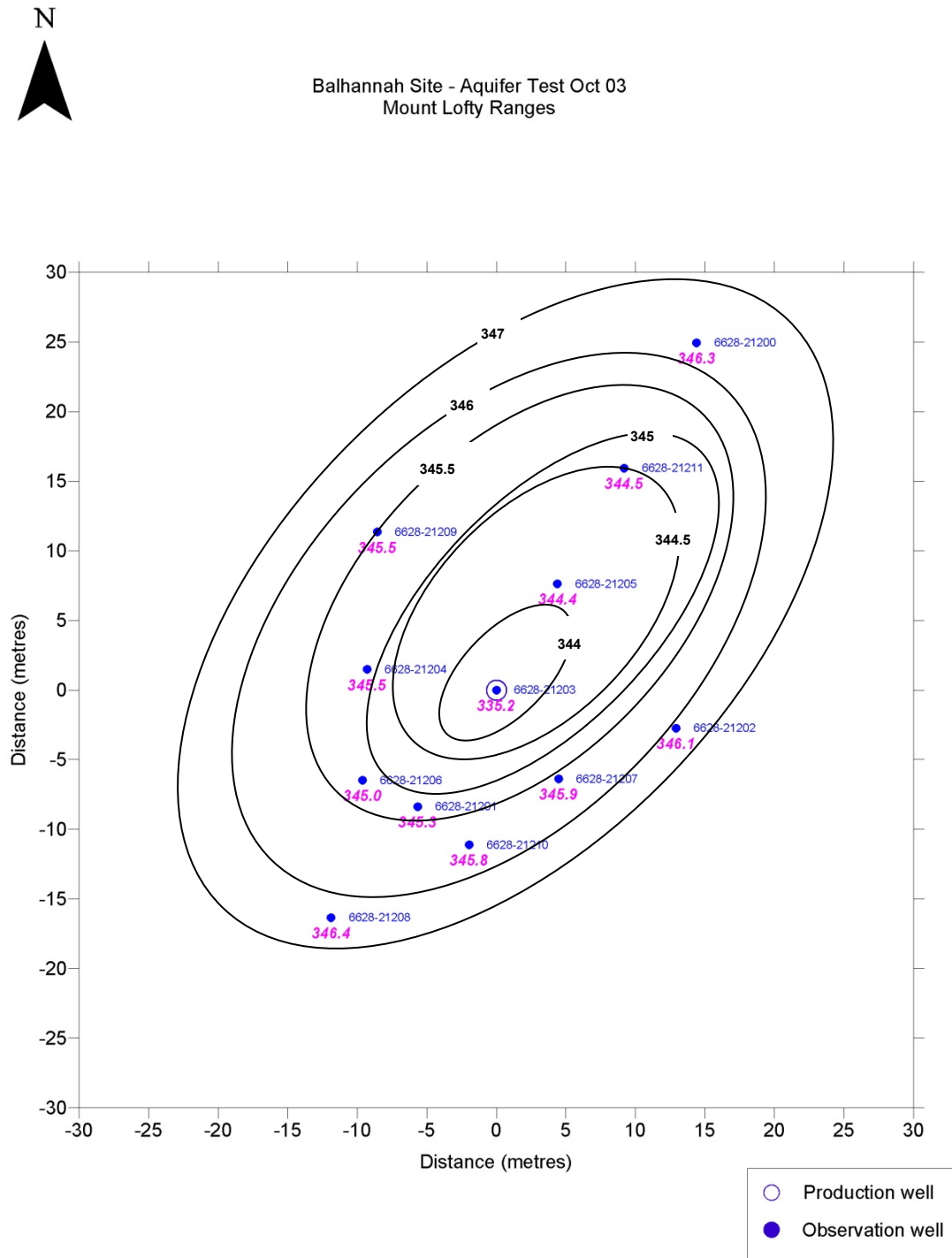


Figure 20. Aquifer test conducted in October 2003. Drawdown contours shown here are after 230 minutes of pumping from well 6628-21203. Well unit numbers are in blue, water levels (mAHd) for each well are in red. Note that water level contours (also mAHd) are approximate and coloured black

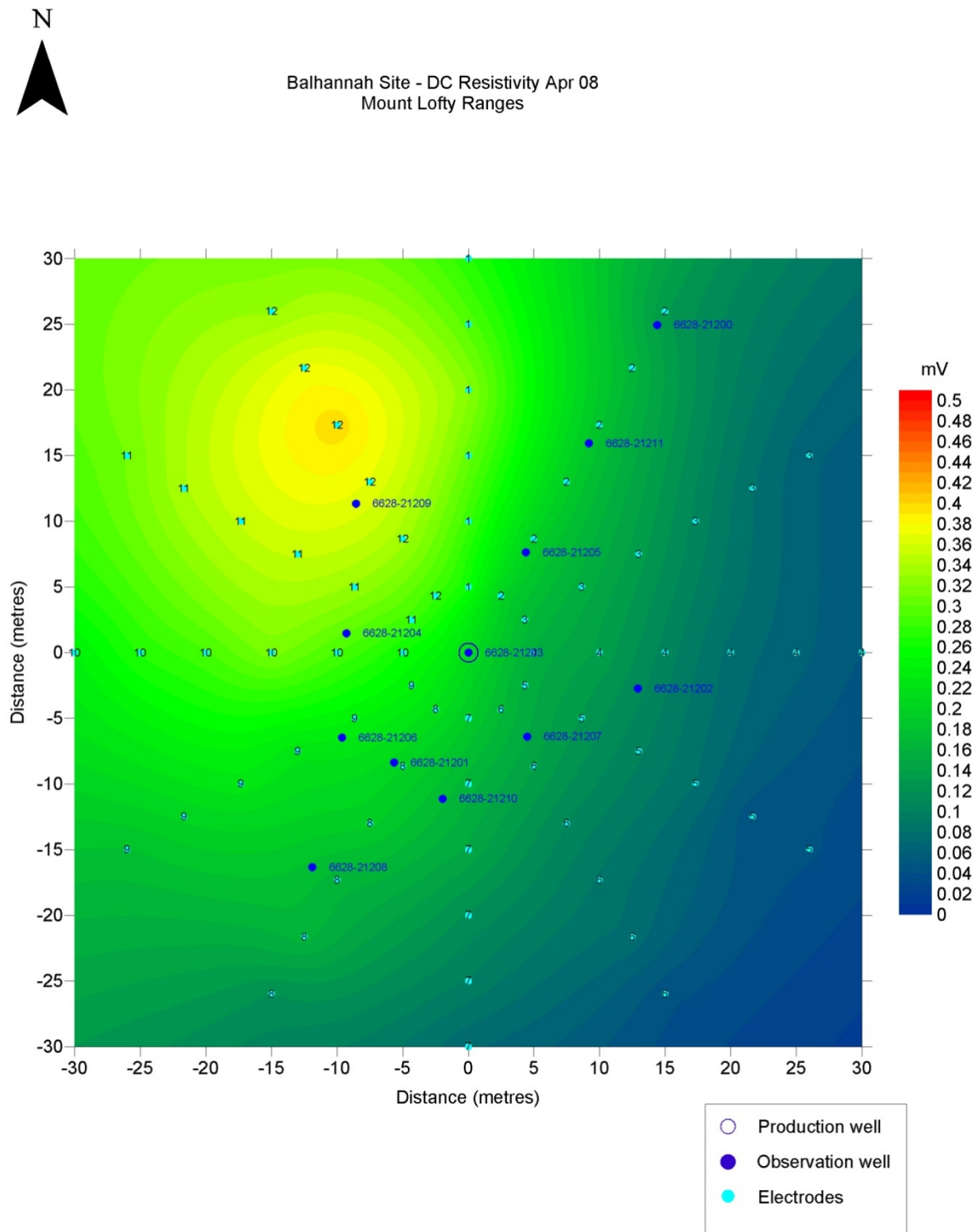


Figure 21. Normalised potential distribution contour map for Balhannah site

In April 2008 a borehole-to-surface DC resistivity survey was conducted at the Balhannah site for purposes of calibration for this investigation. Figure 21 shows the normalised potential distribution contour map for the site.

In order to align with the pumping test, well 6628-21203 was used as the central well where a current potential was lowered to approximately 30 metres. In the same fashion as the other

DISCUSSION

18 sites in the WMLR, 72 electrodes were placed strategically around the central well and their potentials measured.

The same methodology that was applied in the WMLR and in Skinner and Heinson (2004) was applied to the data at Balhannah where the dip and strike of the most conductive elements at this site were inferred from the data. Direction of dip was calculated by measuring the distance of lateral offset of the maximum transfer resistance value from its expected location (directly above the current electrode). The strike was determined from the orientation of the maximum axis of the equipotential ellipse.

For well 6628-21203 the calculated dip of the conductive structures was to the south – south-east. Since the shape of the potentials was not highly elliptical in shape (infers the site is not highly anisotropic) the strike was determined to be to the north – north-east using simple geological mapping geometry. This is also consistent with Figure 22, which shows a peak in the apparent resistivity (Equation 2) at approximately 210° and a south – south-west to north – north-east strike direction.

Data from a pumping test conducted by DWLBC in 2003 (Fig. 20) supports this strike direction.

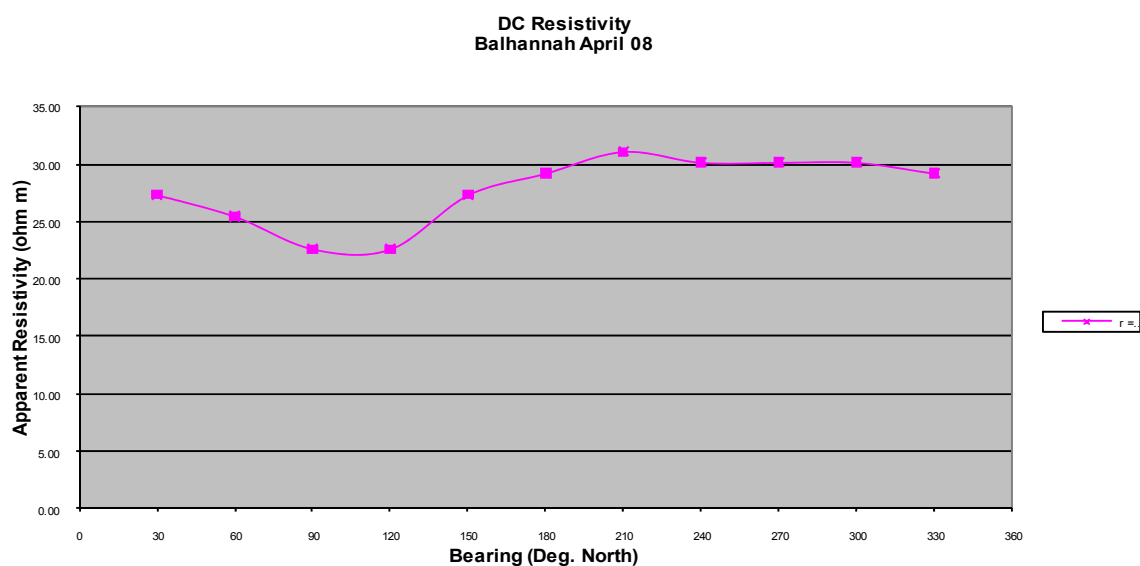


Figure 22. Apparent resistivity of electrodes at 15 m away from the well as a function of bearing

Calculation of maximum to minimum ratio using the normalised potential distribution at $r = 15$ m (lowered due to the offset of the maximum potential), the maximum potential = ~ 0.33 (approximately 31.10 ohm m); the minimum for the same distance = ~ 0.24 (approximately 22.62 ohm m). Therefore an anisotropic ratio using geophysical methods is approximately 1.4.

Due to preferential fracturing, the very nature of a fractured rock environment, there will always be some level of anisotropy (even if low).

DISCUSSION

It is clear from the calibration that the geophysical method (borehole-to-surface DC resistivity) is not as sensitive to anisotropy as the hydraulic equivalent. However the data (Table 3) does suggest that there is a multiplying factor.

Table 3. Summary of anisotropic ratios for the calibration sites

Site	R (m)	Hydraulic Anisotropy	Geophysical Anisotropy	Ratio
Watervale Oval	25	5	2	2.5
Balhannah	15	2	1.4	1.4
Average				~ 2

Using an average of the ratios found at each calibration site, a measured geophysical anisotropy using borehole-to-surface DC resistivity will need to be multiplied by a factor of 2 in order to calculate a hydraulic anisotropy.

5.2 GENERATING HYDRAULIC ANISOTROPY

Using the calibration methodology (Table 3) and applying this to the electrical data (namely borehole-to-surface DC resistivity, Table 2), one can determine a hydraulic anisotropy for each of the 18 sites investigated in the WMLR (Table 4).

Table 4. Summary of electrical data interpretations for 18 selected sites in the Western Mount Lofty Ranges

Site	Anisotropy (Yes/No)	Strike	Dip	Magnitude (V/I)	Geophysical Anisotropic Ratio	Hydraulic Anisotropic Ratio
1	-	-	-	-	-	-
2	Y	NW	SW	Medium	1.5	3
3	Y (low)	NNW	-	High	1.3	2
4	-	-	-	-	-	-
5	Y	NW	SW	Medium	1.5	3
6	Y	ukn (NE*)	SE	Medium	2.5	5
7	-	-	-	-	-	-
8	Y	N	E	Medium	1.5	3
9	ukn	ukn (NE/SW*)	SE	Medium	ukn	ukn
10	ukn	ukn (N/S*)	E	Medium	ukn	ukn
11	Y	NW	-	High	1.5	3
12	Y	NE	SE	Medium	2.0	4
13	Y	NE	SE	Med	1.5	3
14	Y	NNE	-	High	1.5	3
15	-	-	-	-	-	-
16	Y (low)	NNE	ESE	Medium	1.2	2
17	Y	WNW	-	Medium	2.0	4

DISCUSSION

18	Y	NE	-	Medium	1.5	3
19	Y	NNW	ENE	Medium	2.0	4
20	Y	NW	-	Medium	1.5	3
21	Y	NE	-	High	1.5	3

N (strike/dip) – north
 E (strike/dip) – east
 S (strike/dip) – south
 W (strike/dip) – west

unkn – unknown (not enough data)
 * Dip direction implies orthogonal strike direction

Hydraulic anisotropy may be applied to (or refine) existing extraction well buffer guidelines in line with the following example. A nominal buffer for a particular area depending on geology, geological structure and rate of and volume of extraction, may typically have a radius of 200 metres. Current guidelines assume equal drawdown in each direction from the extraction well and hence a circular buffer (with this radius) is applied. However in a fractured rock environment there will be preferential fracturing in a particular direction. Using Site 5 (Table 4) as an example, this site exhibits preferential fracturing in the north-west to south-east direction (direction of strike and anisotropy). The hydraulic anisotropic ratio was calculated to be 3 (Table 4). Therefore the radius of the maximum axis (in the north-west to south-east direction) would be three times that of the minimum axis (in the north-east to south-west direction).

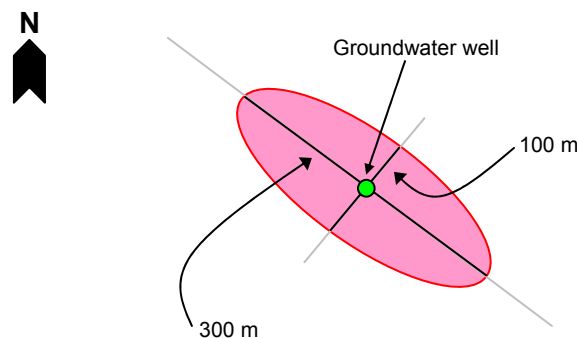


Figure 24. Hypothetical example of anisotropic direction and ratio as applied to circular buffering system. Assuming circular buffer radius of 200 m with an anisotropic strike direction of NW/SE and a hydraulic anisotropic ratio of 3.

In order to maintain an area size similar to the current (circular) buffer guidelines, the radius would be reduced by 50%, this becomes the radius of the minimum axis. The anisotropic ratio is then applied to this minimum axis to generate a radius for the maximum axis. Using the example of Site 5 and an original (circular) buffer of 200 m, an ellipse with the following specifications would apply (Fig. 24):

- Minimum radius in the north-east/south-west direction = 100 m
- Maximum radius in the north-west/south-east direction = 300 m.

CONCLUSION

Borehole-to-surface resistivity data obtained by placing an electrode down a borehole and measuring the distribution of transverse resistance on the surface has been used to delineate the orientation of dominant sub-vertical fractures intersecting the borehole.

Surveys conducted at numerous sites within the WMLR have confirmed that dominant fracture sets in the Adelaidean metasediments and Kanmantoo Group are controlled by the major north – north-west to north – north-east structural trends in the area.

Although the borehole-to-surface technique shows localised results, it is evident from the consistent interpretations throughout the field area that orientations of the dominant hydraulically conductive sub-vertical fractures are consistent with regional trends. Borehole-to-surface electrical measurements exhibited significant variations in magnitude, which are indicative of different porosities and saturations within the area. Bulk electrical resistivity could be estimated from apparent resistivity and, at sites for which electrical conductivity was measured, porosity could also be estimated. The ratio of maximum to minimum apparent resistivity could be attributed to the hydrogeology and used to characterise areas exhibiting substantial differences in fluid flow. Due to the linear versus cubic nature of electric versus hydraulic conductivity, a doubling of electrical conductivity could potentially correspond to an eight-fold increase in fluid flow in the dominant fracture orientation. The bulk resistivity is also linked to the salinity of the groundwater and variations are partially attributed to this.

Deviations of surface potential from those expected within a homogeneous medium can be attributed almost exclusively to fracture or bedding-plane orientations, although other conductive materials may contribute. However, aligned conductive minerals may still be a proxy for fracture orientation due to the nature of the structural control in the area and, as such, could have similar orientation to dominant conductive zones resulting from open fractures. It is unlikely that this is a major concern for the WMLR region as a discernable trend of greater anisotropy was not seen in lithological units with more conductive material.

While borehole-to-surface surveys are limited to sites where at least one borehole exists, the method is neither time-consuming nor labour-intensive. Surveys undertaken (including SP methods) in the WMLR took about four hours per site, meaning that two sites could usually be surveyed per day.

The electrokinetic measurements at some sites show large (up to 60 mV) variations with time due to drawdown associated with pumping, particularly over the first five to ten minutes. These changes showed groundwater movement in the proximity of the electrodes and allowed quantification of the direction of groundwater flow at some sites.

However, at some sites, the potential changes are less than 1 mV, and hence are difficult to detect above the ambient noise levels. The magnitude of changes in the electrokinetic measurement can be attributed to fluid flow rates and the depth of conductive zones. A comparison of surface profiles for analytical and observed solutions of SP can be used to determine an average hydraulic conductivity for the site. This potentially can be related to the drawdown although it is more complicated with depth when attributes of the media act extremely different to porous media. Electrokinetic potentials allow a greater understanding of the subsurface fluid flow and could be used to infer distances for zones of influence around the well.

The interpretation that borehole-to-surface electrical methods are mapping the bedding planes, and not the deeper fractures feeding the system, is consistent with previous work (Skinner and Heinson, 2004). The deeper fractures may be sub-horizontal, such that

CONCLUSION

borehole-to-borehole electrical methods may enhance interpretation of cross connection (a third method not explored in this study).

These two electrical methods are sampling the top 20 metres at most, however this is a depth range from which the majority of pumping occurs in the WMLR. Much of what is being imaged is the water in fractures parallel to bedding planes and these are likely to be open due to uplift and stress relief (Fig. 23).

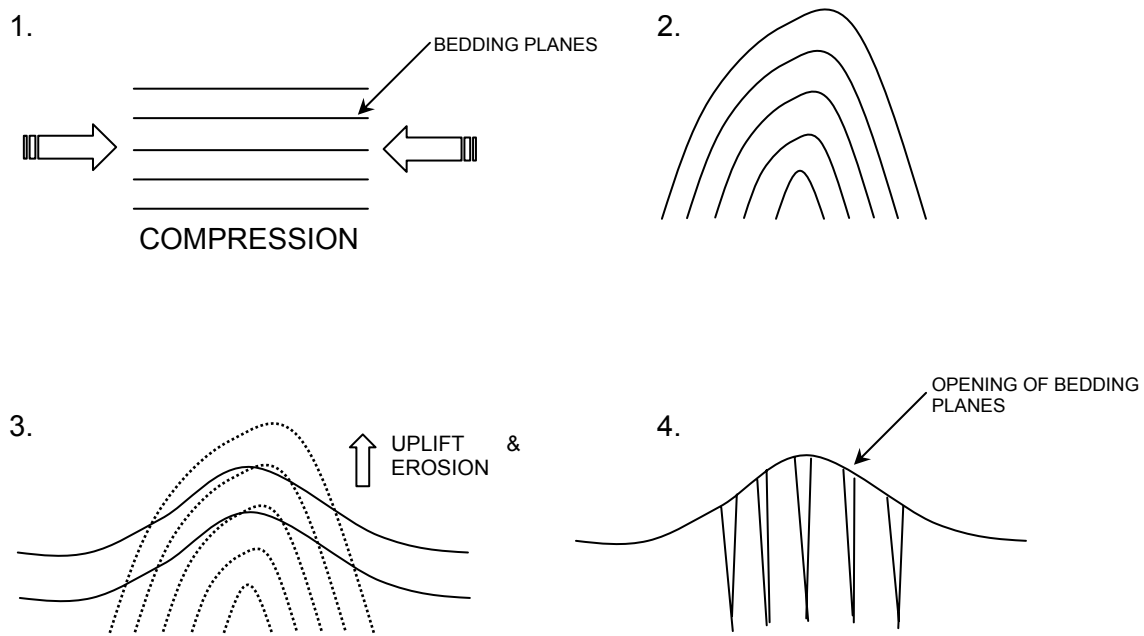


Figure 23. Sequence of events which facilitate fracture development in a fractured rock environment

Recharge in this top 20 metres is a mixture of local rainfall (which moves down the bedding planes) with some contribution from deeper fractures.

Due to the complex distribution of fractures in almost every type of rock, no single method can unambiguously map fractures and their capacity for fluid movement. Although SP is a relatively new technique, using interpretations from the two methods will lead to a greater understanding of characterisation subsurface flow in recharge zones and can be used to define orientation of fractures in terms of strike and dip, as well as broadly defining bulk electric resistivity, bulk porosity and hydraulic conductivity. By using a combination of the methods described it could be possible to determine zones of influence around pumping wells in the future, primarily inferring dominant orientation of strike from resistivity methods and an estimate of the elliptical radius from magnitude of electrokinetic measurements.

7. RECOMMENDATIONS

The investigation showed that the borehole-to-surface DC resistivity proved to be effective in determining preferential fracture orientation as defined by both strike and dip. It compares well with the known structure in the WMLR.

The SP data proved to be a little more challenging than first thought. The results suggest that there are more chemical processes at work that are not fully understood at this early stage. It is recommended, as expressed in earlier chapters, that the ability of these techniques be further investigated.

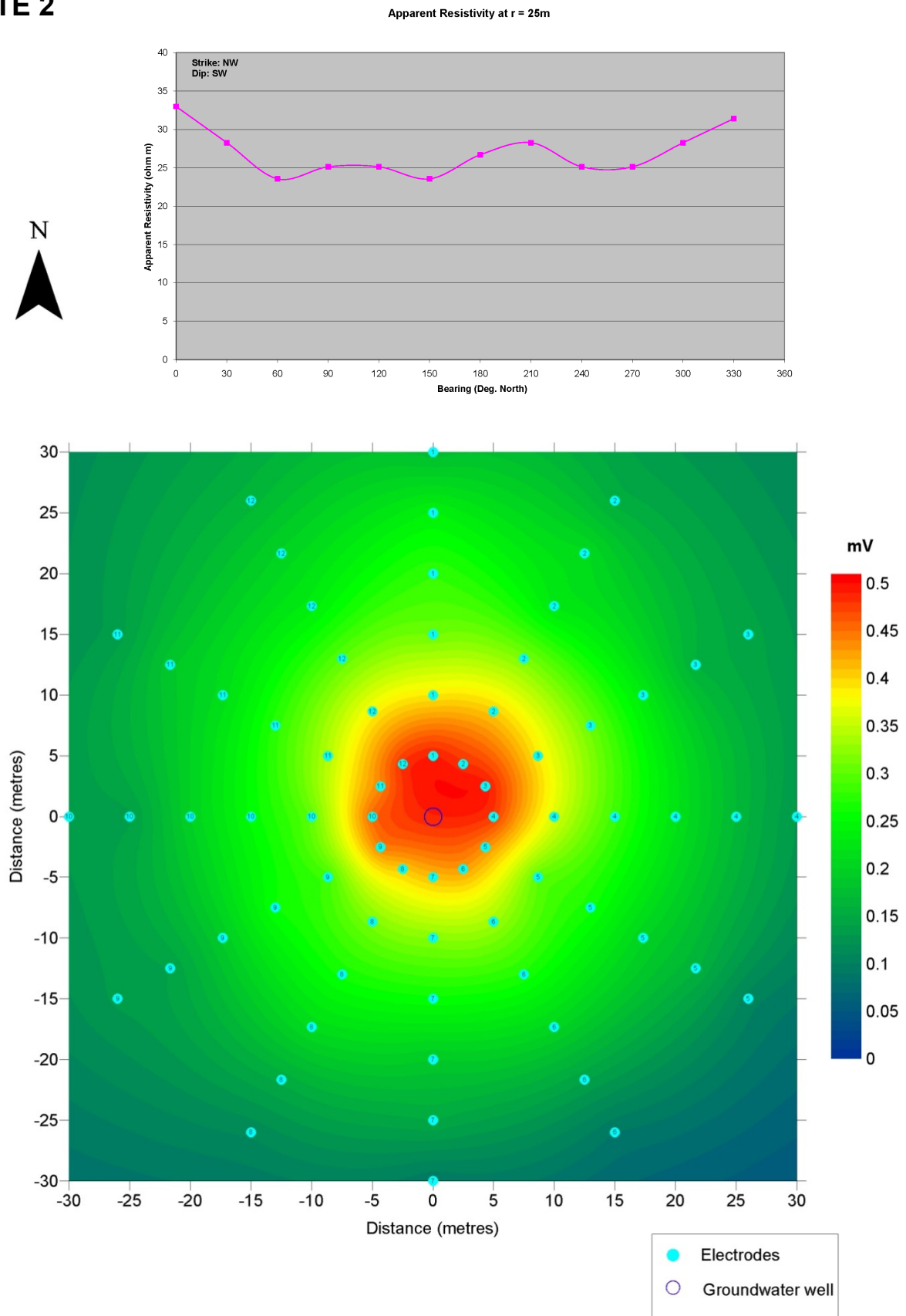
Based upon these geophysical findings, the extents of the zones of influence around a number of extraction wells in the WMLR have been identified. These buffer distances can be recommended for these specific sites and provide a guide to the method by which buffer distances can be determined in water management plans. The direction and range of magnitudes of the hydraulic anisotropy identified at the locations assessed provides a guide to the specification of buffers for wells in similar geological settings.

It is recommended that these guidelines are used when reviewing buffer zones in current and future groundwater resource management plans.

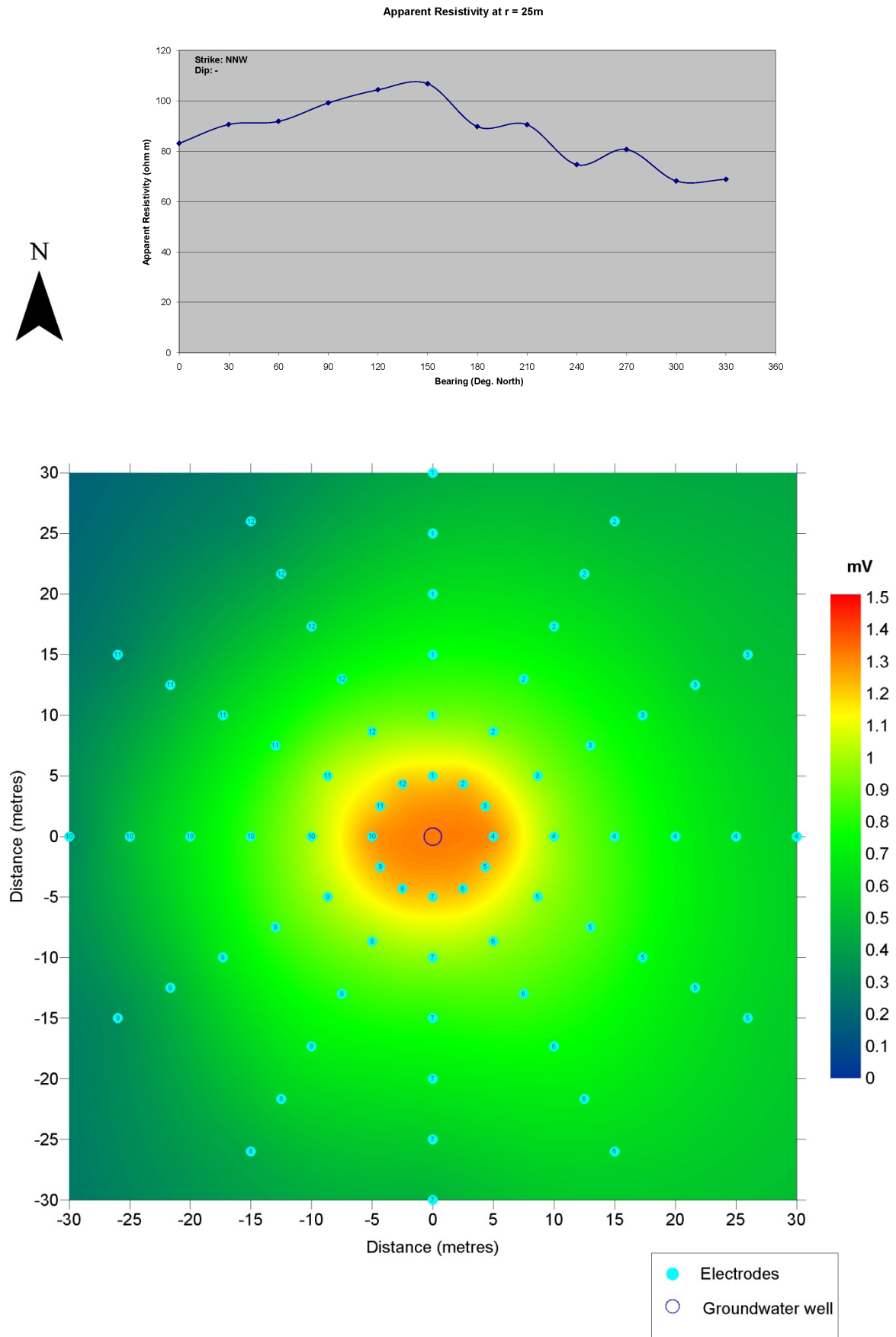
APPENDICES

A. SURFACE MAPS OF ELECTRICAL POTENTIAL FOR ALL 18 SITES IN THE WESTERN MOUNT LOFTY RANGES

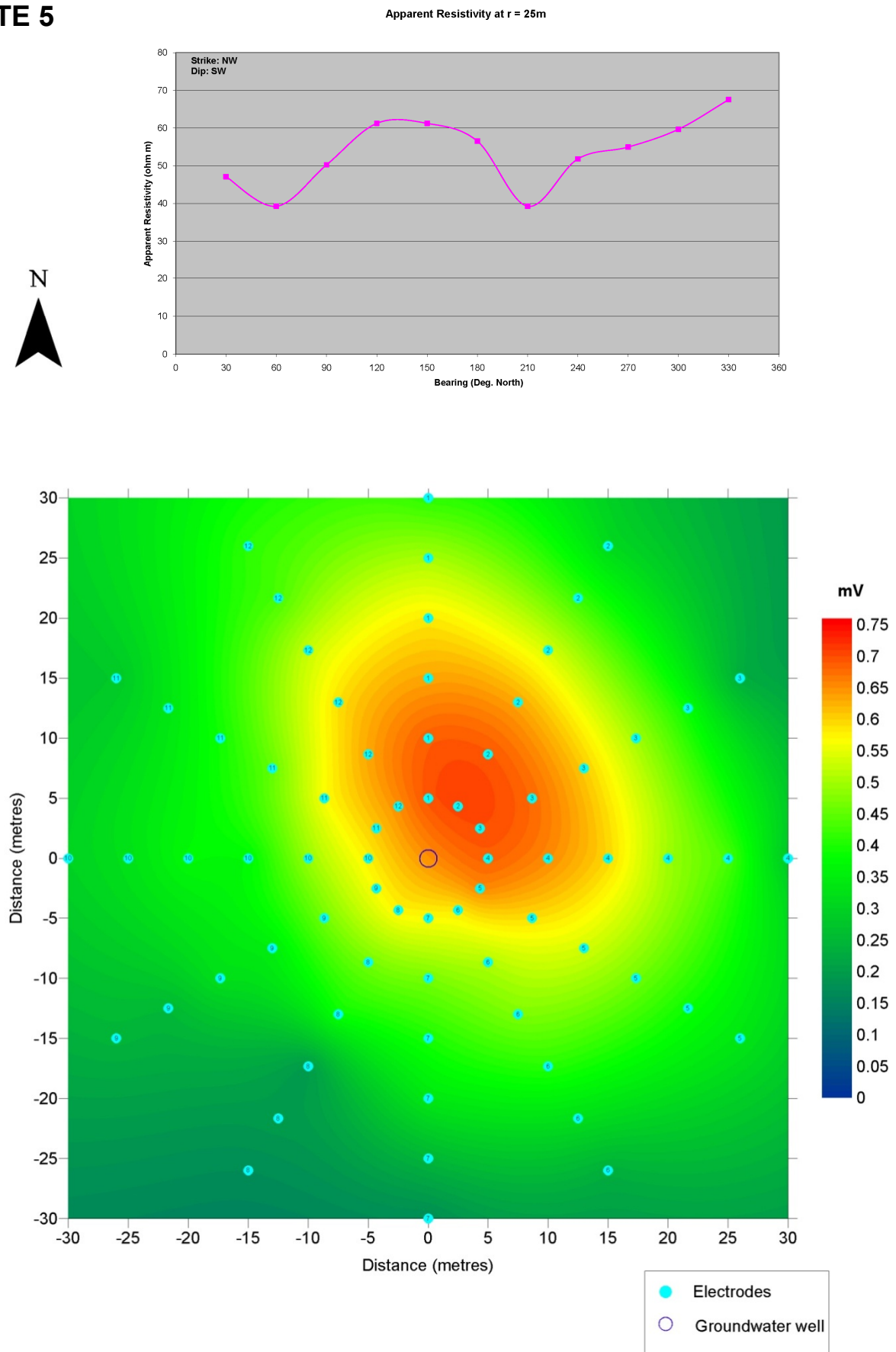
SITE 2



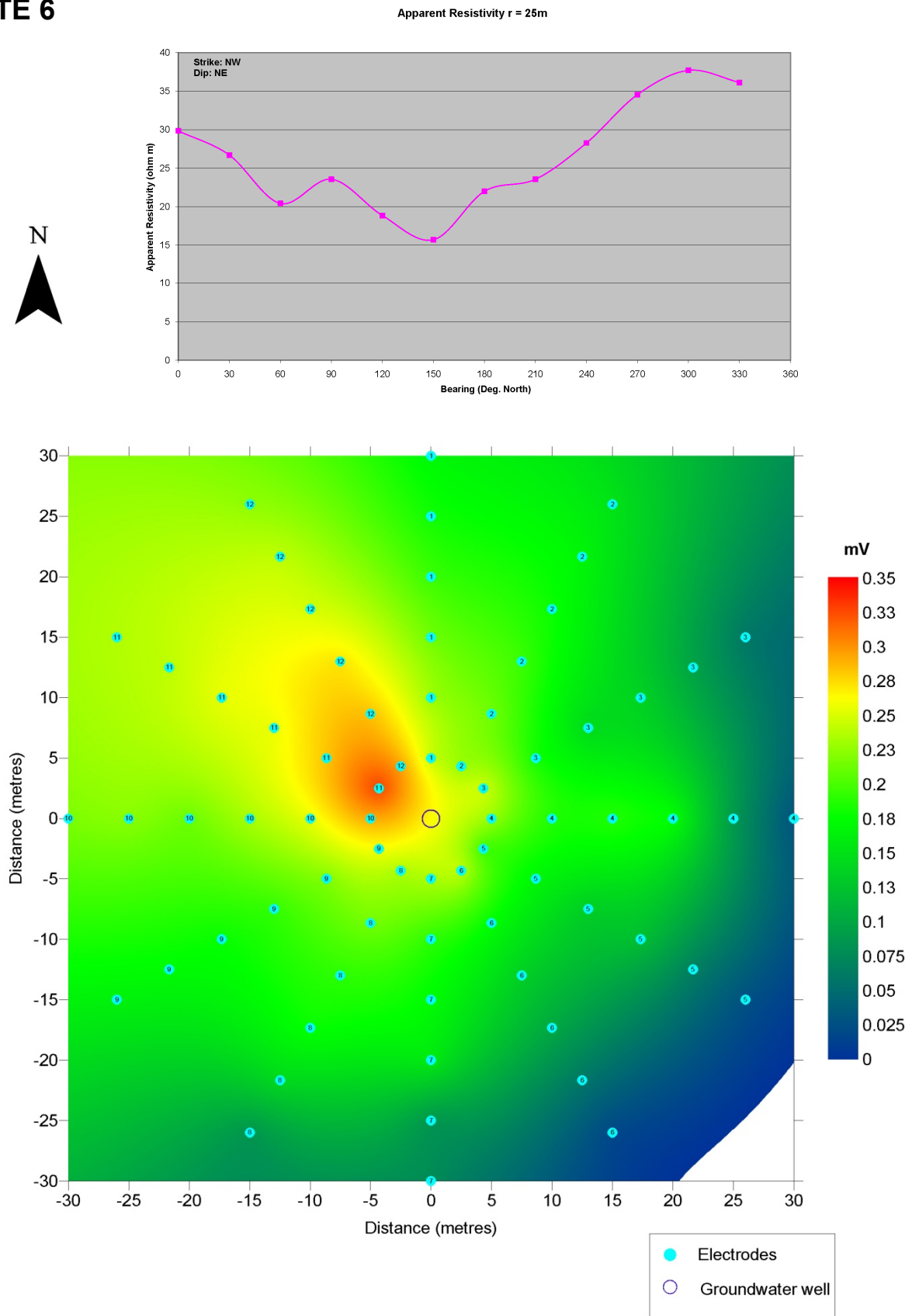
SITE 3



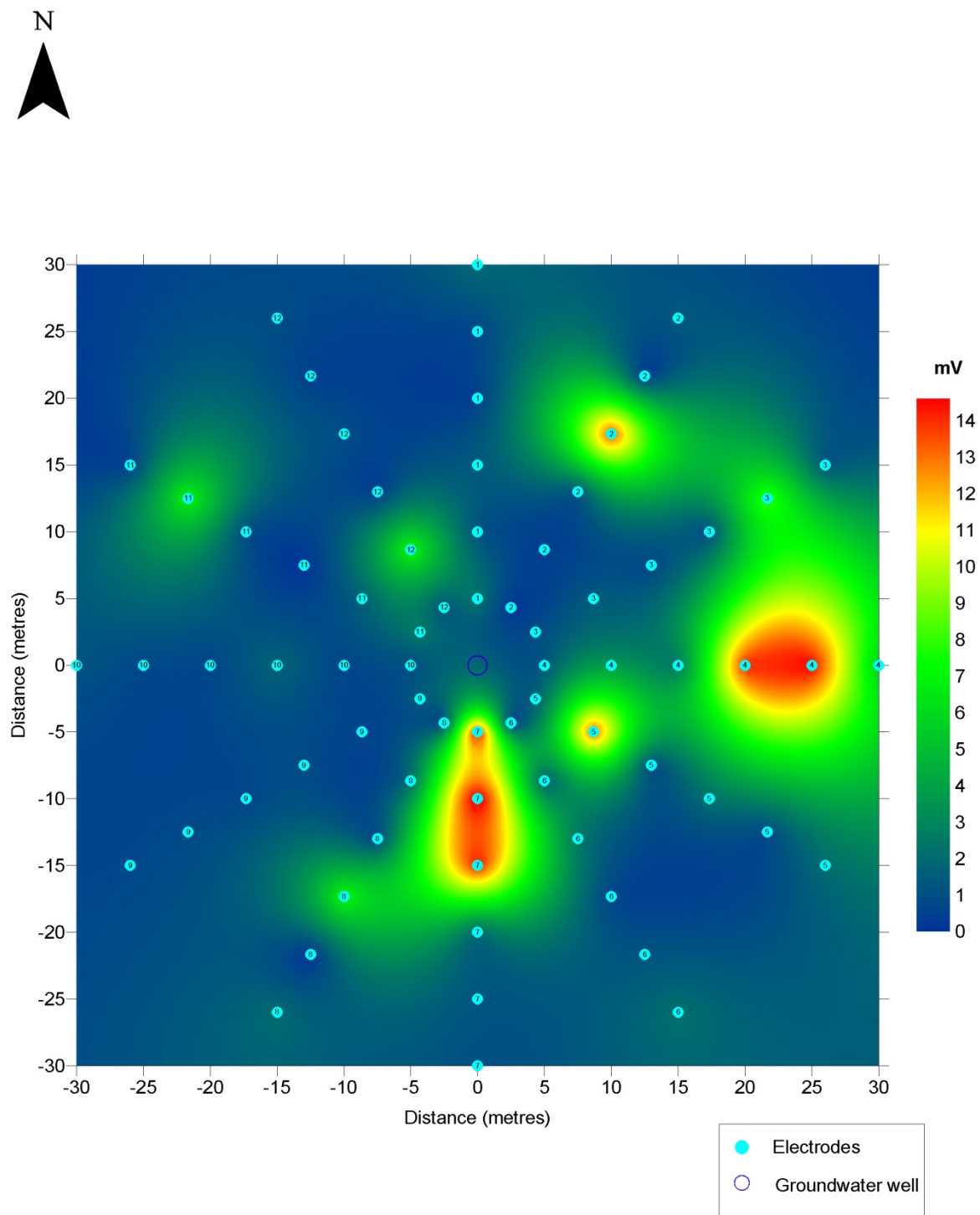
SITE 5



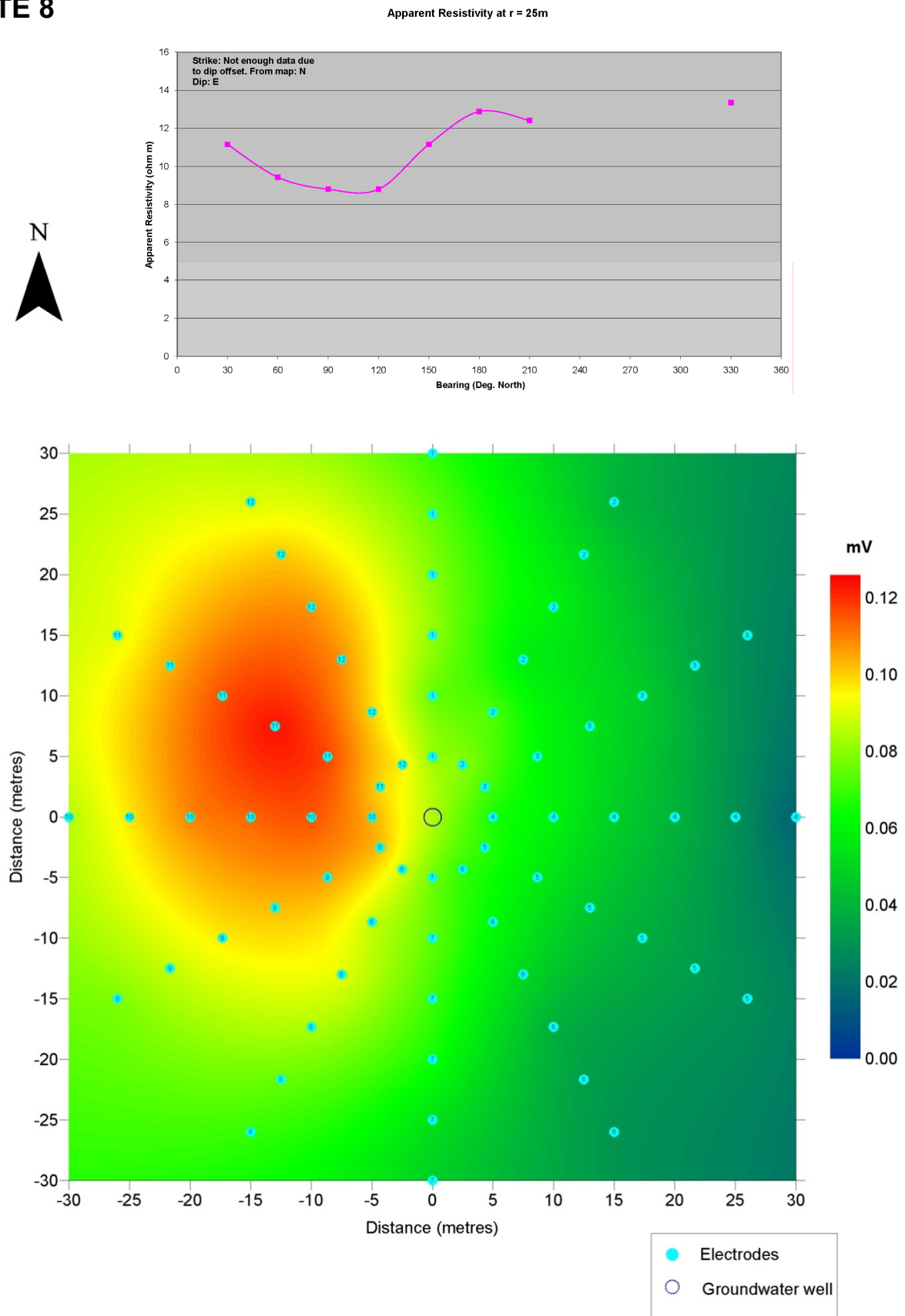
SITE 6



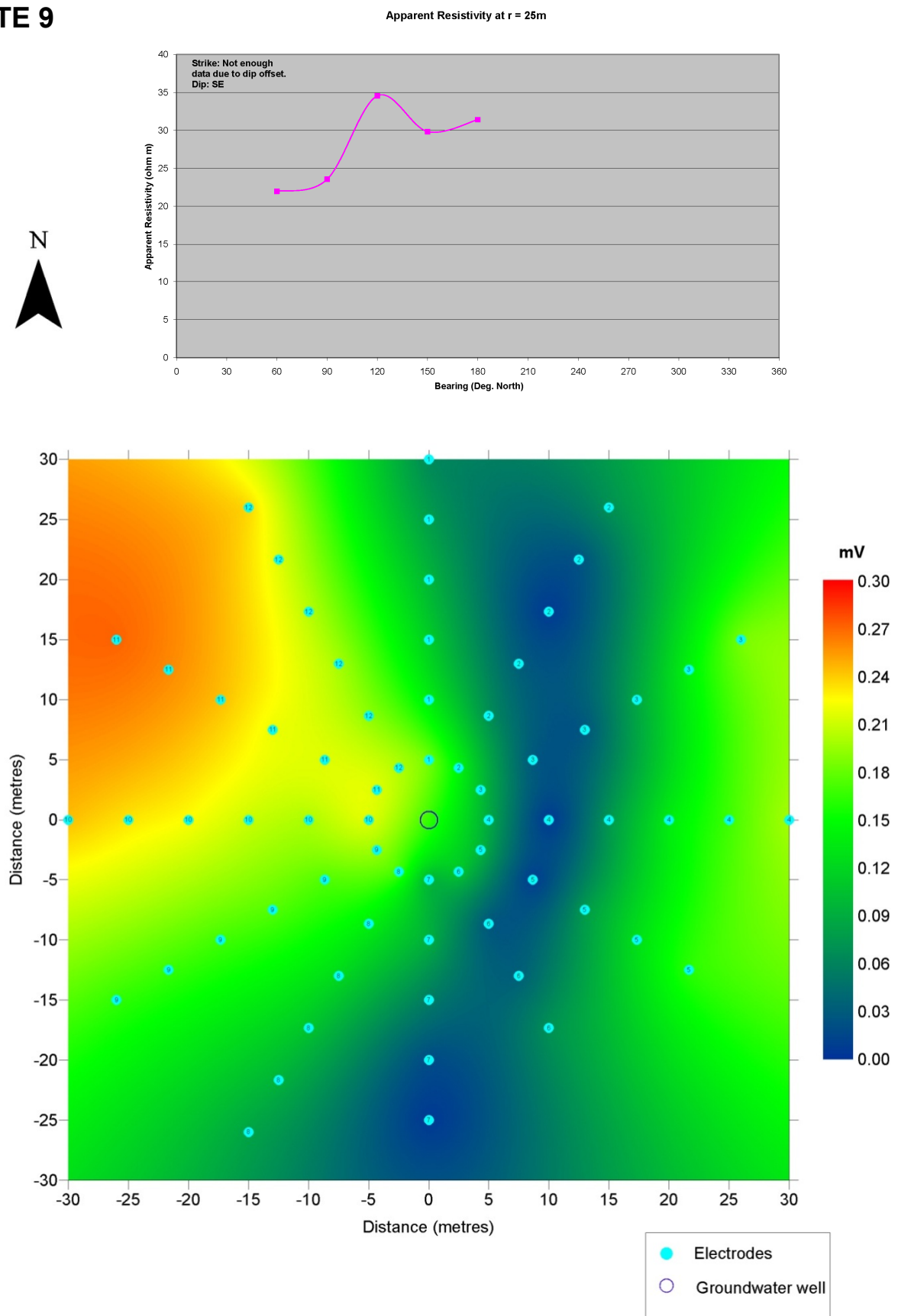
SITE 7



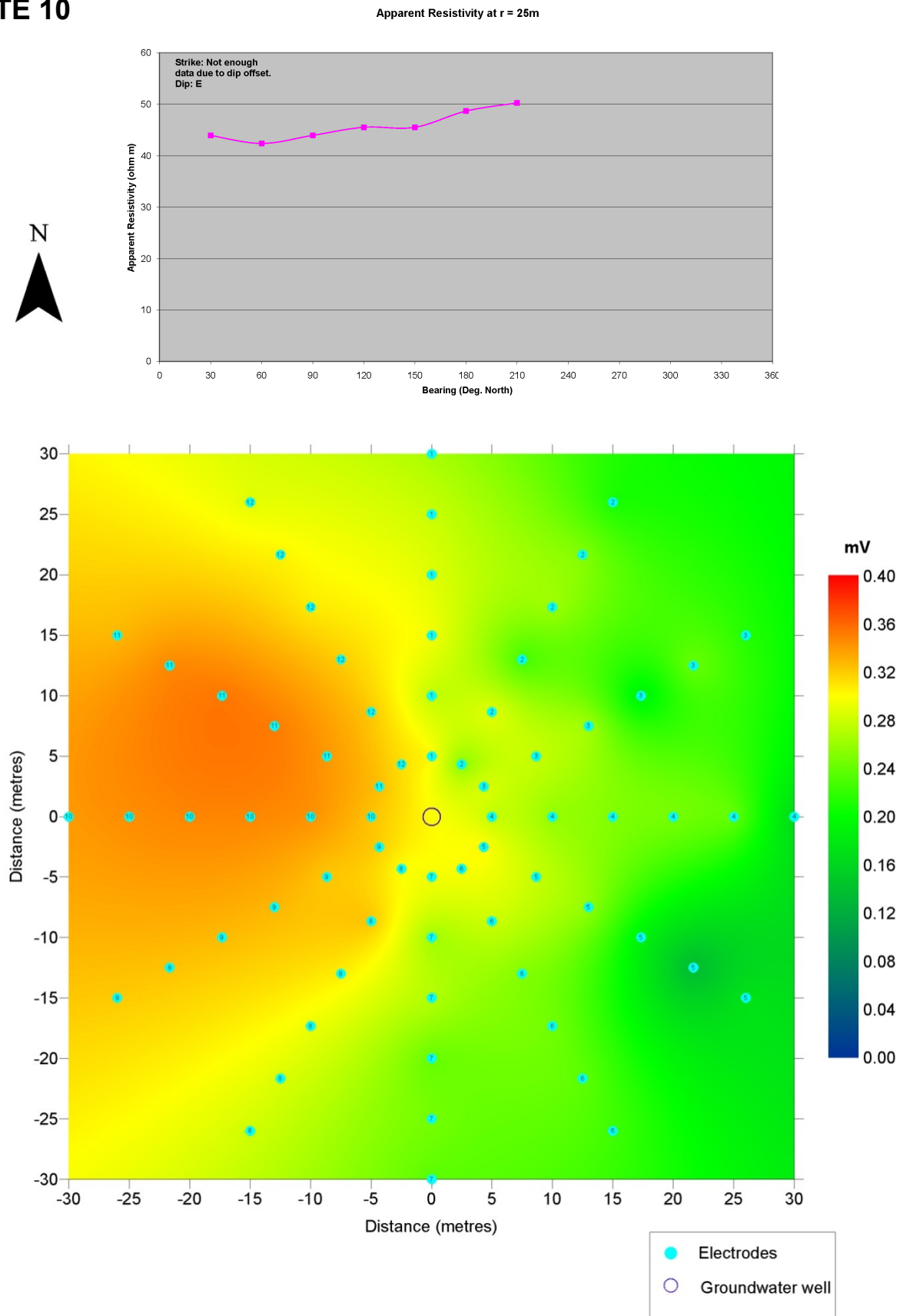
SITE 8



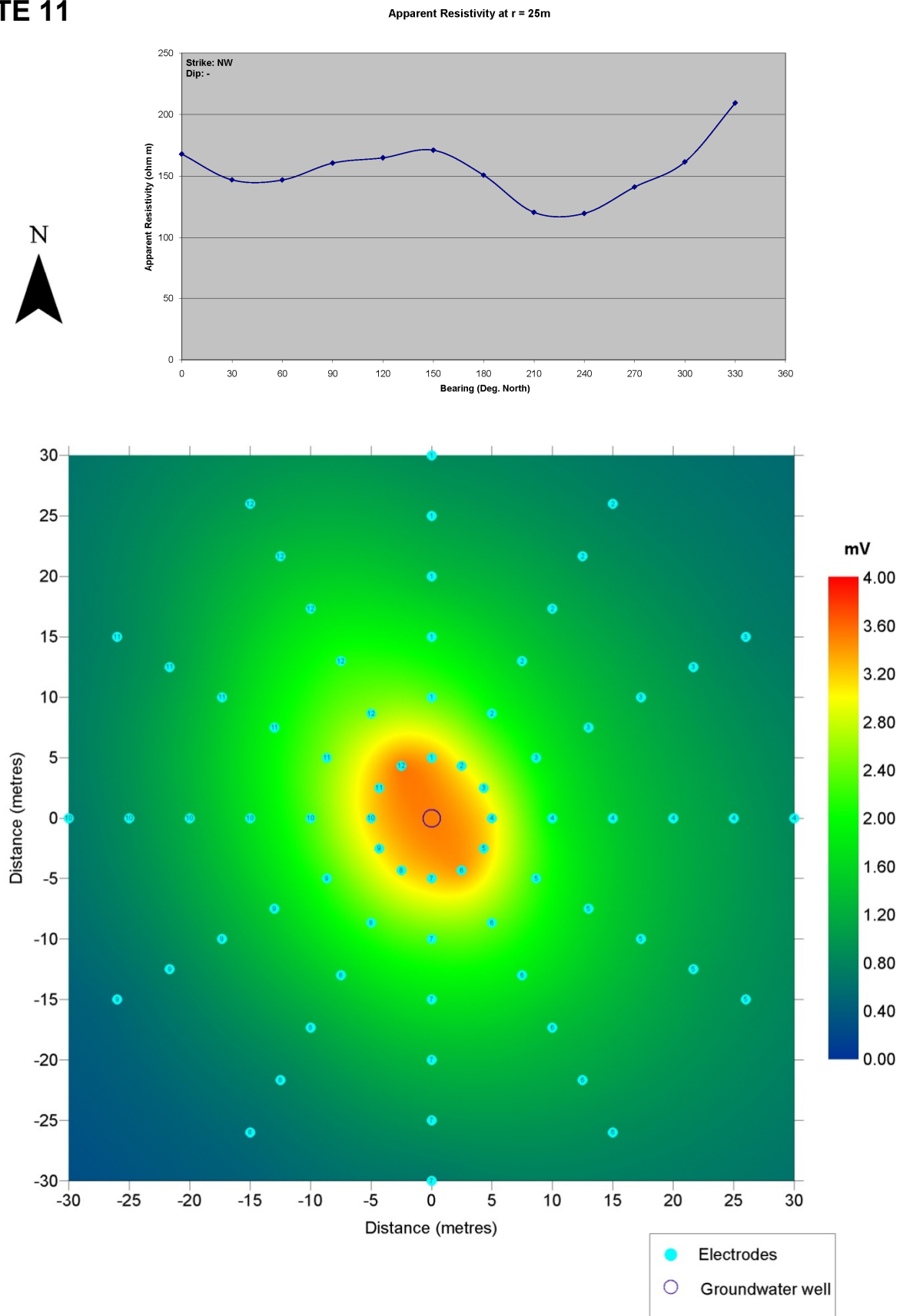
SITE 9



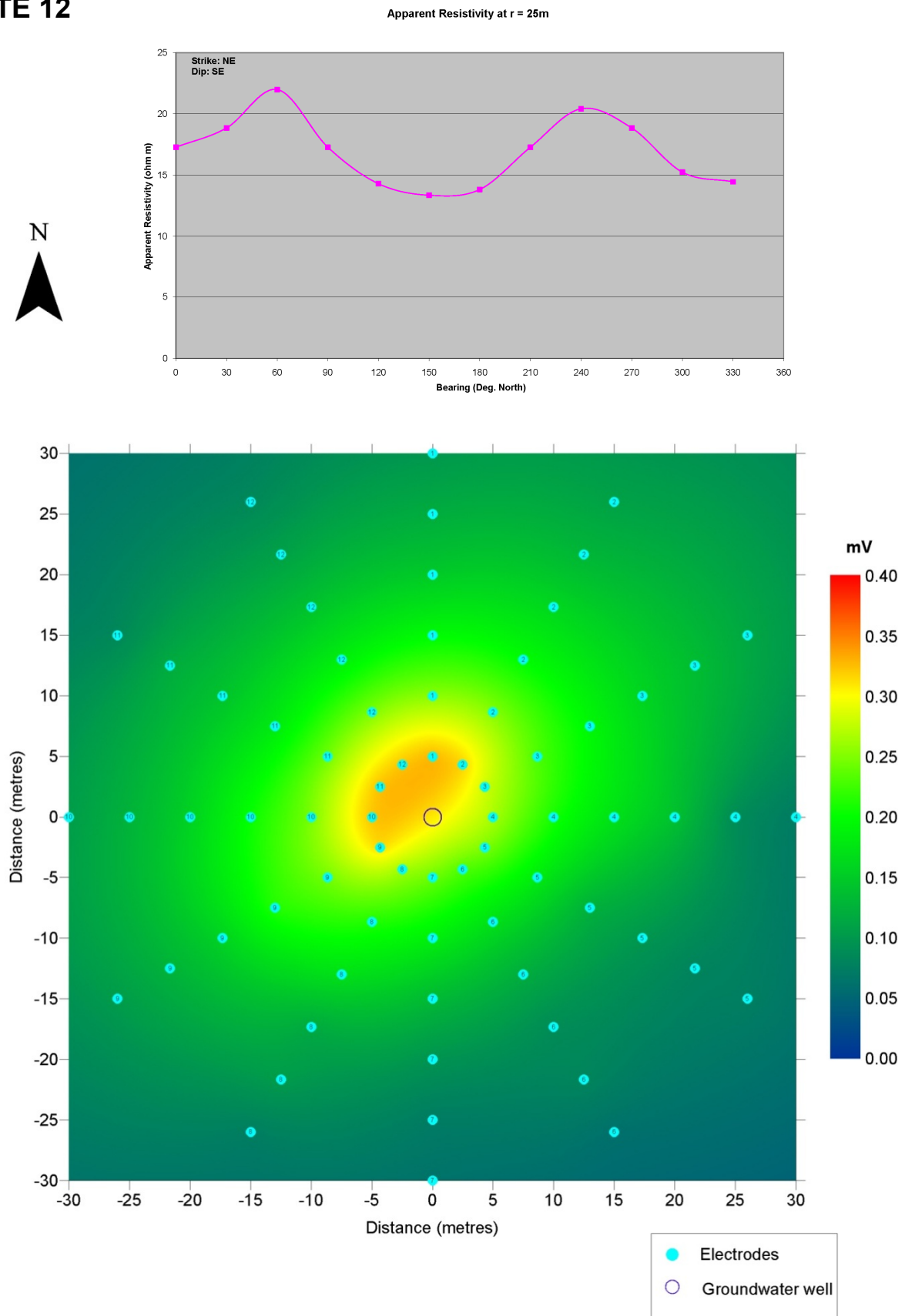
SITE 10



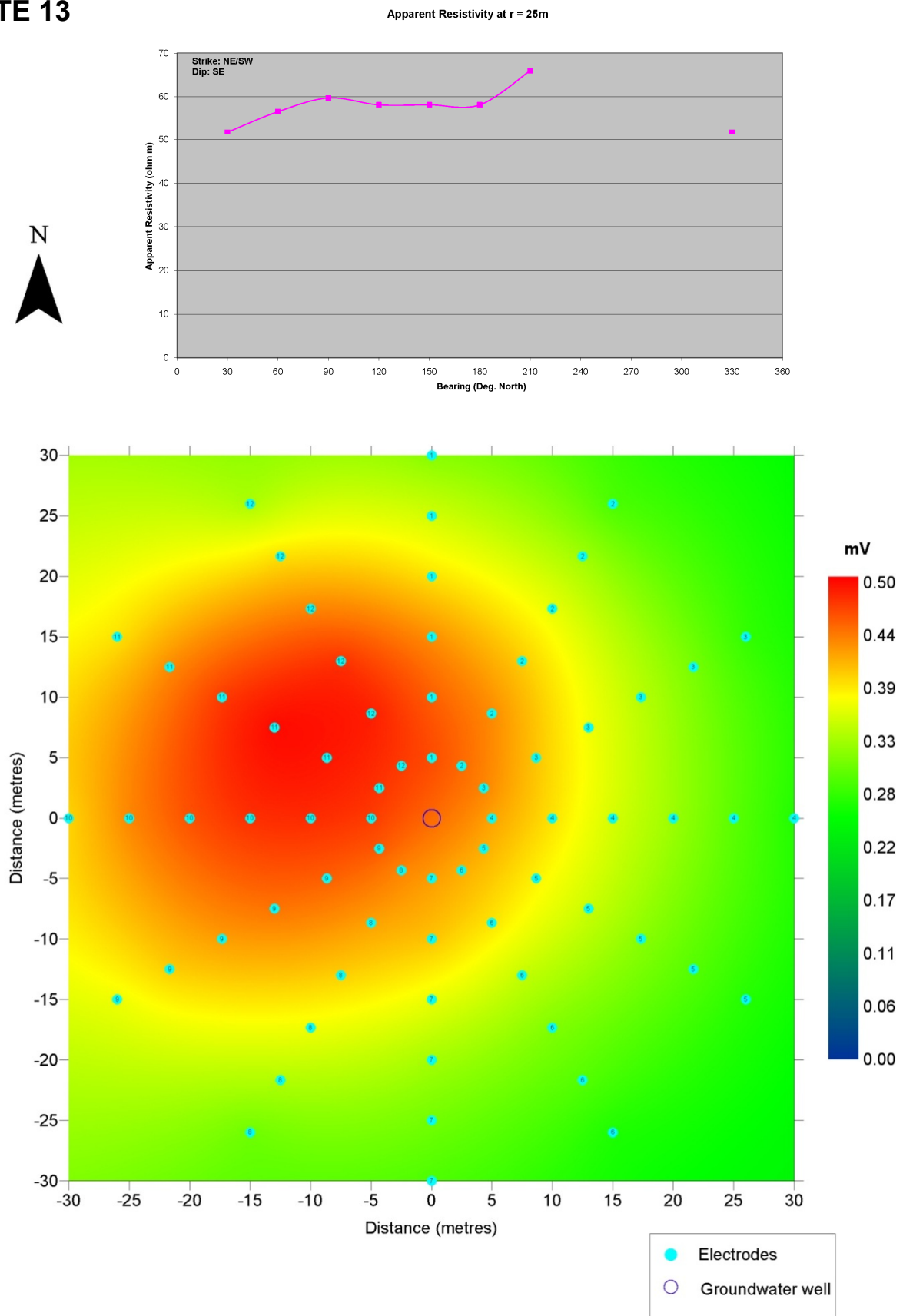
SITE 11



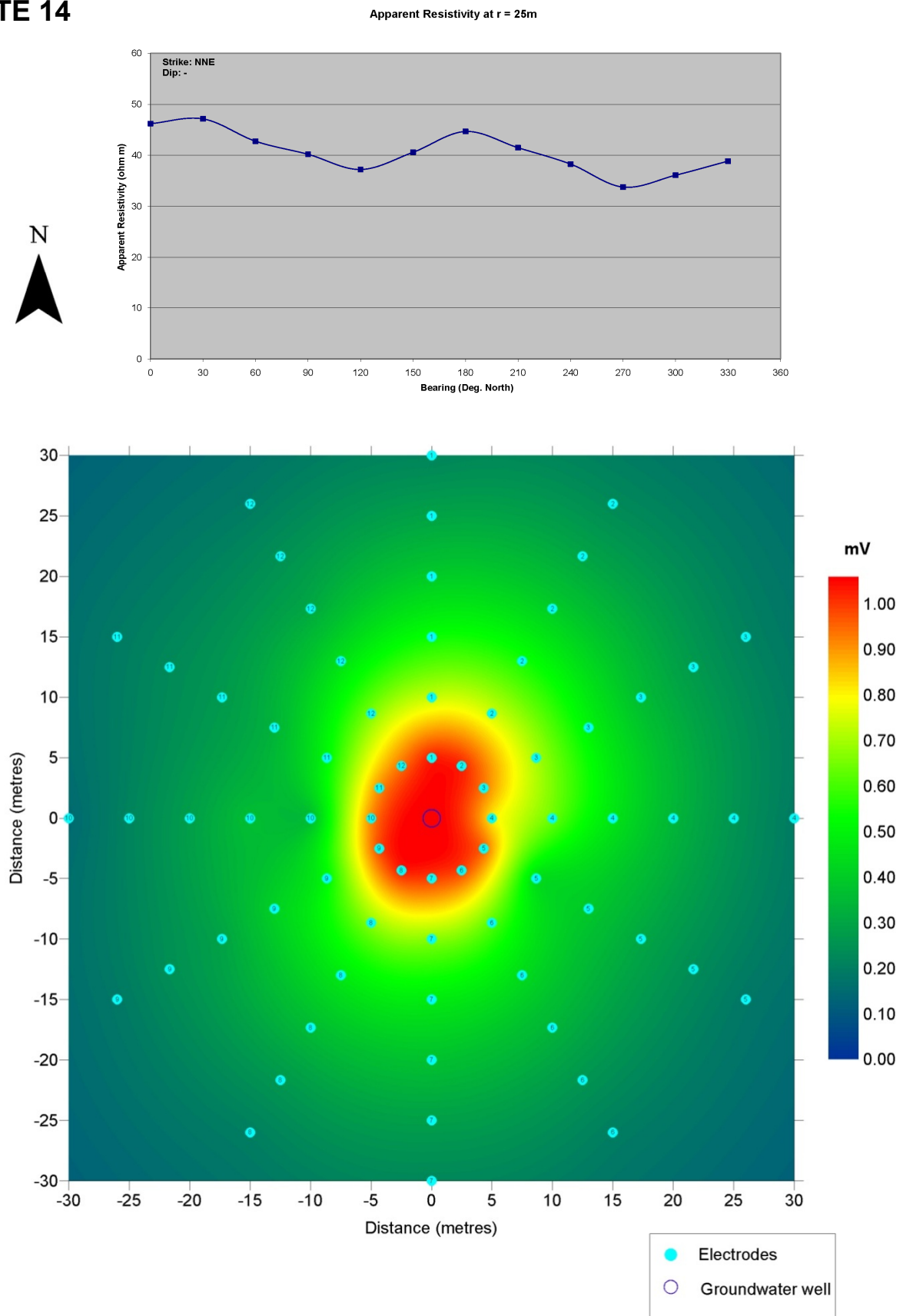
SITE 12



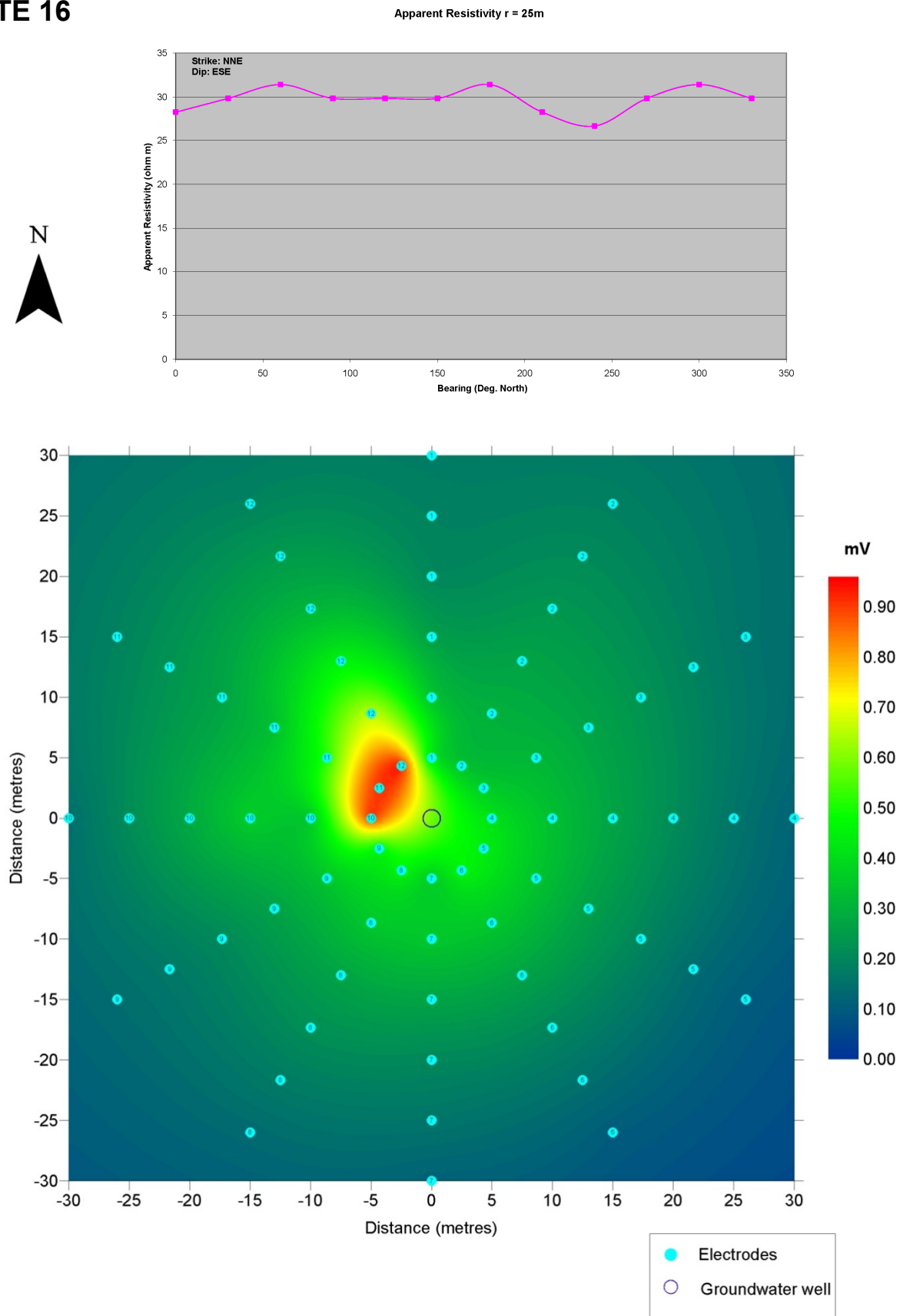
SITE 13



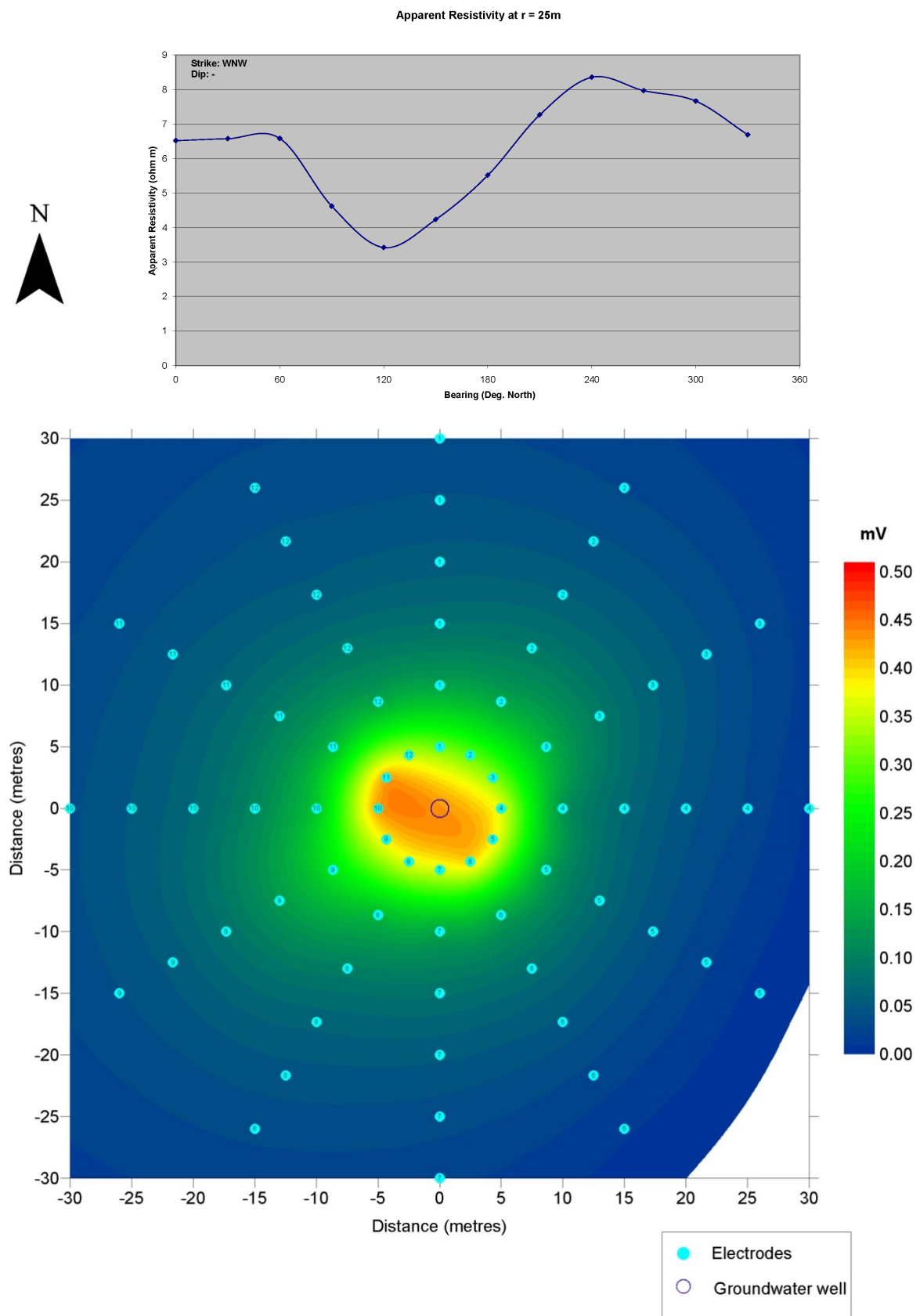
SITE 14



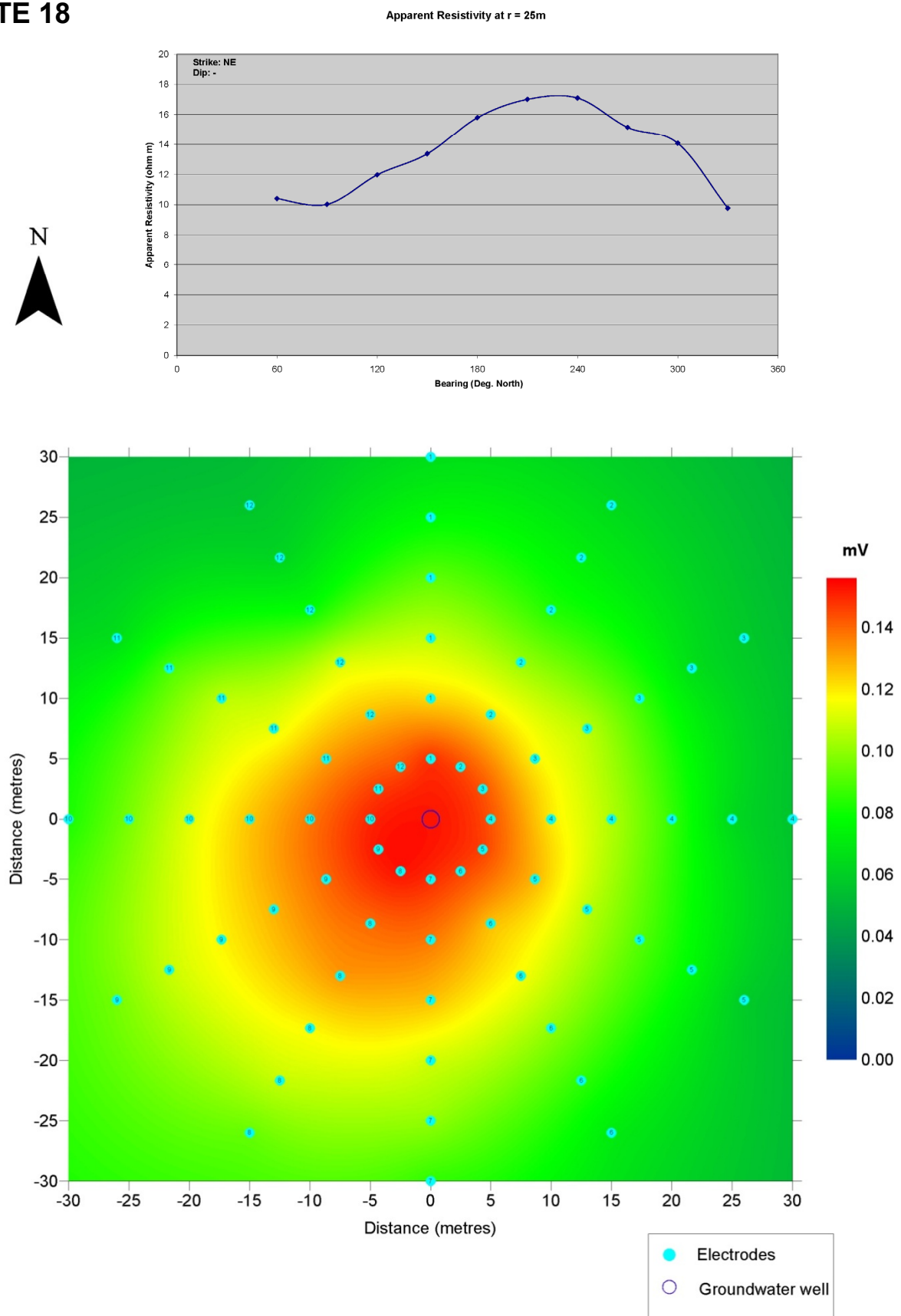
SITE 16



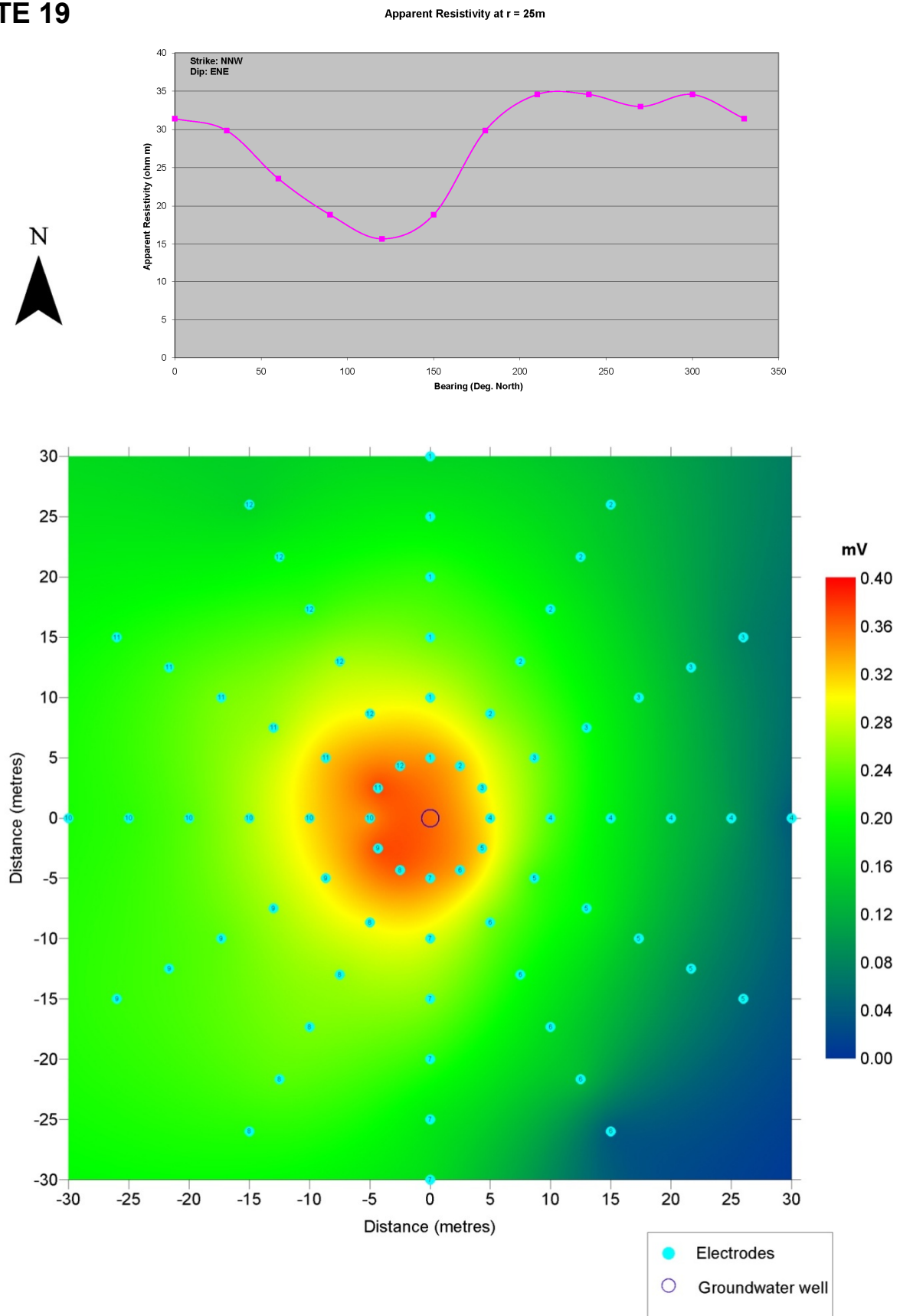
SITE 17



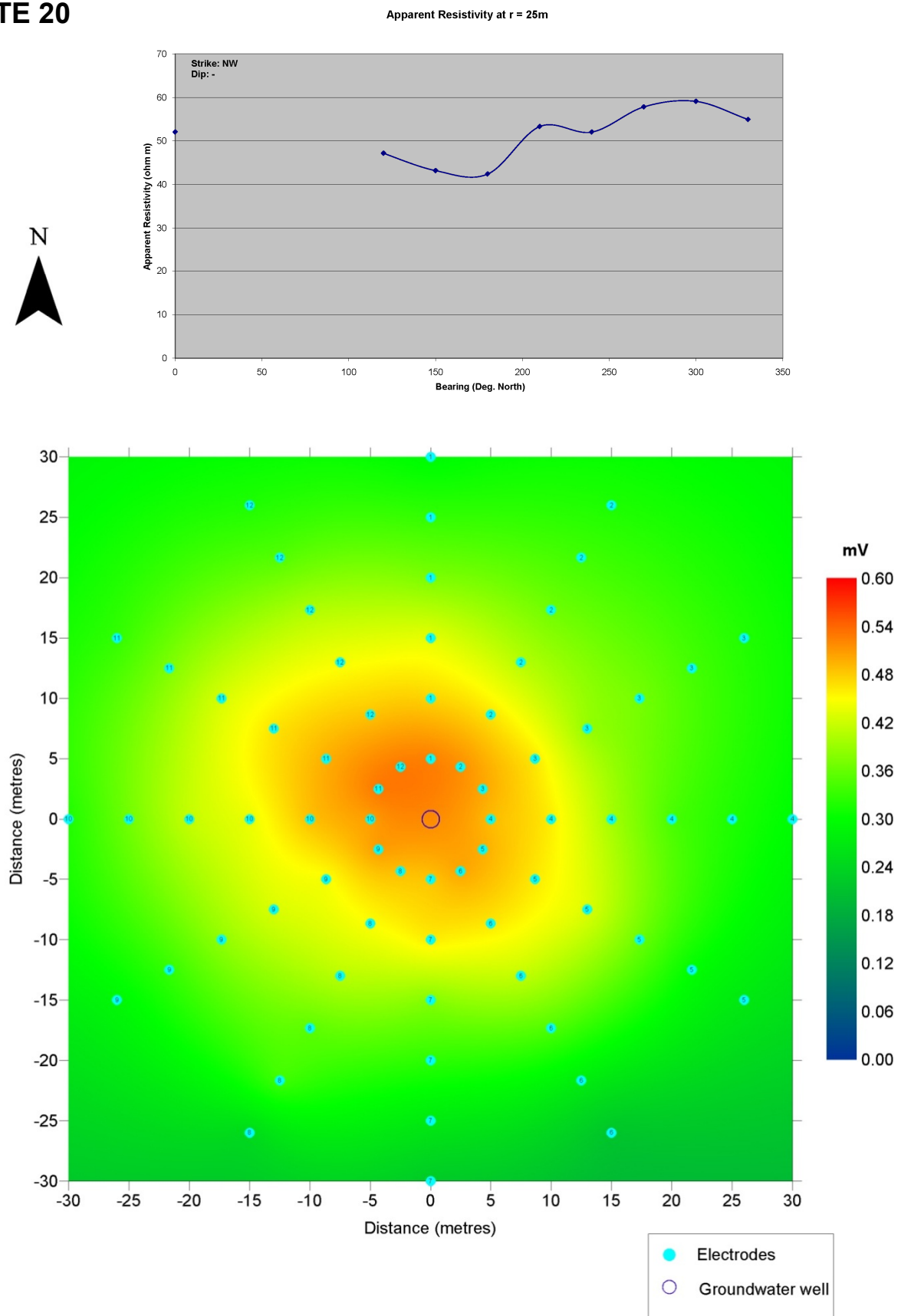
SITE 18



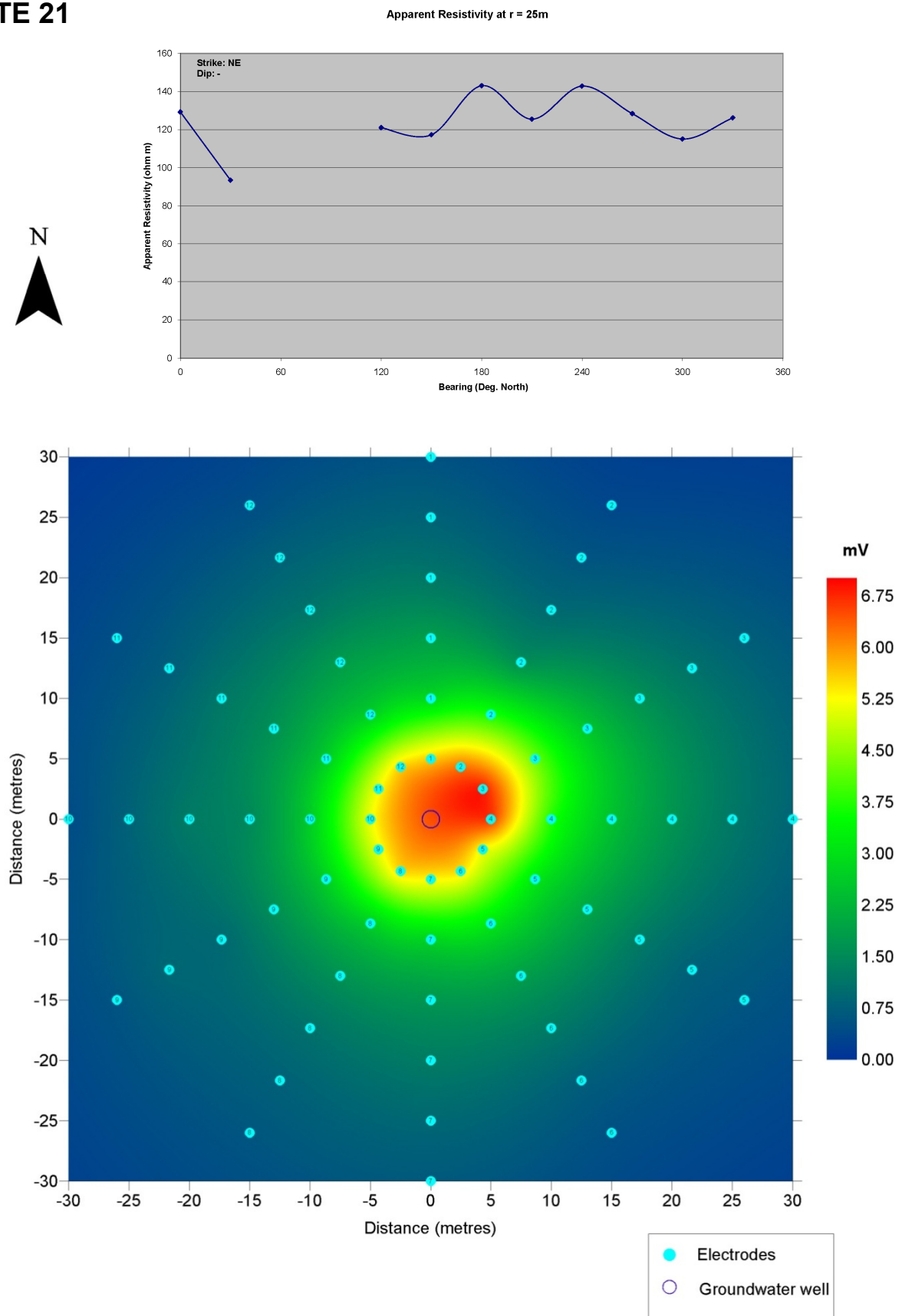
SITE 19



SITE 20



SITE 21



B. WELLS SELECTED FOR SURVEY IN THE WESTERN MOUNT LOFTY RANGES WITH GEOLOGICAL DESCRIPTION

Site	Unit Number	Depth (m)	Geological		Formal Map Description	
			Unit	Formation	Aquifer Type	
1	-	-	-	-	-	-
2	6628-5502	76.2	Lb	Barossa Complex	Basement/Archaean	Gneiss, schist and pegmatite subjected to metamorphism as high temperatures and pressures.
3	6628-6109	152.0	Nmc	Castambul Formation	Burra Group	Dolomite, massive, pale grey to white, finely crystalline. Occurs as 50-100m thick interbeds within green grey silt and phyllite.
4	-	-	-	-	-	-
5	6628-11979	104.0	Ndw	Woolshed Flat Shale	Burra Group	Shale, black; dolomitic siltstone; dolomite; grey laminated siltstone.
6	6628-4602	71.0	Ndw	Woolshed Flat Shale	Burra Group	Shale, black; dolomitic siltstone; dolomite; grey laminated siltstone.
7	6628-11780	118.0	Eeb	Backstairs Passage Formation	Kanmantoo Group	Sandstone, laminated, thick bedded, slumped, crossbedded, with minor siltstone interbeds. Widespread siltstone unit at base.
8	6628-10781	41.0	Eec	Carrickalinga Head Formation	Kanmantoo Group	Sandstone, grey, thick bedded, with thinly bedded, muddy, siltstone interbeds. Minor cross-bedding, ripples, rare trace fossils.
9	6628-12605	123.4	Ndw	Woolshed Flat Shale	Burra Group	Shale, black; dolomitic siltstone; dolomite; grey laminated siltstone.
10	6628-22603	91.0	Ndt	Stonyfell Quartzite	Burra Group	Quartzite, feldspathic, with shale interbeds; silty sandstone in part schistose and calcareous.
11	6628-9333	40.0	Nds	Saddleworth Formation	Burra Group	Slate dolomite quartzite.
12	6628-14068	110.0	Nds	Saddleworth Formation	Burra Group	Slate dolomite quartzite.
13	6628-10214	56.8	Nds	Saddleworth Formation	Burra Group	Slate dolomite quartzite.
14	6628-6576	82.3	Ndw	Woolshed Flat Shale	Burra Group	Shale, black; dolomitic siltstone; dolomite; grey laminated siltstone.
15	-	-	-	-	-	-

APPENDICES

16	6628-6835	59.1	No	Emeroo Subgroup	Burra Group	Quartz, sandstone, dolomite, conglomerate.
17	6628-6739	83.8	No	Emeroo Subgroup	Burra Group	Quartz, sandstone, dolomite, conglomerate.
18	6628-10954	66.5	No	Emeroo Subgroup	Burra Group	Quartz, sandstone, dolomite, conglomerate.
19	6628-21741	140.0	No	Emeroo Subgroup	Burra Group	Quartz, sandstone, dolomite, conglomerate.
20	6628-6854	129.0	Lb	Barossa Complex	Basement/Archaean	Gneiss, schist and pegmatite subjected to metamorphism as high temperatures and pressures.
21	6627-2721	50.0	No	Emeroo Subgroup	Burra Group	Quartz, sandstone, dolomite, conglomerate.

UNITS OF MEASUREMENT

Units of measurement commonly used (SI and non-SI Australian legal)

Name of unit	Symbol	Definition in terms of other metric units	Quantity
Day	d	24 h	time interval
Gigalitre	GL	10^6 m^3	Volume
Gram	g	10^{-3} kg	mass
Hectare	ha	10^4 m^2	area
Hour	h	60 min	time interval
Kilogram	kg	base unit	mass
Kilolitre	kL	1 m^3	volume
Kilometre	km	10^3 m	length
Litre	L	10^{-3} m^3	volume
Megalitre	ML	10^3 m^3	volume
metre	m	base unit	length
Microgram	μg	10^{-6} g	mass
Microlitre	μL	10^{-9} m^3	volume
Milligram	mg	10^{-3} g	mass
Millilitre	mL	10^{-6} m^3	volume
millimetre	mm	10^{-3} m	length
Minute	min	60 s	time interval
Second	s	base unit	time interval
Tonne	t	1000 kg	mass
Year	y	365 or 366 days	time interval

Shortened forms

~	approximately equal to	NS	natural surface
bgs	below ground surface	pH	acidity
DD	drawdown	ppb	parts per billion
DTW	depth to water (measured from a reference point usually top of casing)	ppm	parts per million
		ppt	parts per trillion
		ρ_a	apparent resistivity (Ωm)
EC	electrical conductivity ($\mu\text{S}/\text{cm}$)	SWL	standing water level (measured from ground surface)
K	hydraulic conductivity (m/d)		
mV	millivolts	TDS	total dissolved solids (mg/L)
mBNS	metres below natural surface	TOC	top of casing

GLOSSARY

Anisotropic — Applied to substances whose optical or other physical properties vary according to the direction from which they are observed

Apparent resistivity — A measurement of resistivity which is calculated as the product of the measured resistance and a geomagnetic factor; units are ohms/m. It is important to note that the apparent resistivity is not an explicit measurement of the electrical resistivity of a material and should not be interpreted as being diagnostic of a given material

Aquifer — An underground layer of rock or sediment that holds water and allows water to percolate through

Aquifer test — A hydrological test performed on a well, aimed to increase the understanding of the aquifer properties, including any interference between wells, and to more accurately estimate the sustainable use of the water resources available for development from the well

ASR — Aquifer Storage and Recovery

Cone of depression — An inverted cone-shaped space within an aquifer caused by a rate of groundwater extraction that exceeds the rate of recharge; continuing extraction of water can extend the area and may affect the viability of adjacent wells, due to declining water levels or water quality

Continental margin — Zone that extends from the shoreline to the deep-ocean floor at a depth of 2000 metres. The zone is underlain by continental crust

DC — Direct current

DWLBC — Department of Water, Land and Biodiversity Conservation (Government of South Australia)

E — East

ESE — East – south-east

ENE — East – north-east

EMLR — Eastern Mount Lofty Ranges

Equipotential line — The two-dimensional focus of all points with equal value for a potential field

Equipotential surface — The three-dimensional distribution of all points of equal value for a potential field. Equipotential lines and surfaces are perpendicular to the lines of force associated with the potential field

EC — Electrical conductivity; 1 EC unit = 1 micro-Siemen per centimetre ($\mu\text{S}/\text{cm}$) measured at 25°C; commonly used as a measure of water salinity as it is quicker and easier than measurement by TDS

FRA — Fractured rock aquifer

Fracture — General term applied to any break in a material, but commonly applied to more or less clean breaks in rocks or minerals

Geophysics — The science concerned with all aspects of the physical properties and processes of the Earth and planetary bodies and their interpretation

Geosyncline — Large, downwarp structure generally of considerable extent, which may develop along a continental margin

Groundwater — Water occurring naturally below ground level or water pumped, diverted and released into a well for storage underground; see also 'underground water'

Hydraulic conductivity (K) — A measure of the ease of flow through aquifer material: high K indicates low resistance, or high flow conditions; measured in metres per day

Hydrogeology — The study of groundwater, which includes its occurrence, recharge and discharge processes, and the properties of aquifers; see also 'hydrology'

Lithology — The description of the microscopic features of a rock

LPRC — Little Para River Catchment

m AHD — Defines elevation in metres (m) according to the Australian Height Datum (AHD)

MLR — Mount Lofty Ranges

NE — North-east

NNE — North – north-east

NNW — North north-west

NW — North-west

Observation well — A narrow well or piezometer whose sole function is to permit water level measurements

ORC — Onkaparinga River Catchment

PIRSA — Primary Industries and Resources South Australia

Porosity — Absolute porosity is the total of all void spaces present within a rock, but not all these spaces will be interconnected and thus be able to contain and transmit fluids. The effective porosity is thus defined as the proportion of the rock which consists of interconnected pores. Porosity is expressed as a percentage of the bulk volume of the rock

Potential electrode — An electrode used as a ground contact in a voltage-measuring circuit

Production well — The pumped well in an aquifer test, as opposed to observation wells; a wide-hole well, fully developed and screened for water supply, drilled on the basis of previous exploration wells

PWRA — Prescribed Water Resource Area

SE — South-east

SP — Self potential. A method which measures the naturally occurring potential differences between two non-polarizable electrodes

SW — South-west

TDS — Total dissolved solids, measured in milligrams per litre (mg/L); a measure of water salinity

TRC — Torrens River Catchment

Underground water (groundwater) — Water occurring naturally below ground level or water pumped, diverted or released into a well for storage underground

Unit number — A unique identifier given to all registered wells within South Australia

Well — (1) An opening in the ground excavated for the purpose of obtaining access to underground water. (2) An opening in the ground excavated for some other purpose but that gives access to underground water. (3) A natural opening in the ground that gives access to underground water

WMLR — Western Mount Lofty Ranges

WNW — West – north-west

REFERENCES

- Adepelumi A, Yi J, Kim JH, Ako BD, Son JS, 2006, Integration of surface geophysical methods for fracture detection in crystalline bedrocks of southwestern Nigeria. *Hydrogeological Journal* 14:1283-1306.
- Archie G, 1942, 'The electrical resistivity log as an aid in determining some reservoir characteristics.' *Transactions of American Institute of Mining, Metallurgical and Petroleum Engineers*.
- Batayneh AT, 2006, 'Use of electrical resistivity methods for detecting subsurface fresh and saline water and delineating their interfacial configuration: a case study of the eastern Dead Sea coastal aquifers, Jordan', in *Hydrogeological Journal* 14:1277-1283.
- Benson AK, Payne KL, and Stubben M, 1997, 'Mapping groundwater contamination using DC resistivity and VLF geophysical methods - A case study'. in *Geophysics* 62:80-86.
- Block L, Cheng CH, Fehler M, and Phillips WS, 1994, 'Seismic imaging using microearthquakes induced by hydraulic fracturing', in *Geophysics* 59:102-112.
- Brown, SR, 1989, 'Transport of fluid and electric current through a single fracture', in *Journal of Geophysical Research* 94:9429-9438.
- Cook, PG, 2003, *A guide to regional groundwater flow in fractured rock aquifers*. CSIRO Land and Water.
- Cook PG, Herczeg AL, and McEwan KL, 2001, 'Groundwater recharge and stream baseflow. Atherton Tablelands, Queensland', in *CSIRO Land and Water*, Technical Report 08/01.
- Corwin RF, and Hoover DB, 1979 'The self-potential method in geothermal exploration', in *Geophysics* 44:226-245.
- Costar A, Heinson G, Wilson T and Smit Z, 2008, *Hydrogeophysical mapping of fracture orientation and groundwater flow in the Eastern Mount Lofty Ranges, South Australia*, DWBLC Report 2009/09, Department of Water, Land and Biodiversity Conservation, Adelaide.
- Dailey JW, LaBrecque D, and Nitao J, 1992, 'Electrical resistivity tomography of vadose water movement', in *Water Resources Research* 28(5):1429-1442.
- Daily W, and Owen E, 1991, 'Cross-borehole resistivity tomography', in *Geophysics* 56(8):1228-1235.
- Davies PB, Brush LH, and Mendenhall FT, 1991, 'Assessing the impact of waste-generated gas from the degradation of transuranic waste at the Waste Isolation Pilot Plant', in *Proceedings of the Workshop on Gas Generation and Release from Radioactive Waste Repositories*, Aix-en-Provence, France.
- Fagerlund F, and Heinson GS, 2003, 'Detecting sub-surface groundwater flow in fractured rock using self-potential (SP) methods', in *Environmental Geology* 43:782-794.
- Fehler M, 1989, 'Stress control of seismicity patterns observed during hydraulic fracturing experiments at the Fenton Hill hot dry rock geothermal energy site, New Mexico. *International Journal of Rock Mechanics and Mining Science and Geomechanics Abstracts* 26:211-219.
- Freeze RA, and Cherry JA, 1979, *Groundwater*, Prentice Hall, New Jersey.

REFERENCES

- Gustafsson J, Mikkola P, Jokinen M, and Rosenholm JB, 2000, 'The influence of pH and NaCl on the zeta potential and rheology of anatase dispersions', in *Colloids and Surfaces A: Physicochemical and Engineering Aspects*, 175(3):349-359(11).
- Ishido T, and Pritchett JW, 1999, 'Numerical simulation of electrokinetic potentials associated with subsurface fluid flow', in *Journal of Geophysical Research* 104(B7):15247-15259.
- Johnson CD, Haeni FP, Lane JW, and White, EA, 2002, 'Borehole-geophysical investigation of the University of Connecticut landfill, Storrs, Connecticut', in *US Geological Survey Water-Resources Investigations Report 01(4033)*:187.
- Jouniaux L, and Pozzi J-P, 1995, 'Streaming potential and permeability of saturated sandstones under triaxial stress: consequences for electrotelluric anomalies prior to earthquakes', in *Journal of Geophysical Research* 100:10197–10209.
- Karasaki K, Freifeld B, Cohen A, Grossenbacher K, Cook P, and Vasco D, 2000, 'A multidisciplinary fractured rock characterization study at Raymond field site, Raymond, CA', in *Journal of Hydrology* 236(1/2):17-34.
- Keller GV, and Frischknecht FC, 1966, *Electrical methods in geophysical prospecting*, Pergamon Press, New York.
- Love A, and Cook P, 1999, *The importance of fractured rock aquifers*, Department of Primary Industries and Resources South Australia Rep Book 99/23
- Majer EL, Peterson JE, Daley T, Kaelin B, Myer LR, Queen J, D-Onfro P, and Rizer W, 1997, 'Fracture detection using crosswell and single well surveys', in *Geophysics* 62(2):495-504.
- Nicholas JR, and Healy RW, 1988, 'Tritium migration from a low-level radioactive-waste disposal site near Chicago, Illinois', in *USGS Water Supply Paper 2333*, US Geological Survey, Reston, Virginia.
- Nimmer RE, Osiensky JL, Binley AM, Sprenke KF, and Williams BC, 2007, 'Electrical resistivity imaging of conductive plume dilution in fractured rock' in *Hydrogeological Journal* 15(5):877-890.
- Preiss WV (compiler), 1987, 'The Adelaide Geosyncline – later Proterozoic stratigraphy, sedimentation, palaeontology and tectonics', Bulletin 53 of the Geological Survey of South Australia.
- Revil A, Pezard PA, and Glover PW, 1999, 'Streaming potential in porous media 1. Theory of the zeta potential', in *Journal of Geophysical Research* 104(B9):20021-20032.
- Rizzo E, Suski B, Revil A, Straface S, and Troisi S, 2004, 'Self-potential signals associated with pumping tests experiments', in *Journal of Geophysical Research* 109(B):10203.
- Robinson B, and Tester J, 1984 'Dispersed flow in fractured reservoirs: an analysis of tracer-determined residence time distributions', in *Journal of Geophysical Research* 89:10374-10384.
- Robinson R, Silliman S, and Cady C, 1993, 'Identifying fracture interconnections between boreholes using natural temperature profiling: Application to a fractured dolomite', in *The Log Analyst* 34(1):69-77.
- Sahimi, M, 1995 'Flow and transport in porous media and fractured rock', in *VCH*, Weinheim, Germany.
- Saka, 2006, 'The effects of electrolyte concentration, ion species and pH on the zeta potential and electrokinetic charge density of montmorillonite', in *Clay Minerals* (0009-8558) 41(4):853.
- Sato M, and Mooney H, 1960, The electrochemical mechanisms of sulphide self-potentials', in *Geophysics* 25(1):226.

REFERENCES

- Shapiro AM, and Hsieh PA, 1991, 'Research in fractured-rock hydrogeology: characterizing fluid movement and chemical transport in fractured rock at the Mirror Lake drainage basin', in *USGS Water Resources Investigation Report* 91-4034, US Geological Survey, Reston, Virginia.
- Sheffer MR, and Oldenburg DW, 2007, 'Three-dimensional modelling of streaming potential', in *Geophysical Journal International* 169:839-848.
- Sill RW, 1983 'Self-potential modeling from primary flows', in *Geophysics* 48:76-86.
- Skinner D, and Heinson G, 2004, 'A comparison of electrical and electromagnetic methods for the detection of hydraulic pathways in a fractured rock aquifer, Clare Valley, South Australia', in *Hydrogeological Journal* 12(5):576-590.
- Slater L, Brown D, and Binley A, 1996, 'Determination of hydraulically conductive pathways in fractured limestone using cross-borehole electrical resistivity tomography', in *European Journal of Environmental and Engineering Geophysics* 1(1):35-52.
- Smit Z, 2007, 'Hydrogeophysical Mapping of Fracture Orientation and Groundwater Flow in the Eastern Mount Lofty Ranges, South Australia', Honours thesis, The University of Adelaide.
- Stevens KM, Lodha GS, Holloway AL, and Soonawala NM, 1995, 'The application of ground penetrating radar for mapping fractures in plutonic rocks within the Whiteshell Research Area, Pinawa, Manitoba, Canada', in *Journal of Applied Geophysics* 33(1/3):125-141.
- Taylor RW, and Flemming AH, 1988, 'Characterizing jointed systems by azimuthal resistivity surveys', in *Ground Water* 26(4):464-474.
- Warren BM, 2001, 'Determining ratios of anisotropy using hydrogeological and geophysical methods in the Clare Valley, South Australia', Honours thesis, Flinders University of South Australia.
- Watson KA, and Barker RD, 1999, 'Differentiating anisotropy and lateral effects using azimuthal resistivity offset Wenner soundings', in *Geophysics* 64:739-745.
- Weiss M, Rubin Y, Adar E, and Nativ R, 2006, 'Fracture and bedding plane control on groundwater flow in a chalk aquitard', in *Hydrogeological Journal* 14:1081-1093.
- Wishart DN, Slater LD, and Gates AE, 2006, 'Self potential improves characterization of hydraulically-active fractures from azimuthal geoelectrical measurements', in *Journal of Geophysical Research Letter* 33:L17314, doi:10.1029/2006 GL027092.
- Zulfic D, and Barnett S, 2003, *Eastern Mount Lofty Ranges Groundwater Assessment*, DWBLC Report 2005/05, Department of Water, Land and Biodiversity Conservation, Adelaide.

BIBLIOGRAPHY

Asch, T, and Morrison, HF, 1989, 'Mapping and monitoring electrical resistivity with surface and subsurface electrode arrays', in *Geophysics* 54:235-244.

Bear J, 1979, *Hydraulic of groundwater*, McGraw-Hill, Keterpress, Jerusalem.

Cook, PG, 2003, *A guide to regional groundwater flow in fractured rock aquifers*, CSIRO Land and Water, Australia.

Cook, PG and Simmons, CT, 2000, 'Using environmental tracers to constrain flow parameters in fractured rock aquifers: Clare Valley, South Australia', in Faybishenko, B (ed), *Dynamics of fluids in fractured rocks: Concepts and recent advances*, AGU Monograph, 122, pp.337–347.

Daley, S and Dwyer, T 2004, 'Eastern Mt Lofty Ranges land use survey classification and field survey methodology', internal technical report, Department of Water, Land and Biodiversity Conservation, Adelaide.

Gravestock, DI and Gatehouse, CG, 1995, 'Early and Middle Palaeozoic', in Drexel, JF & Preiss, WV (eds), *The geology of South Australia, Vol 2, The Phanerozoic*, Bulletin 54, Geological Survey, Adelaide, pp.3–61.

Jansen, J, and Zorich, T, 1995, 'Spontaneous potential surveys around pumping wells', in *Proceedings of the Symposium of Applied Geophysics to Environmental and Engineering Problems*, (SAGEEP) 865–869.

Preiss, WV, (compiler) 1987, *The Adelaide Geosyncline: Late Proterozoic stratigraphy, sedimentation, palaeontology and tectonics*, Bulletin 53, Geological Survey, Adelaide.

Preiss, WV 1995, 'Early and middle Palaeozoic orogenesis', in Drexel, JF & Preiss, WV (eds), *The geology of South Australia, Vol. 2, The Phanerozoic*, Bulletin, 54, Geological Survey, Adelaide, pp.45–57.

Renshaw, CE, 1995, 'On the relationship between mechanical and hydraulic apertures in rough-walled fractures', in *Journal of Geophysical Research* 10:24629-24636.

Renshaw, CE, 1999, 'Connectivity of joint networks with power law length distributions', in *Water Resources Res* 35:2661-2670.

Renshaw, CE, Dadakis, JS, and Brown, SR, 2000, 'Measuring fracture apertures: A comparison of methods', in *Geophysical Research Letters* 27:289-292.

Reynolds, JM, 1997, *An introduction to Applied and Environmental Geophysics*, John Wiley and Sons Ltd, Chichester.

Slater, LD, Binley A, and Brown, D, 1997, 'Electrical imaging of fractures using groundwater salinity change', in *Ground Water* 35(3):436-442.

Snow, DT, 1968, 'Rock fractures spacings, openings and porosities', in *Journal of Soil Mechanics and Foundations Division*, SM1:73-91.

Zhang, X, and Sanderson, DJ, 1998, 'Numerical study of critical behaviour of deformation and permeability of fractured rock masses', in *Marine and Petroleum Geology* 15:535-548.

BIBLIOGRAPHY

Zhou, B, 1998, 'Crosshole resistivity and acoustic velocity imaging: 2.5-D Helmholtz equation modelling and inversion, Doctorate of Philosophy, University of Adelaide.

Zulfic, D, and Barnett, S, 2003, *Eastern Mount Lofty Ranges groundwater assessment*, Report DWLBC 2003/25, Department of Water, Land and Biodiversity Conservation, Adelaide.